

Project 97-14 Effect of Stratification on Ecosystem Changes in Lake Erie

David A. Culver and Ellen T. McDonald The Ohio State University

ABSTRACT

Lake Erie has undergone tremendous changes since 1970, notably a 70% decline in external phosphorus loading and the introduction of zebra mussels. An understanding of the physical processes that affect the vertical transport of nutrients and algae in the lake is essential in order to help integrate these changes into future management of lake resources. In this LEPPF-sponsored research project, we studied the role of nutrient and phytoplankton transport in the Lake Erie ecosystem of the central basin of Lake Erie, emphasizing the relationships among the physical, biological and chemical processes controlling vertical transport in the Lake.

We compared the spatial and temporal variation in nutrients, phytoplankton, and zooplankton in the 3 Lake Erie basins, quantified the vertical turbulent mixing rates throughout the water column at a single site in the central basin, used these results together with vertical profiles of nutrient concentrations and phytoplankton abundance to estimate the fluxes of nutrients and phytoplankton within the water column, and adapted the results for use in models of the effects of phosphorus and nitrogen loading and cycling on the production of plankton and fish. Central to this research was the use of a Self-Contained Autonomous Microprofiler (SCAMP). The SCAMP falls through the water column at 10 cm/s and samples at 100 scans/s, giving a measurement resolution of 1 mm for depth, temperature, oxygen, and chlorophyll fluorescence throughout the profile.

Preliminary findings discussed in this report:

Objective 1: Spatial and temporal variation of Lake Erie nutrients and plankton

May 1997: Total nitrogen concentration (TN) ranged between 400 and 600 $\mu\text{gN/L}$ at our site and across most of the southern portion of the central basin, and between 200 and 400 $\mu\text{gN/L}$ on the northern shore. TN in the western basin was 600-800 $\mu\text{gN/L}$, except in the Sandusky and Maumee river mouths where it was $\approx 1000 \mu\text{gN/L}$. Phosphorus concentrations in the central basin were $\approx 14 \mu\text{g/L}$ except near Cleveland and the mouths of the Grand and Cuyahoga Rivers, where TP was as high as 42 $\mu\text{g/L}$. Eastern basin concentrations were below 14 $\mu\text{gP/L}$, while those in the western basin were between 28 and 42 $\mu\text{gP/L}$. Phytoplankton biomass was below 1 mg wet weight/L at our study site and for much of the rest of the central basin. Phytoplankton biomass near the Bass Islands (6 mg/L) exceeded concentrations in the western basin which were all $\geq 3 \text{ mg/L}$. Great Lakes Forecasting System (GLFS) data for currents, wave height, temperature (10-12 $^{\circ}\text{C}$) and wind direction supported our assumptions of minimal horizontal gradients at our site and its being characteristic of the central basin as a whole.

August 1997: Surface TN was lower in the stratified eastern and central basins (240 - 320 $\mu\text{gN/L}$), but remained high in the unstratified western basin (up to 800 $\mu\text{gN/L}$). Central basin TP concentrations were 6 to 12 $\mu\text{gP/L}$, while they were 6 to 9 $\mu\text{gP/L}$ in the eastern basin. Just as in May, values were higher to the northeast of Cleveland, reaching 18 $\mu\text{g/L}$ P. Western basin values were comparable to those in May. Phytoplankton ranged from 0.5 to 0.75 mg/L except west of Kelly's Island (3.5 mg/L). There was again very little variation in the various parameters (e.g. surface temperature, 24-25 °C) across the central basin. The largest spatial heterogeneity in both May and August came from the Grand and Cuyahoga River inputs, upwelling events near Long Point, and occasional transport of western basin water masses into the central basin.

Objective 2: Quantify the vertical mixing rates throughout the water

In May 1997, the water column 5 miles off Fairport, OH, was weakly stratified, whereas in August it had developed a strong seasonal thermocline at 17 m. The rate of turbulent mixing (eddy diffusivity) was calculated from each of over 20 SCAMP temperature distribution profiles from a week of sampling in May, and again in August. In both months, four mixing processes were identified: Wind-induced mixing at the surface, over night cooling of the surface waters which caused penetrative convection, shear instability associated with thermal gradients at the thermocline, and shear instability caused by currents (seiche activity) at the bottom of the lake. For most of the profiles, very little mixing was occurring. The greatest amount of mixing was due to daily penetrative convection, and wind-induced mixing associated with storm events (e.g. 21 May and 6 August).

Objective 3: Estimate the fluxes of nutrients and phytoplankton within the water column.

We used the eddy diffusivities and measured gradients of nutrient concentration and phytoplankton abundance and chlorophyll *a* to estimate flux rates. Even extreme gradients do not produce turbulent fluxes in the absence of turbulent mixing (i.e., when the eddy diffusivity is equal to zero). Similarly, high diffusivities generate no net fluxes in the absence of concentration gradients in the same water mass.

There were three primary regions in the water column for which there was a measurable flux of nutrients, corresponding to the four types of mixing found at our sample site in May and August 1997. At the surface, both penetrative convection and wind/wave-driven mixing dominate, influencing both chlorophyll and nutrients. At the bottom of the epilimnion, shear causes fluxes when the epilimnion and the hypolimnion move in different directions. Finally, at the base of the hypolimnion, bottom currents create shear, which resuspends nutrients from the lake bottom and mixes the hypolimnion. On calm days (e.g. 23 May and 8 August), in the absence of penetrative convection, the fluxes of chlorophyll *a* are on the order of 0.1 $\text{mg m}^{-3} \text{sec}^{-1}$ in the surface waters, an order of magnitude less than the fluxes caused by the storm events. Shear at the base of the hypolimnion results in both the mixing of nutrients within the hypolimnion and resuspension of phosphorus from the sediment on the order of 1 $\text{g m}^{-2} \text{day}^{-1}$.

Objective 4: Adapt the results for use in models of the effects of P and N loading and cycling on the production of plankton and fish.

Flux estimates allow us to address the role of vertical mixing in the central basin in plankton and fish production. Our results contribute to two primary modeling components: 1) nutrient regeneration from the sediments as a source of internal loading in the central basin, and 2) that under strong thermal stratification, little mixing occurs across the thermocline, but it does occasionally occur. We will combine these results with information on the impacts of zebra mussel grazing obtained in field experiments, to estimate phytoplankton fluxes into the benthic boundary layer, where the zebra mussels consume the algae. Upon measuring turbulent mixing rates in the western and eastern basins as well, we will be able to more accurately estimate vertical transport affects zebra mussel consumption of algae, mass transport of oxygen and nutrients, and many other aspects of lake function.

PROBLEM STATEMENT

Since 1970, the functioning of the Lake Erie pelagic ecosystem has been constantly changing. As in most freshwater ecosystems, the limiting nutrient in algal production is phosphorus. The influx of phosphorus from detergents, agricultural runoff and human waste was estimated to be 26 thousand metric tons phosphorus in 1967/68 (Janus and Vollenweider 1981). Such loading led to extensive eutrophication and a resulting deterioration of water quality. Public concern prompted government intervention, and in 1978, the Great Lakes Water Quality Agreement introduced new EPA controls to reduce phosphorus inputs into the Great Lakes. The EPA's reduction targets for point-source phosphorus loading were met in 1982-1983 and have been exceeded many years since. Low rainfall in 1987-88 brought phosphorus input levels to a post-1970 low, causing concern among some that Lake Erie may now actually receive too little phosphorus to maintain fish populations. By 1995, however, it was clear that nutrient levels were again on the rise in the lake, and a bloom of *Microcystis* (a toxic cyanobacterium often associated with high phosphorus availability) occurred. Increased nutrient levels could be caused by increased external loading of phosphorus and/or by the introduction of the zebra mussels (a possible source of internal loading via mineralization of algae). The increased nutrient levels affect algal, zooplankton and fish production throughout the lake, major points of concern for industries dependent on the lake's resources.

An understanding of the physical processes that affect the vertical transport of nutrients and algae in the lake is essential in order to track the continually changing Lake Erie ecosystem, as well as to help with future management of lake resources. The introduction of the zebra mussel has stimulated Lake Erie research, resulting in numerous efforts to estimate the impact of the mussel on lake ecology. Nearly all of these studies, however, have investigated the biological and/or chemical components of the ecosystem, without adequately considering the coupling of these processes to the physical dynamics of the lake. For example, zebra mussels are benthic suspension feeders, living on the bottom, while the algae they eat are primarily produced in the upper water column. They therefore rely on a combination of turbulent mixing and settling to bring algae down to the benthos where they feed. It is also known that the zebra mussels increase the concentrations of nitrogen and phosphorus near the benthos (Heath et al. 1995). These elevated nutrient levels may contribute to alteration of algal species composition and abundance. The magnitude of the impacts on phytoplankton dynamics from increased benthic nutrient release will depend both on the amounts of nutrients excreted and on the extent of vertical transport of nutrients up from the benthos by turbulent mixing into the euphotic zone where the nutrients can be utilized. In addition, the intensity of mixing determines the light levels encountered by the phytoplankton, an important factor in the rate of photosynthesis (MacIntyre 1993). These processes illustrate the intricate role of physical processes in all levels of the lake's ecology.

In this LEPF-sponsored research project, we studied the role of nutrient and phytoplankton transport in the Lake Erie ecosystem of the central basin of Lake Erie, emphasizing the relationships among the physical, biological and chemical processes

controlling vertical transport in the Lake. We organized our project activities around four research objectives. This report summarizes work performed on the four study objectives and the research results obtained to date, and has been written by William Edwards (doctoral student), Kyle McCune (Master's Student), and David Culver and Ellen McDonald (Project Directors).

STUDY OBJECTIVES

- 1) Compare the spatial and temporal variation in nutrients, phytoplankton, and zooplankton in the 3 Lake Erie basins.
- 2) Quantify the vertical mixing rates throughout the water column at selected sites in the central basin.
- 3) Use the results of 2), together with vertical profiles of nutrient concentrations and phytoplankton abundance to estimate the fluxes of nutrients and phytoplankton within the water column.
- 4) Adapt the results for use in models of the effects of P and N loading and cycling on the production of plankton and fish.

PROJECT ACCOMPLISHMENTS

Objective 1) Compare the spatial and temporal variation in nutrients, phytoplankton, and zooplankton abundance in the 3 basins of Lake Erie.

Introduction

Because our studies of turbulent transport were limited to a site in the central basin, it is important to determine to what extent this site is characteristic of the remainder of the central basin and of Lake Erie as a whole. This objective is thus part of a major initiative underway to investigate the horizontal and temporal variation of nutrients, algae and zooplankton in the three basins of Lake Erie. Field work, including sampling of algae, zooplankton, seston, chlorophyll *a*, and nutrients, was performed by the Ohio Division of Wildlife (ODW), and the Canadian National Water Research Institute (NWRI) and Department of Fisheries and Oceans (DFO) at the Canadian Centre for Inland Waters (CCIW), Burlington, Ontario, as part of their contributions to the binational Lake Erie Lakewide Management Plan program (LaMP) activities.

Methods

Laboratory analysis of phytoplankton biomass, chlorophyll *a* and zooplankton abundance was performed at our Ohio State University laboratories, while nutrient analysis was performed both at CCIW by NWRI personnel, and at Heidelberg College, Tiffin, OH, by D. Baker. Much of the information used in this part of the project was obtained from results of the LEPF *Microcystis* collaborative research project (D. Culver, director, plus 13 other scientists) and LaMP research sponsored by grants from ODW and the Ohio EPA to the Ohio State University. Analyses performed specifically as part of this project, primarily those used in our study of vertical mixing in the central basin of Lake Erie, form about 20% of the biological data used in this project, and themselves contribute to the overall Lake Erie study initiative.

Spatial variations of phytoplankton and nutrients in the central basin were examined in 1997 for the months of May (Lake Erie central basin unstratified thermally) and August (Lake Erie central basin under strong seasonal stratification), the two time periods during which we performed vertical mixing studies in the central basin. The spatial variation in concentrations of the various nutrients and algal biomass were plotted in order to investigate whether our study site was representative of the basin as a whole during those time periods. The Great Lakes Forecasting System (GLFS) was used to examine wind fields, surface elevation, water temperature and water currents in order to insure that our sampling of mixing characteristics was spatially and temporally representative of the Lake Erie central basin.

Results and Discussion:

May Sampling Series

Total nitrogen (TN) in May, between 400 and 600 $\mu\text{g/L}$ at our site, varied little across most of the southern portion of the central basin (Figure 1.1). On the northern edge, TN was much less, between 200 and 400 $\mu\text{g/L}$ N. Near the outlets of the Grand and

Cuyahoga Rivers, there was an increase in nitrogen concentration, to as high as 1600 $\mu\text{g/L N}$, curling along the shore to the northeast due to Coriolis forces. The eastern basin ranged from 400 to 600 $\mu\text{g/L N}$ while the western basin was slightly higher, 600 to 800 $\mu\text{g/L N}$, except around the mouths of the Maumee and Sandusky Rivers, where it reached 1000 $\mu\text{g/L N}$.

Phosphorus concentrations in the central basin were low, approximately 14 $\mu\text{g/L P}$ (Figure 1.2). Along the shore to the northeast of Cleveland and the mouths of the Grand and Cuyahoga Rivers, TP was as high as 42 $\mu\text{g/L P}$, due to loading from these rivers. In addition, there appeared to be an upwelling event along the north shore, probably causing a large phytoplankton bloom that is reflected in our TP data. The eastern basin concentrations were below 14 $\mu\text{g/L P}$, while those of the western basin were higher, between 28 and 42 $\mu\text{g/L P}$.

May 1997 phytoplankton biomass data are available for the central and western basins (Figure 1.3). Central basin biomass estimates are below 1 mg wet weight/L at our study site and for much of the rest of the basin. However, at the border of the central and western basins, there was a large phytoplankton bloom, with concentrations as high as 6 mg/L. The concentrations for the western basin all exceeded 3 mg/L.

August Sampling Series

Surface TN values in August 1997 were much lower in the stratified eastern and central basins, ranging between 240 and 320 $\mu\text{g/L N}$, except along the coast to the northeast of Cleveland (Figure 1.4). The unstratified western basin ranged much higher, up to 800 $\mu\text{g/L P}$. The highest values are along the southern shore of the western basin, likely due to agricultural runoff.

TP concentrations (Figure 1.5) were very low compared with May values, ranging from 6 to 12 $\mu\text{g/L P}$ in the central basin and 6 to 9 in the eastern basin. Just as in May, values were higher to the northeast of Cleveland, reaching 18 $\mu\text{g/L P}$. In the western basin, concentrations were comparable to those in May. However, there is a much higher gradient of TP from the Maumee River, indicating that much of the TP could be in the form of agricultural runoff rather than algae (spring diatom bloom) as seen in May.

Phytoplankton levels in August were lower than those in May in the central basin (Figure 1.6), ranging from 0.5 to 0.75 mg wet weight/L. The exception was the bloom of phytoplankton (as high as 3.5 mg/L) to the west of Kelly's Island. There was very little variation in algal abundance across much of the central basin during August 1997.

Great Lakes Forecasting System Physical Data

On 23 May 1997, analysis of Great Lakes Forecasting System (GLFS) there were variations in surface temperature from inshore to offshore (Figure 1.7), but integrated vertical water velocity data indicated that horizontal water velocities at our site were negligible (<4.5 cm/s at 12:00 p.m.) (Figure 1.8), supporting our assumption of minimal horizontal advection at our site. Wave heights were less than 0.3 m throughout the entire

central basin (Figure 1.9). Water surface temperatures in the central basin were between 10 and 12 °C, except for the warmer waters in the near-shore areas to the northeast of the Grand and Cuyahoga Rivers (Figure 1.7). Our sample site (see Figure 2.1) was well beyond this irregularity.

GLFS data from August were again used to check that our site was representative of the central basin as a whole. Wave heights were less than 0.5 m (Figure 1.10) but we observed slightly higher vertically-integrated horizontal velocities on 8 August 97, ranging from 4.5 to 9.0 cm/s at our site (Figure 1.11), than those we had seen in May. Surface temperatures were uniform (between 24 and 25 °C) across the central basin but there was a prominent area of upwelling east of Long Point (Figure 1.12).

There were three main factors influencing and causing irregularities in the central basin during the two months we sampled. The first is the effects of the Grand and Cuyahoga Rivers, apparent both in May and August. Coriolis forces cause the rivers to turn clockwise upon leaving the mouths of the rivers. However, the shore interferes, causing flow to the northeast along the shore. This flow contained higher amounts of nutrients, both in May and August due to the runoff in the rivers. In fact, we observed the muddy water of the Grand River leaving Fairport Harbor (the mouth of the river) and turning to the northeast (the river flow was easily discernible from the lake water because of the muddy brown coloration). Our sample site was well beyond the possible effects of this disturbance.

The second cause of disturbance was upwelling events off Long Point in May and again in August. High TP concentrations off this point and colder surface waters indicate that it is indeed an upwelling. However, we have no phytoplankton data for this area in May to confirm this. Though water currents do flow out of this region to the southwest toward our sample site, the currents do not reach far enough to disturb it.

The last cause of disturbance noted in the central basin during May and August was the blooms of phytoplankton that are transported by currents from the western basin. The May patch (Figure 1.3), likely to have drifted longer in the central basin, is more diffuse, while the patch in August is still concentrated and on the western central basin border and has not yet progressed into the central basin proper. Though our central basin site is clearly not representative of the whole lake, its horizontal and temporal variation in chemical, biological and physical dynamics are characteristic of the central basin for May and August 1997.

Objective 2) Quantify vertical mixing rates at sites in the Lake Erie central basin

Introduction

The extent and intensity of vertical mixing in the water column is dependent on the strength of vertical density gradients within the water column, as well as on the local sources and sinks of turbulent kinetic energy (TKE). For example, shear stress applied to the surface by wind is a source of TKE while the water's viscosity acts as a sink of TKE, dissipating some of the energy through heat. Where the net amount of TKE is the mechanism for mixing, a vertical density gradient acts as a stabilizing element and hinders mixing.

The sources and sinks that contribute to or hinder mixing may vary temporally, occurring over a range of time scales from minutes to months. For example, the lake's structure changes seasonally from a nearly uniform density through the cooler months of the year to a strongly stratified structure, which reduces mixing during the warmer summer months. A similar process occurs daily as the lake surface is heated throughout the daylight hours, forming a diurnal thermocline. During the night, the surface again cools, resulting in complete or partial mixing of this diurnal thermocline. The seasonal thermocline is, in fact, the net result of these daily inputs of heat over the whole summer.

In addition to temporal variation, the sources and sinks of TKE vary spatially. At the surface, mechanisms for mixing include wind-induced shear and penetrative convection due to surface cooling and the formation of an unstable density gradient. At the bottom of the well-mixed epilimnion, in the presence of a strong thermocline, we see more shear induced turbulence. In this case, as in the above wind-induced mixing, shear instabilities provide a source of TKE, which leads to entrainment of the underlying water into the surface layer. At the same time, the density gradient resists mixing and much of the TKE provided by shear is dissipated without producing active mixing. Using water temperature as a tracer, we can measure the amount of the TKE being dissipated and use this value to calculate a vertical diffusivity coefficient, K_z that varies with depth. This vertical diffusivity coefficient can be used with concentration gradients to calculate fluxes of nutrients, oxygen, phytoplankton or any other constituent that is convected along with the fluid motion.

The sampling site:

The data were collected from the central basin of Lake Erie, the largest (16,425 km²) of the three lake basins. The topography is relatively uniform with a mean depth of 18.3 m and a maximum depth of 25 m. The physical dynamics of the central basin are different from the well-studied western basin, which is shallower and tends to remain well-mixed for most of the year. The structure of the temperature stratification in the central basin frequently leads to late summer deoxygenation of the hypolimnion.

Within the central basin we chose a sampling site corresponding to a grid point used by the Ohio Department of Natural Resources in their ongoing trawling studies of sport fish species (see Figure 2.1). As such, we have historical phytoplankton and zooplankton data

to incorporate into our efforts. A station five miles from the coast was chosen in order to avoid any near-shore current effects, which would make the primary assumption of this study, horizontal homogeneity, invalid. All sampling was conducted at this point, longitude west 81° 18' 10.7" latitude north 41° 51' 0.8" at a depth of approximately 21 m.

Methods

The data were collected using a free-falling instrument designed by Precision Measurement Engineering called a Self -Contained Autonomous Microprofiler (SCAMP) (Figure 2.29). The SCAMP falls through the water column at 10 cm/s and samples at 100 scans/s, giving a resolution of 1 mm throughout the profile. The main sensors include fast and slow response thermistors, a fast dissolved oxygen probe, a pressure transducer to determine depth, and a miniature fluorometer (Figure 2.2). The manufacturer calibrated the temperature probes. Therefore it was only necessary to calibrate the dissolved oxygen sensor and the fluorometer. The oxygen sensor was calibrated by recording the sensor output when placed in water of known temperature and oxygen concentration (via Winkler titration) and varying (separately) the oxygen and temperature. This allowed for accurate oxygen measurements in situations where the temperature and oxygen concentrations varied widely (as in the stratified central basin in August). The fluorometer was calibrated by measuring chlorophyll *a* values along with the voltage outputs of the fluorometer and fitting them to a third-order polynomial.

The SCAMP was deployed approximately hourly during daylight hours for a week in May 1997, just as the lake was beginning to form a seasonal thermocline and again for a week in August 1997 after a strong stratification had developed (Figures 2.3 and 2.4). This frequent sampling of the water column allowed us to study the development of the diel thermocline and the effects of varying wind velocity.

In order to calculate the vertical transport in the central basin, it is necessary to calculate the turbulent eddy diffusivity, K_z . In order to calculate K_z , two quantities must be known: 1) the flux Richardson number, R_f , and 2) the turbulent energy dissipation, ϵ . The flux Richardson number is defined as the ratio of buoyancy flux to the turbulent production. Thus, it relates the turbulent displacement of less dense (warmer) water down into more dense (cooler) water versus the buoyancy that counteracts it. Ellison (1957) obtained R_f approximations from laboratory experiments, which have been found to be accurate in most cases (Ivey and Imberger 1991). Therefore we calculated the buoyancy flux from the R_f for use directly in the estimation of K_z .

The turbulent energy dissipation, ϵ , can be calculated with the use of the Batchelor Spectrum (Batchelor 1959), which is the theoretical spectrum of a dynamically passive, conservative, scalar quantity (such as temperature) at large wave numbers. As suggested above, we have assumed that the temperature field of a fluid in turbulent motion acquires the same statistical properties as the fluid itself. The Batchelor spectrum takes into account the effects of convection with the mean fluid motion as well as molecular diffusion. In our case, we used temperature as a tracer quantity to derive a fit between the

turbulence sampled by the microprofiler and a nondimensional form of the Batchelor spectrum and then used the theoretical spectrum to describe the turbulence and to calculate the TKE dissipation, ϵ . The method used compared temperature gradient spectra to the Batchelor spectrum of temperature gradient fluctuations (Caldwell et al. 1980, Dillon and Caldwell 1980). The fit to the spectrum was done as a nonlinear, weighted least-squares fit. After determining if, indeed, we have a stationary turbulence patch, the theoretical spectrum can be used to find the cutoff wave number, k_c . This number was then used to calculate ϵ as in Dillon and Caldwell (1980). The eddy diffusivity, K_z , was then calculated using the method described by Imberger and Ivey (1991), a modification of Osborn's (1980) method, where K_z is the ratio of the buoyancy flux b (evaluated from R_f and ϵ) to the buoyancy frequency squared, N^2 .

Results

On 23 May 97, the water column was weakly stratified (Figures 2.5-2.14). The day was calm, partially overcast during the morning, but by 9:30 am when we began sampling, the sky had begun to clear, initiating the formation of a diurnal thermocline approximately 1 m beneath the surface (Figure 2.5). Figure 2.5 and the succeeding figures like it have three separate, but related, parts. First, the solid line indicates the temperature ($^{\circ}\text{C}$), with the scale given across the top axis. The TKE dissipation (ϵ) is displayed as solid bars (m^2s^{-3}), with a logarithmic scale displayed across the bottom axis. The width of the bars indicates the width of the segment of TKE dissipation in terms of depth (m, on the left axis). Overturns, the third quantity represented, were too small at 9:30 am to be displayed on the figure except for a small layer at approximately 1 m from the surface.. Both TKE dissipation and overturns are necessary to produce turbulent mixing, which is indicated by the eddy diffusivity (K_z) versus depth (Figure 2.6). Due to waves of less than 0.3 m height and wind under 4.1 m/s, there is virtually no mixing taking place. As the day progressed, the wind speed remained steady at 4.1 m/s, but wave height increased slightly.

In the subsequent profiles (Figures 2.7-2.14) dissipation is occurring primarily, though not exclusively, at three places: at the surface ($\approx 10^{-9} \text{ m}^2\text{s}^{-3}$), at the deeper seasonal thermocline (at 10-12 m) ($\approx 10^{-10} \text{ m}^2\text{s}^{-3}$), and at the bottom ($\approx 10^{-9} \text{ m}^2\text{s}^{-3}$). Though TKE dissipations are present in three locations in the water column, overturns are only evident near the surface. As the day progressed (Figures 2.9, 2.11, 2.13), TKE dissipations and overturns continued to increase near the surface. These combine to produce increasing diffusivities in the upper 2 m of the water column (Figures 2.10, 2.12, 2.14). Furthermore, the diurnal thermocline is progressively moving deeper as more solar energy heats the surface, and wind causes mixing (the odd-numbered series of Figures 2.7-2.13). Thus, we are witnessing the formation of the wind-mixed layer described by Ivey and Imberger (1991). Though TKE dissipation is occurring at various depths throughout the water column, mixing is only evident at the surface on this relatively calm day (the even series of Figures 2.6-2.14).

In the presence of strong, seasonal stratification, the lake's diurnal processes stay much the same (Figures 2.15-2.22). On 8 August 97, when the lake had become strongly stratified, we began sampling at 6:30 am, in order to observe processes at work before the sun rose (Figure 2.15). A large amount of mixing is present in the epilimnion, most likely due to penetrative convection (Figure 2.16). However, the falling plumes are not energetic enough to cause mixing across the thermocline by entraining water from the hypolimnion. Diffusivity values as high as $0.042 \text{ m}^2/\text{s}$ persist until almost 9:00 am (Figures 2.16, 2.18 and 2.19). On this day, the morning was calm with negligible wind and waves. However, a 2.6 m/s wind developed, causing a small wind-mixed layer to develop by 11:30 am (Figure 2.20). The weather conditions remained constant throughout the day, and again TKE dissipation became weak throughout the water column except at the surface, at the bottom and at the thermocline. In Figures 2.19 and 2.21, there are high TKE dissipation values across the thermocline, as well as small mixing events just under the thermocline. This provides evidence of a strong bottom current eroding the thermocline from below. This unusual phenomenon was identified by Blankton and Winklhofer (1972) and later by Ivey and Boyce (1982). It is suspected that the presence of such a thin layer metalimnion causes a strong bottom current as the lake oscillates back and forth, as basically a two-layered system.

Mixing During Storms

The two storm events encountered on 21 May and 6 August 1997 were of approximately the same magnitude, both lasting about 24 hours with wind speeds of 23 knots. The presence of strong thermal stratification during the August storm event, but not in May, causes the resulting mixing to be very different in the two events. The 21 May 1997 storm registered winds of 23 knots out of the northwest for most of the day and night before. Wave height was between 1.5 and 2.1 m and the sky was overcast. Due to the weather conditions, we were able to make only one cast of the SCAMP (Figures 2.23 and 2.24) before it became unsafe. The water column was very active, with TKE dissipations reaching $1.8 \times 10^{-6} \text{ m}^2/\text{s}^3$ at a depth of 2 m. The temperature profile is almost uniform from top to bottom and two large overturns may be observed as deep as 10 m (Figure 2.23). The resulting diffusivities reach $8.1 \times 10^{-3} \text{ m}^2/\text{s}$. A small gradient is barely detectable at 10 m, just below the deepest overturns.

On 5 August 1997, the weather conditions were much the same, but with wind out of the northeast. This wind direction allows for a much longer fetch and, therefore, much more violent surface conditions. The resulting 2.4 to 3.0 m waves precluded any sampling during the storm. Profiles taken before (Figures 2.25-2.26) and after the storm (Figures 2.27-2.28) show a definite sharpening of the metalimnion as a result of the storm. The thermocline is at 14.5 meters prior to the storm, with the metalimnion extending from 13.5 m to 16 m from the surface (Figure 2.25). At this time, the storm was already developing, with 17 knot winds out of the northeast and 0.9 to 1.2 m waves, causing the water column to become very active above the thermocline, similar to the May storm event, but calm below the thermocline (Figure 2.26). Following the storm event, the thermocline was at 15 m, with a metalimnion less than 1 m thick (Figure 2.27). This suggests that the thermocline was eroded from both the top and the bottom, perhaps from

strong shear generated by the internal seiche. No mixing is evident below the thermocline, but for two days following the storm (Figures 2.28 and 2.14) we see evidence of mixing occurring just below the thermocline in the presence of a sharp temperature gradient.

Discussion

Four physical processes can be identified from the profiles taken in the central basin of Lake Erie during May and August of 1997. These four processes include wind-induced surface mixing, penetrative convection, and two forms of shear-induced mixing: above the thermocline at the base of the epilimnion and below the thermocline at the base of the hypolimnion.

At the surface, wind blowing across the water exerts a drag on the water surface. This drag generates turbulence, which is exported downward through turbulent diffusion. Rates of turbulent diffusion in this region of the water column were generally similar in May and in August. Turbulent diffusivities were found as high as $3.1 \cdot 10^{-4}$ in the presence of a weak, 6 knot wind (Figure 2.14) and as high as $3.9 \cdot 10^{-2}$ during a storm event with winds reaching 23 knots (Figure 2.24).

Production of the wind-mixed surface layer is most apparent in the presence of a small temperature gradient (Figure 2.29). Consecutive SCAMP temperature profiles, offset by 0.5°C , illustrate the deepening of the mixed layer. The relative temperature axis shows the scale of the temperature variations in a single profile, but the 0.5°C offset must be applied when comparing consecutive profiles. The temperature profile taken at 1558 (3:58 PM) shows a large inversion at the surface, indicated by an increase in temperature from the surface down to 4 m. Thus, we have slightly colder water on top of warmer water, and therefore an unstable water mass from the surface to almost 4 m. Subsequent profiles show the wind-driven turbulence transported downward over time. The small temperature gradient is deepened and sharpened as the turbulence propagates and entrains the underlying water. Over a 2 h period, the gradual temperature gradient is replaced by a sharper, deeper temperature gradient, which separates the well-mixed surface region from the rest of the water column.

Daytime heating and nighttime cooling in the atmosphere cause penetrative convection, generating diurnal temperature fluctuations at the water surface. During the day, the surface of the water column is heated, creating stable density stratification. At night, however, the water surface radiates heat to the cooler atmosphere. This surface cooling causes the surface water to become unstable, creating negatively buoyant plumes that fall in the water column causing mixing. This process is called penetrative convection and is an important contributor to the daily mixing of the epilimnion. At the base of the epilimnion, the plumes encounter resistance from density stratification in the metalimnion. At this point, whatever TKE that has not been dissipated by inducing mixing as it falls can deepen the epilimnion. In our SCAMP profiles, falling plumes can be seen as overturns and the progression of the plumes falling over time can be viewed from one profile to the next (Figures 2.17, 2.19). The plumes have insufficient energy to

penetrate the thermocline and thus do not contribute to mixing across the thermocline, remaining isolated in the epilimnion (Figures 2.18 and 2.20).

Shear-induced mixing, generated at the base of the epilimnion, is likely the result of shear instabilities produced by the presence of a velocity gradient across a density interface. This physical process only occurs in the presence of a strong, well-defined thermocline where the magnitude of TKE dissipation is directly proportional to the strength of the density gradient. This occurs because larger density gradients can maintain larger velocity differences across the thermocline, causing the lake to act as a two-layer system. Both larger velocity differences and stronger stratification contribute to increased TKE dissipation. Therefore this process is evident in summer when a strong seasonal thermocline has formed and is magnified by seiche activity in the lake caused by random storm events. Whereas TKE dissipation is directly proportional to both the strength of the density gradient and the velocity difference across the thermocline, the resulting turbulent diffusion is inversely proportional to the strength of the density gradient, because the turbulence is formed by entrainment of underlying water into the epilimnion. If the turbulence is not energetic enough to overcome the stable density gradient and cause entrainment, the TKE is dissipated.

In the presence of weak stratification on a calm day (Figures 2.4-2.14), there is little TKE dissipation (on the order of $10^{-9} \text{ m}^2\text{s}^{-3}$) and there is no mixing. In the presence of strong stratification on a calm day, the TKE dissipation is much higher (on the order of $10^{-7} \text{ m}^2\text{s}^{-3}$), but still causes no mixing as the strong stratification resists entrainment of the underlying waters. Mixing only occurs prior to (and presumably during) the late summer storm event (Figure 2.26). In this case, the mixing is strong enough to cause entrainment of the underlying waters.

Just as shear-induced mixing occurs at the base of the epilimnion, it also occurs in the hypolimnion. However, the mixing is not isolated to just below the thermocline. It extends as far as 2 m below the thermocline (Figures 2.19-2.22), suggesting that processes other than shear production at the density interface may be involved in the mixing events. Ivey and Imberger (1991) and Thorpe (1987) speculate that such turbulence may be due to a focusing of kinetic energy, by internal wave motion. Many processes have been identified as possible sources of the kinetic energy, including wave-shear instabilities, wave-wave instabilities, and convective instabilities. Convective instabilities can be ruled out, as mentioned above, because penetrative convection cannot penetrate a strong density gradient (i.e. the thermocline). This hypolimnetic mixing is persistent during strong stratification, producing diffusivities as high as $3.4 \times 10^{-7} \text{ m}^2/\text{s}$.

Objective 3) Measure the effects of turbulent mixing on the vertical fluxes of nutrients and phytoplankton

Introduction

The impact of changes in the biological and chemical character of Lake Erie on the ecosystem as a whole has been subject to significant debate. For example, based on estimates of population densities and grazing rates, researchers have speculated that zebra mussels could theoretically remove all the algae from the entire western basin in less than one day, or even upwards of 18 times per day (MacIsaac et al. 1992). Lower phosphorus loading since 1970 is correlated with declines in algal abundance. However, although phytoplankton abundance is now lower than it was before zebra mussels invaded and cyanobacterial blooms are rare, the pre-zebra mussel seasonal algal succession patterns have persisted (Wu and Culver 1991). Hence, zebra mussel filtration has not completely overwhelmed phytoplankton production and suggests zebra mussel consumption rates are limited by physical factors such as the rate of delivery of algae to the bottom. Feeding rate estimates such as those of MacIsaac et al. (1992) have generally been based on laboratory work with well-mixed tanks rather than on more realistic *in situ* field studies. These laboratory studies do not take into account the algal delivery rates from the surface to the benthos, or to the implications of the mussels' re-filtering the same water they, or adjacent mussels, had already cleared of algae.

Thus, while there has been a large quantity of research devoted to understanding the biological processes in Lake Erie, there has been little research devoted to the study of the effect of the physical dynamics of the lake on those processes. With effort being devoted to the management of Lake Erie by both the U.S. and Canada by such agencies as the Ohio Division of Wildlife, the Ohio EPA, the USEPA, the International Joint Commission on the Great Lakes, the Great Lakes Fishery Commission, The Canadian National Water Research Institute, the Canadian Department of Fisheries and Oceans, and the Ontario Ministry of Natural Resources, it is important to understand the lake dynamics through the modeling of the lower trophic levels that are central to the Lakewide Management Plan program (LaMP). However, if research fails to include the effects of physical processes, the present models (i.e. the Lake Erie Ecosystem Model-LEEM by Joseph Koonce, CWRU) will always be limited in their usefulness both as management tools and as a means to further our basic understanding of the lake ecosystem. For example, the western basin of the lake is commonly thought to be completely mixed, and many estimates of zebra mussel grazing (e.g., MacIsaac *et al.* 1992) have been based upon this assumption. However, the western basin has been shown to have temperatures that vary as much as 1-2°C (Pontius and Culver, unpublished data), indicating the water column is not so completely mixed as has been assumed. Although relatively small, temperature differences of this magnitude can significantly influence the rate of turbulent mixing in the water column, as we have already seen in the central basin.

Methods

Turbulent mixing is measured by two basic features: 1) the turbulent diffusivity, K_z , and 2) the movement of materials caused by the mixing. In order to determine the movement, or flux, of material down its concentration gradient, the equation

$$J = K_x \partial F / \partial x + K_y \partial F / \partial y + K_z \partial F / \partial z \quad (1)$$

where J is the flux through a point, K_x and K_y are the horizontal eddy diffusivities, $\partial F / \partial x$ and $\partial F / \partial y$ are the horizontal gradients, K_z is the vertical diffusivity, and $\partial F / \partial z$ is the vertical concentration gradient. If we assume that the horizontal gradients are negligible (which we investigated in Objective 1), the equation simplifies to:

$$J = K_z \partial F / \partial z \quad (2)$$

Thus, if we know K_z , we will be able to determine the flux of a solute, F , by determining the concentration gradient.

In order to find this concentration gradient in the solutes of interest (i.e. chlorophyll a , phosphorus and nitrogen), we sampled them concurrently with physical (SCAMP) sampling in May and August (Objective 2). We sampled the gradients approximately every two hours with a twelve-channel water sampler deployed on the bottom of the lake, sampling every 5 cm near the bottom, and every 25 or 50 cm further up, to 300 cm above the sediment-water interface. In addition, Van Dorn water bottle samples were taken at 1-m intervals throughout the water column each day of the sampling period. D. Baker (Water Quality Lab, Heidelberg College) analyzed nutrient concentrations from both these sets of water samples. Algal biomass was enumerated at our Ohio State University laboratories. Fluorescence was sampled using the miniature fluorometer on the SCAMP. Fluorescence was calibrated to chlorophyll a vertical distribution samples analyzed via spectrophotometry.

We fit polynomials to concentrations of nutrients (Total N and Total P) and chlorophyll α (from fluorescence data) as a function of depth and calculated first-order derivatives to obtain the concentration gradients. Because we had fluorescence data for each 4 mm interval, we fit their polynomials by segments throughout the water column (between 30 and 80 segments per profile, depending upon its variability).

We combined the nutrient and chlorophyll a gradients with the physical SCAMP data to produce fluxes with respect to depth. We evaluated the gradients in depth segments corresponding to those for which we had diffusivity (K_z) values. We then combined these, as in equation (2), to produce flux values. Even extreme gradients do not produce fluxes (beyond molecular diffusion) without eddy diffusivities to drive them.

Results

Profiles from 23 May 1997 show decreased chlorophyll *a* in the upper epilimnion, with an increase to a maximum at between 10 and 13 meters (Figure 3.1). This corresponds to the slight seasonal thermocline (Figure 2.7) and even this 0.25 °C change appears to be enough to inhibit nutrient transport to the epilimnion in the absence of strong mixing, demonstrated by the low chlorophyll concentrations near the surface (between 0 and 0.05 mg/m³). The chlorophyll *a* concentrations represented two main groups of algae: the chrysophytes (i.e. the diatoms) and the cryptophytes (i.e. *Cryptomonas* spp. and *Rhodomonas* spp.) (Figure 3.2). Algal biomass in the epilimnion ranged from 0.1 mg wet weight/L at the surface to between 0.4 and 0.6 mg/L at the base of the epilimnion. Beneath the thermocline (10-13 m) algal biomass increased to as high as 0.8 mg/L. Figure 3.3 shows the gradient, and the rate of change of chlorophyll concentrations with respect to depth. The gradients are positive to 10 m, indicating that there are increasing amounts of chlorophyll as depth increases. However, once beneath the seasonal thermocline (13 m), there is wide variation in the gradient, corresponding to local chlorophyll maxima and minima that we were able to observe with the fine scale resolution of the SCAMP fluorometer (1 cm, 4 cm after filtering the data to remove noise). When these data are combined with the eddy diffusivity (Figure 2.8), we can find the flux in chlorophyll *a* with respect to depth in mg/m²/s (Figure 3.4). Positive numbers indicate fluxes down the water column, negative up. There is some correspondence between the eddy diffusivity (Figure 2.8) and the chlorophyll *a* flux (Figure 3.4). However, there is a large flux at just below, but not penetrating, the thermocline (Figure 3.4), whereas the eddy diffusivity is too small to appear on Figure 2.8. Due to the very large chlorophyll concentration gradient at this depth (Figure 3.3), this small diffusivity translates into a large flux of chlorophyll. Succeeding fluxes are summarized in Table 3.1.

As wave height increased from morning until evening on 23 May 1997, a relatively calm day, so did the fluxes of chlorophyll in the surface waters (Table 3.1). However, the numbers are extremely variable. The absence of detectable turbulent mixing at the base of the hypolimnion resulted in no flux of chlorophyll into or out of the sediment at any time during the day. In the metalimnion, there was detectable mixing only at 11:25 am causing a flux of chlorophyll from the hypolimnion across the weak thermocline. Because we sampled nutrients at this time, we combined these SCAMP data with our nutrient gradient measurements to calculate nutrient fluxes. Metalimnetic turbulent mixing, detected only once in our 23 May sampling, thus is driving the flux of nutrients across the thermocline and must be assumed to be very sporadic on such a calm day. The fluxes of both TP and TN (on the order of 10⁻⁷ and 10⁻⁶ mg m⁻²s⁻¹) were in a positive direction, indicating a flux out of the hypolimnion into the nutrient poor epilimnion.

For the 8 August 1997 sampling we were able to begin early enough in the day to find evidence of penetrative convection, which is primarily a nighttime phenomenon. This caused fluxes one order of magnitude higher than anything we found in May (Table 3.1). We observed fluxes of chlorophyll both in the lower epilimnion toward the surface and in the thermocline out into the metalimnion. The plumes of cold water that caused the

penetrative convection did not penetrate the thermocline into the hypolimnion, so the small fluxes from the metalimnion originated in the layer just above the hypolimnion, not within it. By 10:00 am, the fluxes of nutrients were much reduced in the surface waters, resulting from the lack of wind and wave action, though at all times these were greater than those in May. By noon, there were measurable nutrient fluxes resulting from wind-driven mixing in the surface waters, although by this time penetrative convection had ceased due to solar heating of the surface waters. Local TP and TN fluxes in the top 1 m caused a net flux of nutrients back down into the water column. Although there was no net flux of nutrients across the thermocline there was both regeneration of TP from the sediment and a flux of TN into the sediment. These fluxes were caused by turbulent mixing generated from shear along the bottom and resulted in mixing of nutrients within, but not transport out of, the hypolimnion.

Two storm events, on 21 May and 4 August 1997 resulted in very high wind-driven diffusivities in the surface waters. As a result, fluxes of chlorophyll were also extremely high (Table 3.1). They were also extremely variable, with local chlorophyll minima and maxima causing fluxes both up and down in the water column at extremely high rates. In the August storm, the wind and waves were out of the northeast, and thus with (instead of across) the major axis of the lake, and thus created greater maximum fluxes and generally more mixing. However, neither storm penetrated the hypolimnion nor caused mixing across the thermocline. In addition, as strong as the fluxes caused by the storms were, in both cases they were comparable to the mixing caused by penetrative convection on a completely calm night.

Discussion

There were three primary regions in which there was a measurable flux of nutrients within the water column, corresponding to the four types of mixing found at our sample site in May and August 1997 (Objective 2). At the surface, both penetrative convection and wind/wave-driven mixing dominate. At the bottom of the epilimnion, shear causes fluxes as the epilimnion and the hypolimnion move in different directions. Finally, at the base of the hypolimnion, bottom currents create shear, which regenerates nutrients from the bottom and mixes the hypolimnion.

Surface mixing caused by wind/wave action is strongly influenced by weather conditions. On calm days (e.g. 23 May and 8 August), in the absence of penetrative convection, the fluxes of chlorophyll *a* are on the order $0.1 \text{ mg m}^{-3} \text{ sec}^{-1}$ in the surface waters (Table 3.1), an order of magnitude less than the fluxes caused by the storm events on 21 May and 4 August. These numbers represent chlorophyll *a* fluxes toward the surface of the water at a rate of approximately $10 \text{ to } 100 \text{ g m}^{-2} \text{ day}^{-1}$, depending on the weather conditions. However, there is a no-flux boundary at the surface (algae cannot fly), so either 1) there is a chlorophyll sink near the surface (i.e. zooplankton grazing or decreased production due to surface nutrient depletion); or 2) the conditions are temporary, and when our 200 sec snapshot of the water column is over, the conditions could change. However, because the flux of algae toward the surface is evident on all our sampling dates, we believe that (2) is unlikely. Since large zooplankton (e.g. *Daphnia*) that consume most of the algae are

typically found in the deeper waters during the day, it is likely that the flux of chlorophyll towards the surface represents a net loss of algae at the surface caused by decreased algal production.

Nutrient fluxes were observed down from the surface, but within the epilimnion, during both sampling periods, perhaps representing photoinhibition of the phytoplankton in the top 0.5 m of the water column. This is the only point at which both TN and TP gradients were negative, toward the benthos. Photoinhibition could cause decreased algal production in the top 0.5 m, especially on calm days when there are no turbulent convection cells to mix the algae away from the surface. Decreased production would result in decreased nutrient uptake, which could explain the gradients we observed during our 12:00 PM samples.

Earlier in the morning, we expect there would be little or no gradient due to the overnight penetrative convection that would thoroughly mix the upper layers of the epilimnion. The fluxes of nutrients caused by nightly penetrative convection caused much higher fluxes of chlorophyll *a* than any other factor except the storms. Fluxes on the order of $10 \text{ g m}^{-2} \text{ d}^{-1}$ were observed throughout the entire epilimnion. Though the convection cells did not cause release of nutrients from the hypolimnion, the upper, well-mixed epilimnion stays well-mixed due to nightly penetrative convection in addition to random storm events. Unfortunately we were unable to measure nutrient gradients during storm events.

Though shear at the base of the epilimnion is evident from the continuous TKE dissipations in the metalimnion, rarely do these dissipations translate into turbulent mixing across the thermocline. In fact, at only one time on 23 May did we observe this. Thus, though we can translate the fluxes of TP and TN into $0.02 \text{ mg m}^{-2} \text{ day}^{-1}$ P and $0.20 \text{ mg m}^{-2} \text{ day}^{-1}$ N respectively, it is not appropriate to extrapolate in this manner. Instead, we must assume a two-layer system connected only by molecular diffusion even during periods of weak stratification.

Shear at the base of the hypolimnion, however, may be more important for nutrient regeneration. Bottom currents, caused by seiches and internal waves in the two-layer system, cause turbulence due to the velocity differences of the water and the bottom of the lake. This results in both the mixing of nutrients within the hypolimnion and regeneration of phosphorus from the sediment. Phosphorus regeneration was on the order of $1 \text{ g m}^{-2} \text{ day}^{-1}$ and was persistent across all strong-stratification. With a central basin area of $16,425 \text{ km}^2$ this results in 16,425 tonnes of phosphorus regenerated into the hypolimnion each day.

Objective 4) Adapt the results for use in models of the effects of P and N loading and cycling on the production of phytoplankton and fish.

Introduction

Mathematical models, with their potential to help us understand and predict changes in Lake Erie, have been used in management of the lake since the 1970s (DiToro et al. 1975); however, phosphorus loading has decreased by 75% and zebra mussels have been introduced into the lake since their models were written. New computer models to assist Lake Erie management are needed to address ecosystem change caused by these changes in system parameters. Constructing such a model requires: 1) understanding of the trophic interactions among nutrients, algae, zooplankton, and fish, 2) understanding of the physical processes that affect the horizontal and vertical transport of nutrients and algae in the lake, and 3) knowledge of the temporal and 3-dimensional spatial variation in the abundances of nutrients and lower trophic level biotic components on which these physical processes act.

Trophic interactions among nutrients, algae, zooplankton and fish are currently being investigated on several levels. We are collaborating with researchers at the National Water Research Institute (Canada) and the University of Toronto (Canada) to investigate the effects of nutrient loading changes and zebra mussel introduction on the lake in a project funded the Ohio Sea Grant College Program. We are comparing the results of ecological models and fluid mechanics models using combined monthly estimates of phosphorus and nitrogen loading as forcing functions (1970 to present). Observed nutrient changes will be correlated with plankton abundance data from both historical sampling and western basin samples from 1995-1998. Physical models of lake circulation will be combined with spatial and temporal variations identified by the Great Lakes Forecasting System (GLFS) to integrate physical and biological processes in the lake. In addition, this project will attempt to estimate the changes in nutrient regeneration caused by zebra mussels in the western basin and the effects expansion of mussels will have on that internal source of loading.

A second project, funded by the LEPF, "Calibration of Lake Erie foodweb models with field data", has just begun, and also investigates lower trophic level dynamics. This focuses not only on the nutrient/zebra mussel effects on the lake, but will combine these results with models of the biotic components of the lower trophic levels, including phytoplankton, zooplankton and protozoa. Physical components include light intensity, turbidity, photoperiod and temperature, as these are all major forcing functions on the lake. This model is being calibrated with field data from 1995-1997.

Methods

The current LEPF project addressed the last of the three problems in Lake Erie modeling identified above: the physical process of vertical mixing. We have calculated eddy diffusivities (Objective 2) at a location that reflects the majority of the central basin in physical, chemical and biological factors (Objective 1). We obtained seasonal information on changes in this mixing, comparing May versus August changes in diel

mixing (from nightly penetrative convection to daily generation of wind-mixed layers) and the impacts of storm events relative to other forms of mixing. We used these diffusivities to calculate fluxes in both nutrients and chlorophyll within the epilimnion, between the epilimnion and the hypolimnion, and regeneration from the sediments (Objective 3). With these flux estimates, we are able to address the problem of vertical mixing within the central basin and apply our results to the other two modeling efforts mentioned above. This application will have two primary components: 1) we will use our estimates of nutrient regeneration from the sediments to quantify this source of internal loading in the central basin and 2) although we have identified that in strong stratification, little mixing occurs across the thermocline, we have observed that it does occasionally occur (Objective 3) and will use this information to estimate fluxes of nutrients and phytoplankton into the light-rich epilimnion. Both of these factors will have a profound impact on the estimation of primary productivity within the models. In addition, we are combining these results with information on the impacts of zebra mussel grazing obtained in field experiments (1995). With these data, we are estimating phytoplankton fluxes into the benthic boundary layer, where the algae are consumed by the zebra mussels, in relation to various weather conditions. We will therefore be able to more accurately estimate how the zebra mussels act as a phytoplankton sink within the western basin.

LITERATURE CITED

- Batchelor, G. K., 1959. Small-scale variations of convected quantities like temperature in turbulent fluids. *J. Fluid Mech.* 5:113-133.
- Blankton, J. O., and A. R. Winkhofer, 1972. Physical processes affecting the hypolimnion of the Central Basin of Lake Erie. In *Project Hypo*, N. M. Burns and C. Ross, pp 9-38. Paper No. 6. Canada Centre for Inland Waters, Burlington, Ontario. USEPA Tech. Rept. TS-05-71-208-24.
- Caldwell, D. R., T. M. Dillon, J. M. Brubaker, P. A. Newburger, and C. A. Paulson, 1980. The scaling of vertical temperature gradient spectra. *J. Geo. Res.* 85: 1910-1916.
- Dillon, T. M., and D. R. Caldwell, 1980. The Batchelor Spectrum and dissipation in the upper ocean. *J. Geo. Res.* 87: 9601-9613.
- DiToro, D., D. J. O'Connor, R. V. Thomann, and J. L. Mancini. 1975. Phytoplankton-zooplankton-nutrient interaction model for western Lake Erie, pp. 424-473. In B. C. Patten (ed.) *Systems Analysis and Simulation in Ecology*, Vol. III.
- Ellison, T. H., 1957. Turbulent transport of heat and momentum from an infinite rough plane. *J. Fluid Mech.* 2:456-466.
- Heath, R. T., G. L. Fahnenstiel, W. S. Gardner, J. R. Johnson, R. H. Sada, J. F. Cavaletto, and S-J. Hwang, 1995. Ecosystem-level effects of zebra mussels (*Dreissena polymorpha*): an enclosure experiment in Saginaw Bay, Lake Huron. *J. Great Lakes Res.* 21: 501-516.
- Ivey, G. N., and F. M. Boyce, 1982. Entrainment by bottom currents in Lake Erie. *Limn. Oceanogr.* 27: 1029-1038.
- Imberger, J. and G. N. Ivey. 1991. On the nature of turbulence in a stratified fluid. 2. Application to lakes. *J. Physical Oceanography* 21:659-680
- Ivey, G.N. and J. Imberger. 1991. On the nature of turbulence in a stratified fluid. 1. The energetics of mixing. *J. of Physical Oceanography* 21:650-658
- Janus, L. L. and R. A. Vollenweider, 1981. The OECD co-operative programme on eutrophic: Summary report: Canadian Contribution. Nat. Water Res. Inst., Canada Centre for Inland Waters, Sci. Ser. No. 131, 131-S (Background data supplement). Burlington, Ontario.
- MacIntyre, S. 1993. Vertical mixing in a shallow, eutrophic lake – possible consequences for the light climate for phytoplankton. *Limnology and Oceanography* 38:798-817

MacIsaac, H. J., W. G. Sprules, O. E. Johansson, and J. H. Leach, 1992, "Filtering impact of larval and sessile zebra mussels (*Dreissena polymorpha*) in western Lake Erie," Oecologia 92:30-39.

Osborn, T. R., 1980. Estimates of local rates of vertical diffusion from dissipation measurements. *J. Physical Oceanography* 10:83-89.

Thorpe, S. A., 1987. Transitional phenomena and the development of turbulence in stratified fluids: a review. *J. Geo. Res.* 92:5231-5248.

Wu, L., and D. A. Culver. 1991. Zooplankton grazing and phytoplankton abundance: An assessment before and after invasion of *Dreissena polymorpha*. *J. Great Lakes Res.* 17(4): 425-436.

Table 3.1 Flux estimates in three depth zones of the central basin of Lake Erie for chlorophyll *a*, total phosphorus, and total nitrogen for two calm days (23 May and 8 August 1997) and two storm days (21 May and 4 August 1997). Positive fluxes represent fluxes toward the bottom of the lake, while negative fluxes are toward the surface.

Date	Solute	Time	Flux ($\text{mg m}^{-2}\text{s}^{-1}$)		
			Surface	Metalimnion	From sediment
23-May-97	Chlorophyll <i>a</i>	11:25	0.03	0.05	0
23-May-97	Chlorophyll <i>a</i>	13:26	0.2	0	0
23-May-97	Chlorophyll <i>a</i>	15:58	0.07	0	0
23-May-97	Chlorophyll <i>a</i>	17:39	0.3	0	0
23-May-97	TP	12:00	-1.00×10^{-7}	2.50×10^{-7}	0
23-May-97	TN	12:00	-5.00×10^{-7}	2.25×10^{-6}	0
8-Aug-97	Chlorophyll <i>a</i>	6:37	3.5	0.02	0
8-Aug-97	Chlorophyll <i>a</i>	10:00	0.8	0.05	0
8-Aug-97	Chlorophyll <i>a</i>	13:29	1	0	0
8-Aug-97	TP	12:00	-1.00×10^{-4}	0	4.50×10^{-5}
8-Aug-97	TN	12:00	-2.00×10^{-3}	0	-1.30×10^{-3}
21-May-97	Chlorophyll <i>a</i>	12:28	3.5	0	0
4-Aug-97	Chlorophyll <i>a</i>	12:43	4.8	0	0

May 1997 Total Nitrogen

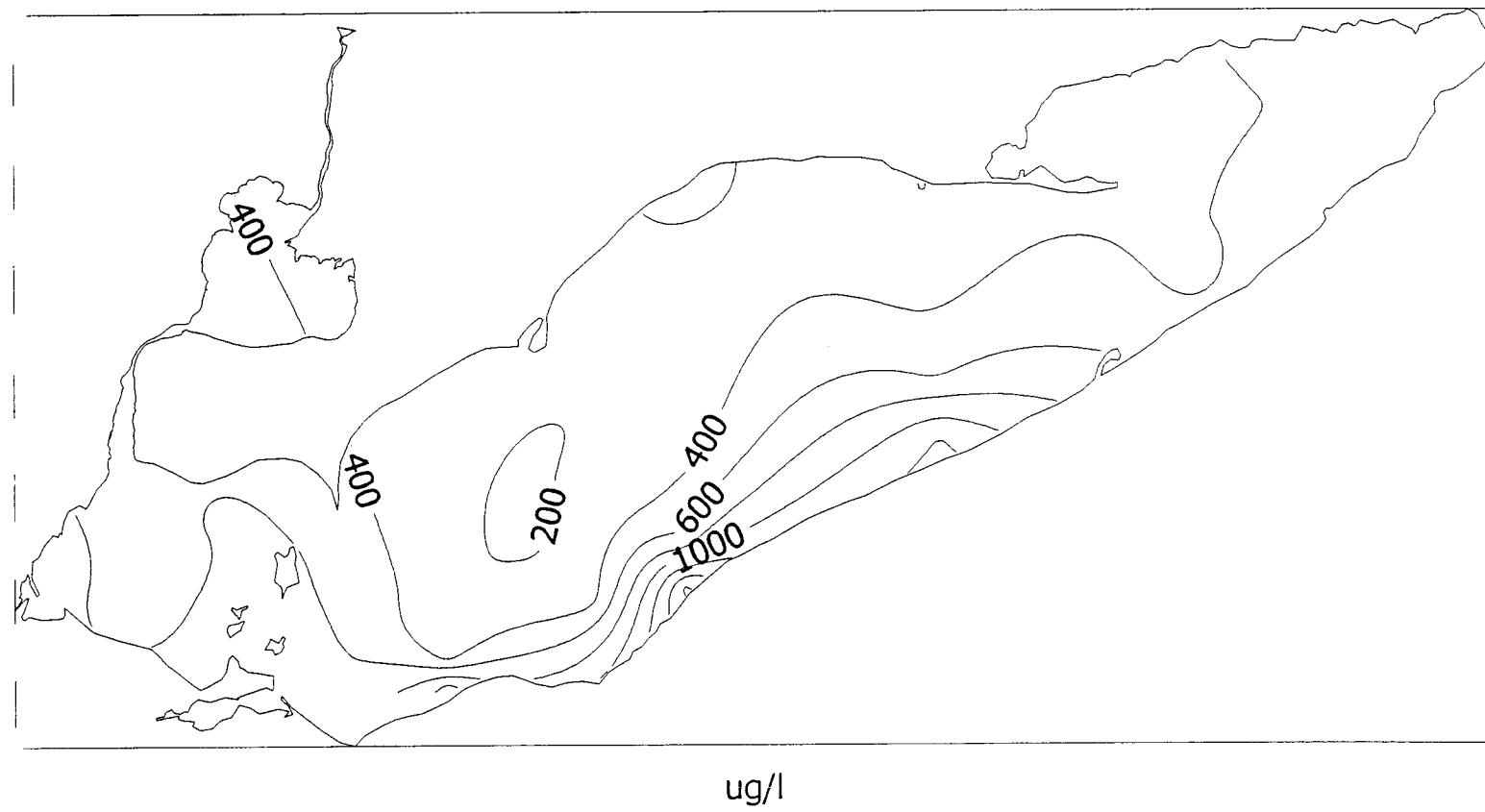


Figure 1.1: Total nitrogen in the surface waters of Lake Erie during May 1997. Each contour represents a change of 200 $\mu\text{g/L N}$. The samples were taken over the entire month and combined into one figure.

May 1997 Total Phosphorus

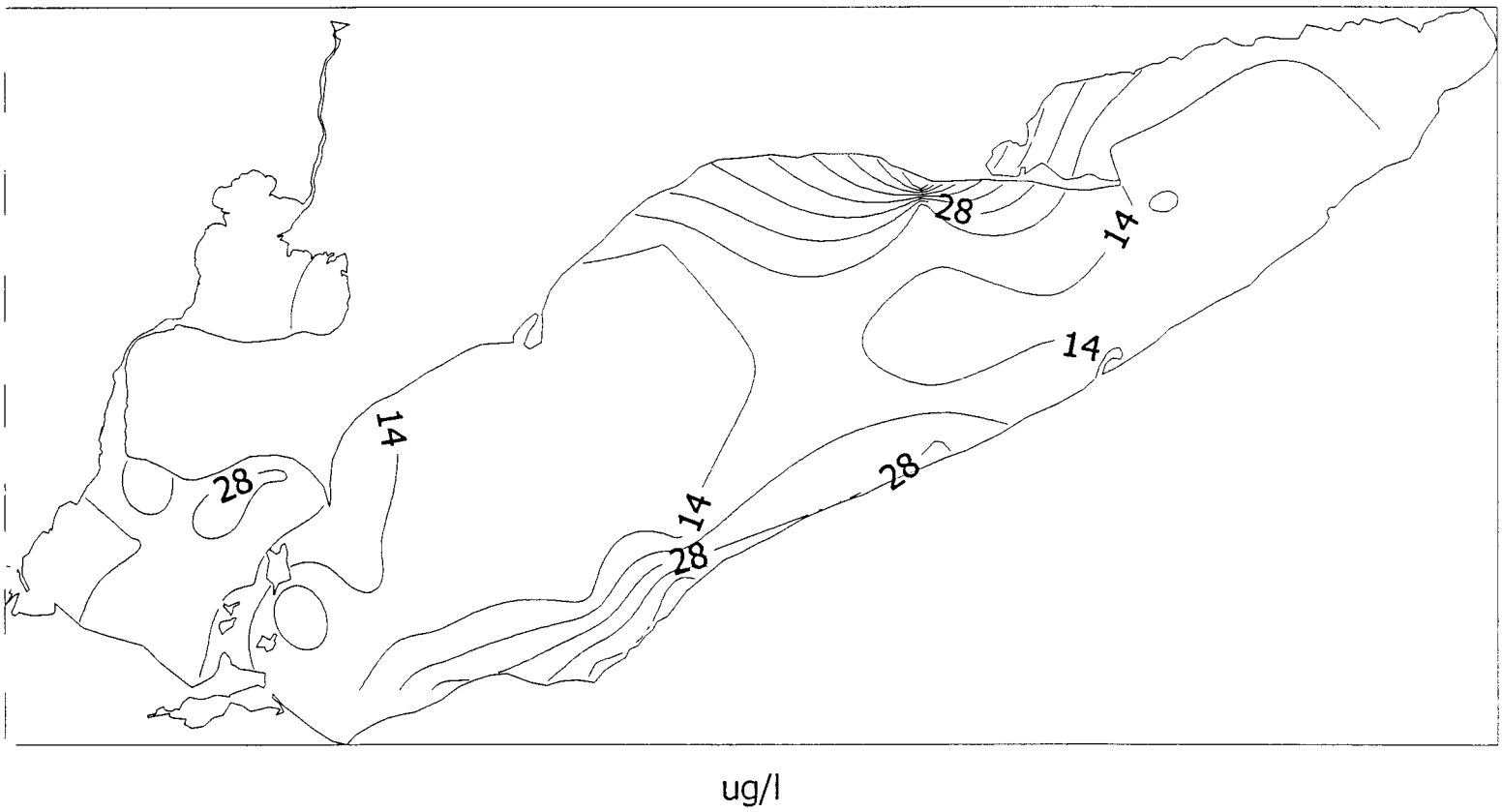


Figure 1.2: Total phosphorus in the surface waters of Lake Erie during May 1997. Each contour represents a change of 7 $\mu\text{g/L P}$. The samples were taken over the entire month and combined into one figure.

May 1997 Total Phytoplankton Biomass

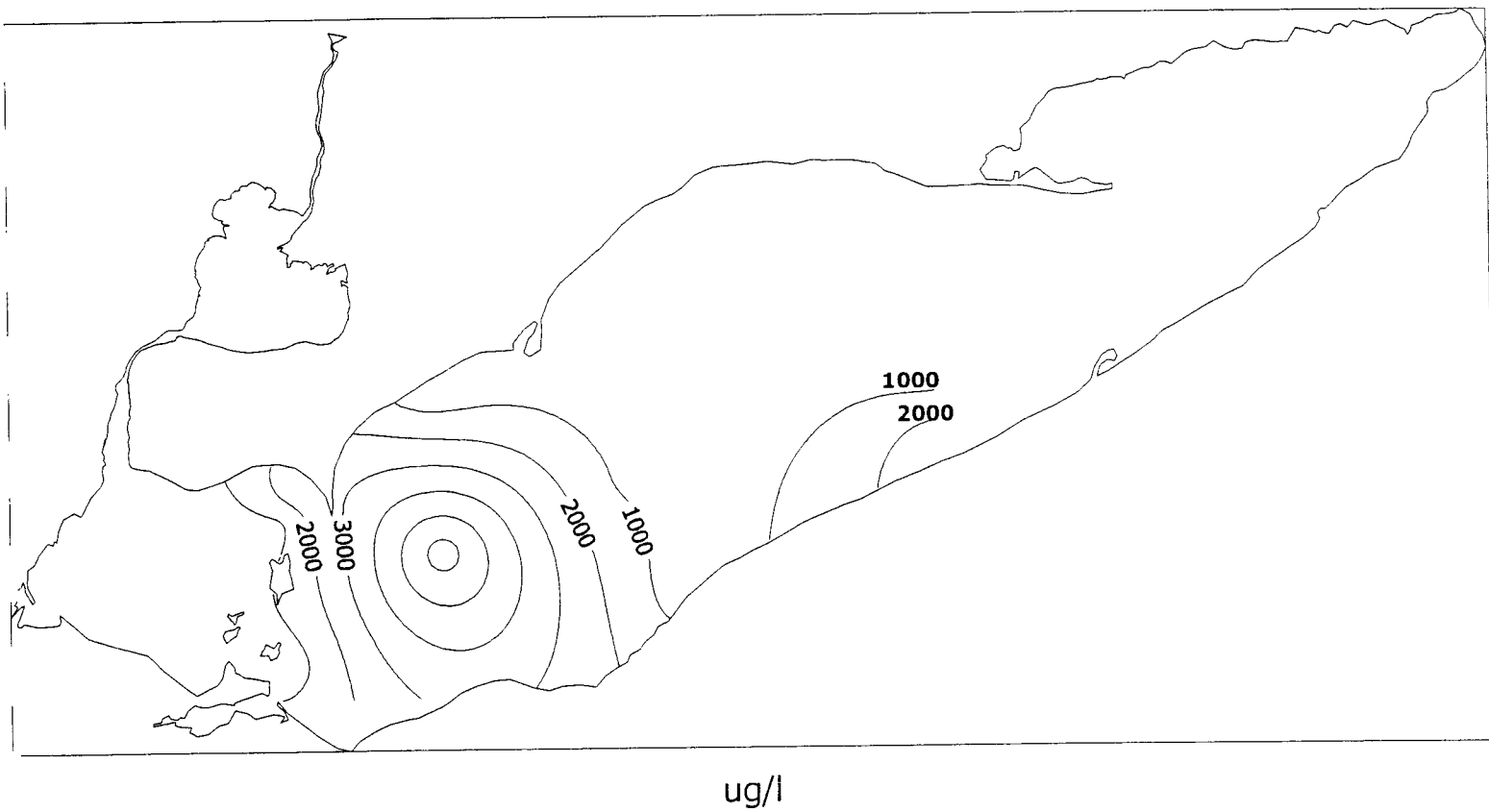


Figure 1.3: Total phytoplankton biomass in the surface waters of Lake Erie during May 1997. Each contour represents a change of 1 mg/L. The samples were taken over the entire month and combined into one figure. There were no samples available in the northeastern central basin or in the eastern basin.

August 1997 Total Nitrogen

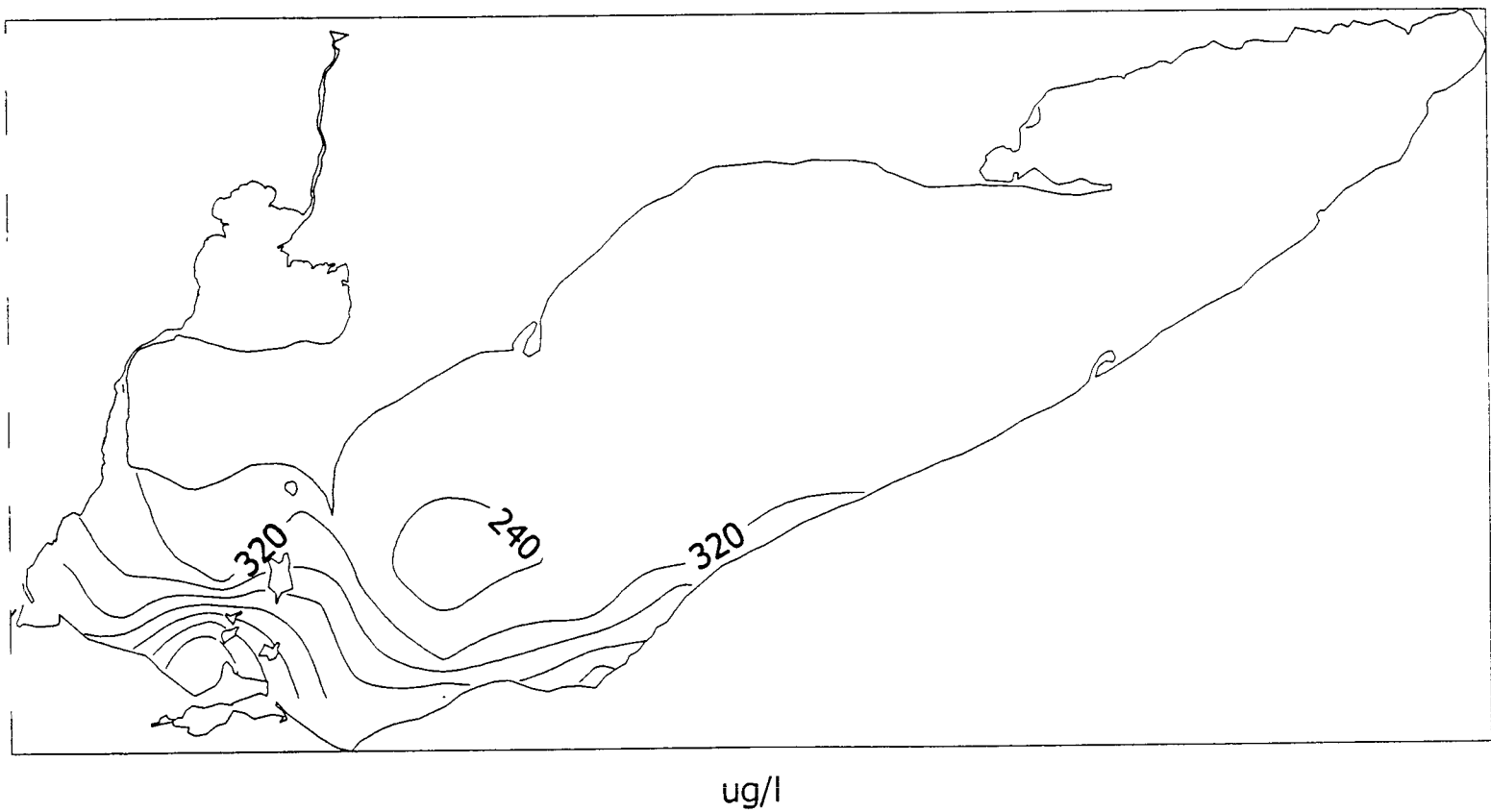


Figure 1.4: Total nitrogen in the surface waters of Lake Erie during August 1997. Each contour represents a change of $80 \mu\text{g/L N}$. The samples were taken over the entire month and combined into one figure. Samples were taken in the eastern basin and were similar to central basin values, causing the absence of contour lines.

August 1997 Total Phosphorus

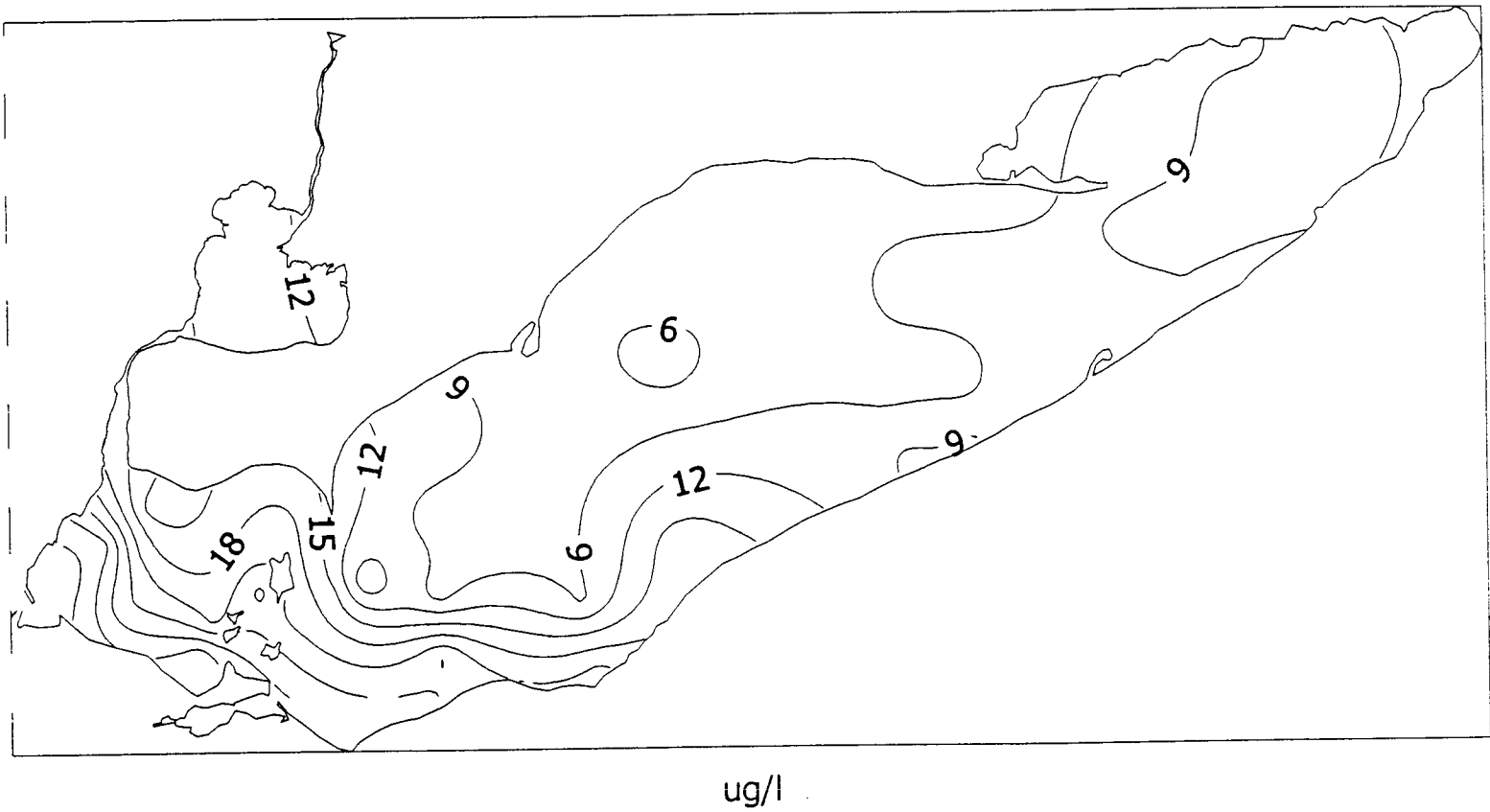
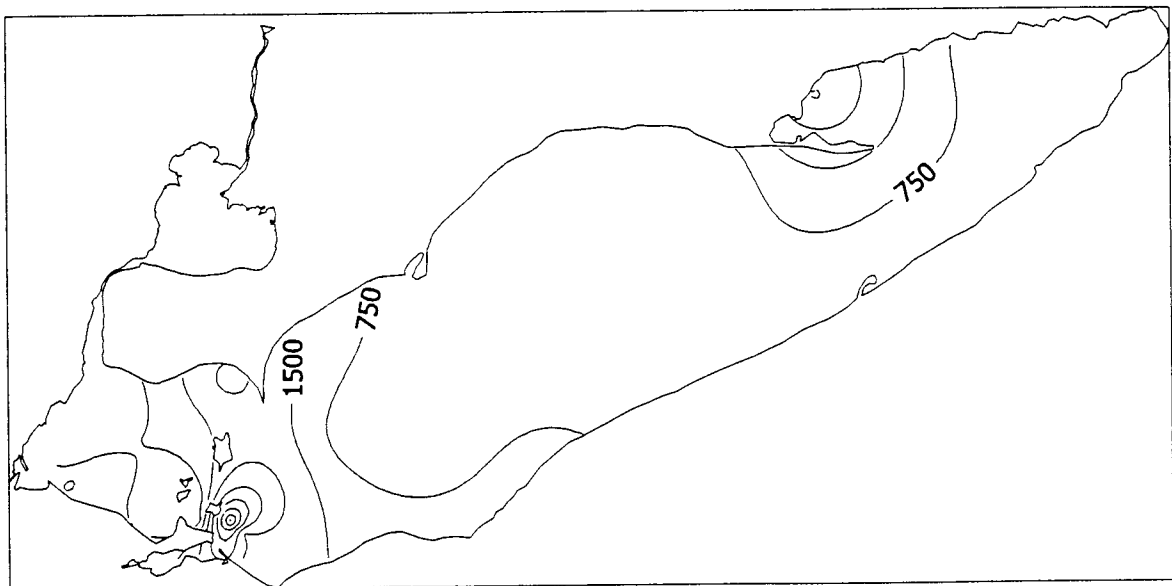


Figure 1.5: Total phosphorus in the surface waters of Lake Erie during August 1997. Each contour represents a change of $3 \mu\text{g/L}$ P. The samples were taken over the entire month and combined into one figure.

August 1997 Total Phytoplankton Biomass



ug/l

Figure 1.6: Total phytoplankton biomass in the surface waters of Lake Erie during May 1997. Each contour represents a change of 0.75 mg/L. The samples were taken over the entire month and combined into one figure.

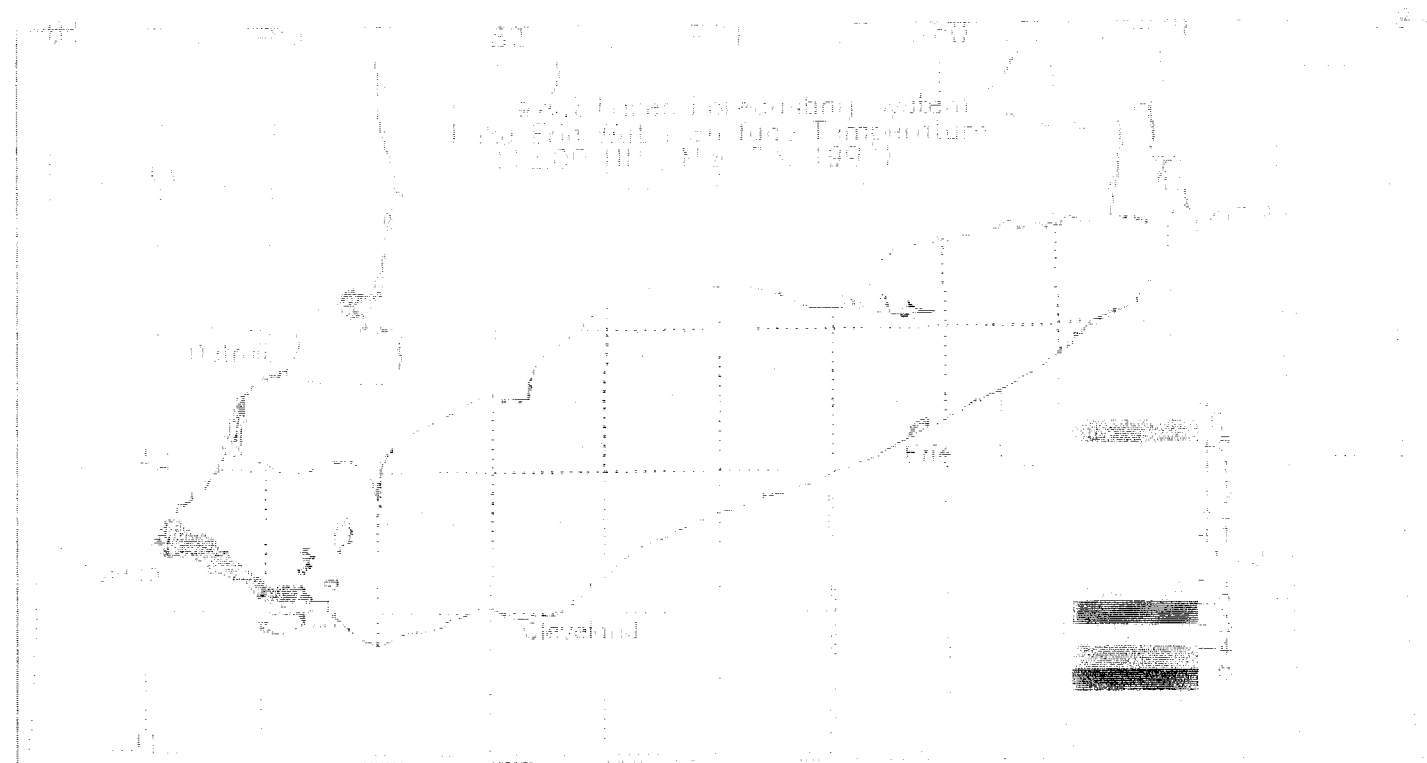


Figure 1.7 : Great Lakes Forecasting System surface temperature for Lake Erie on 23 May 1997. The colors indicate the magnitude of the difference in temperature from 10 °C.

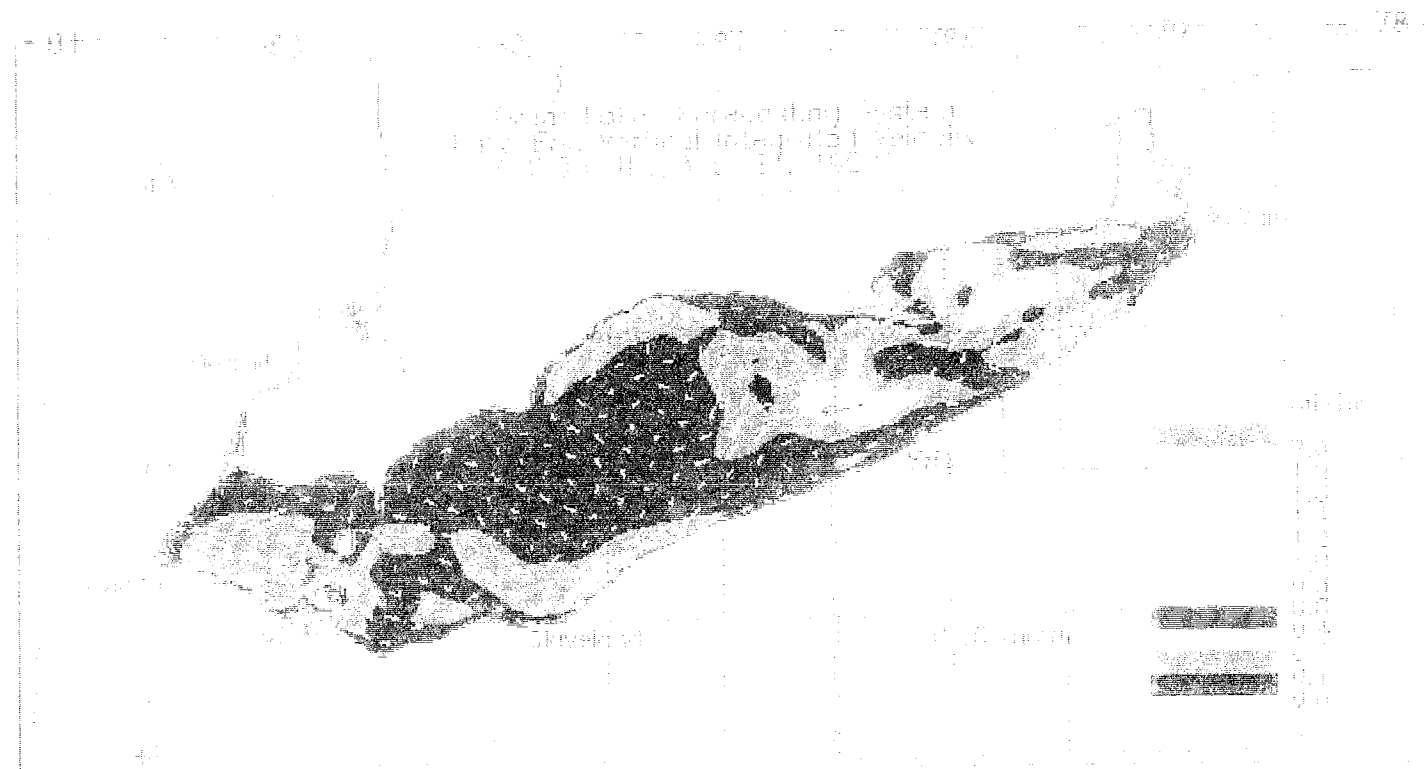


Figure 18: Great Lakes Forecasting System vertical integrated water velocity for Lake Erie on our sampling date, 23 May 1997. The legend colors indicate the magnitude of the velocity, while the small arrows on the map show the direction of the velocity as well as the magnitude.

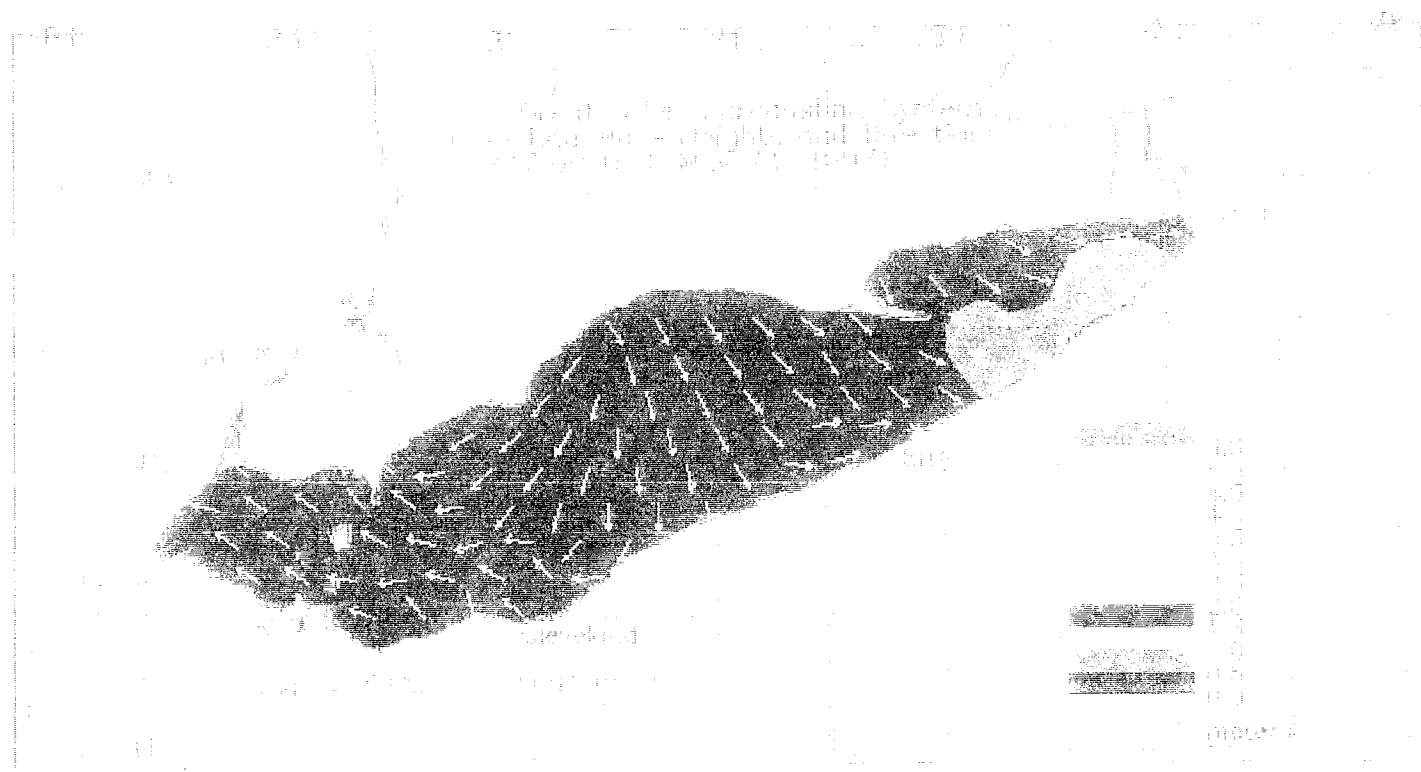


Figure 1: Geological cross-section of the Lake Superior region. Note the presence of the Precambrian basement rock, while the rest is the deviation.

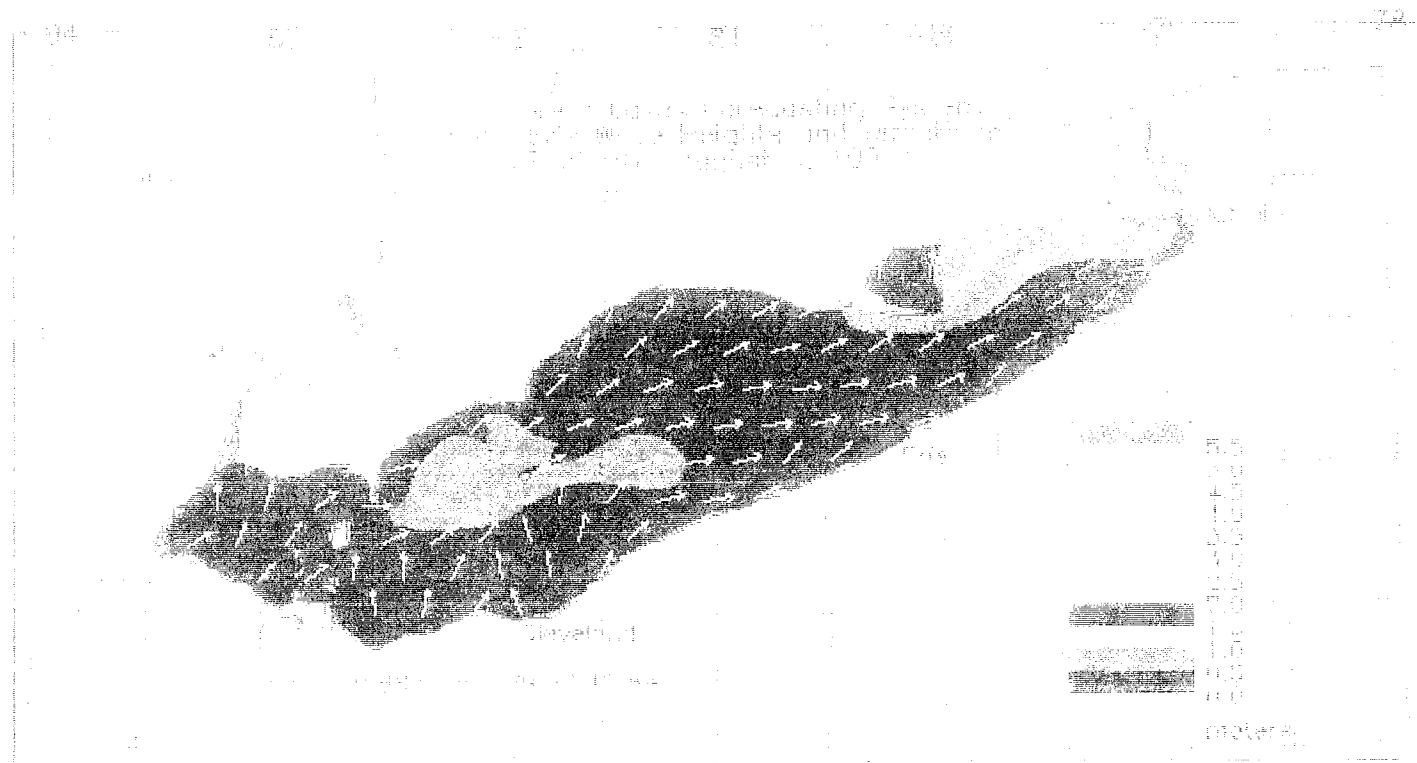


Figure 1.10: Great Lakes Forecasting System wave heights and directions for Lake Erie on 8 August 1997. The colors indicate the height of the wave, while the arrows give the direction.



Figure 1.11. Great Lakes Forecasting System vertical integrated water velocity for Lake Erie on our sampling date, 8 August 1997. The legend colors indicate the magnitude of the velocity, while the small arrows on the map show the direction of the velocity as well as the magnitude.

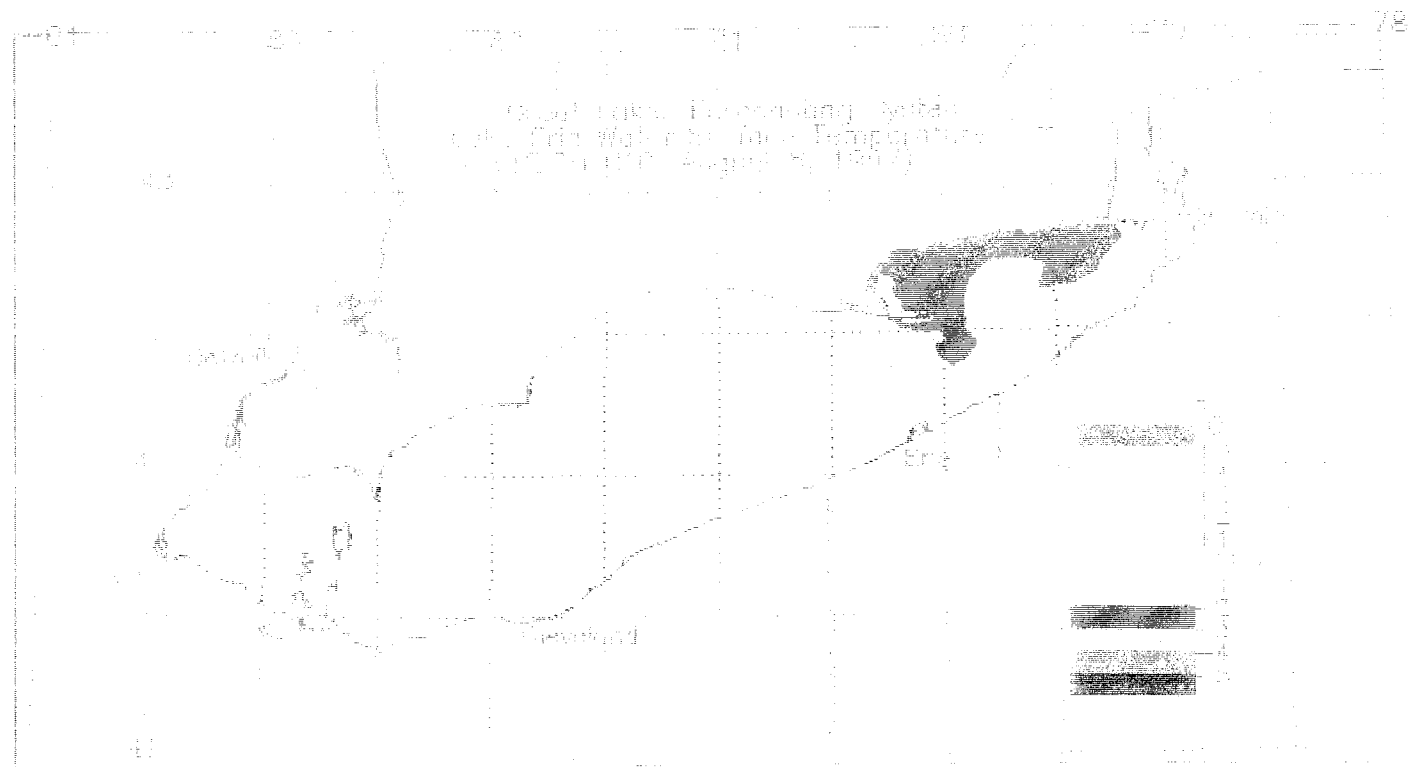


Figure 1.12. Great Lakes Forecasting System surface temperature for Lake Erie on 8 August 1997. The colors indicate the magnitude of the difference in temperature from 24 °C.

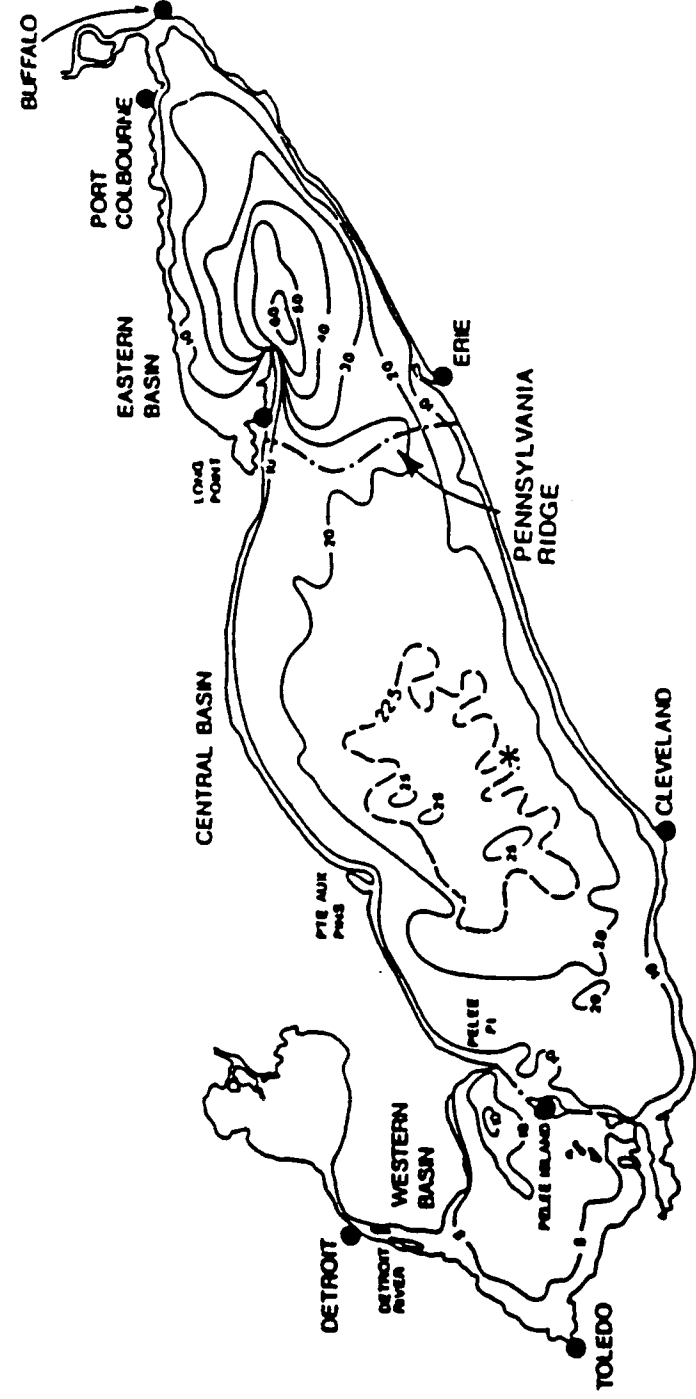
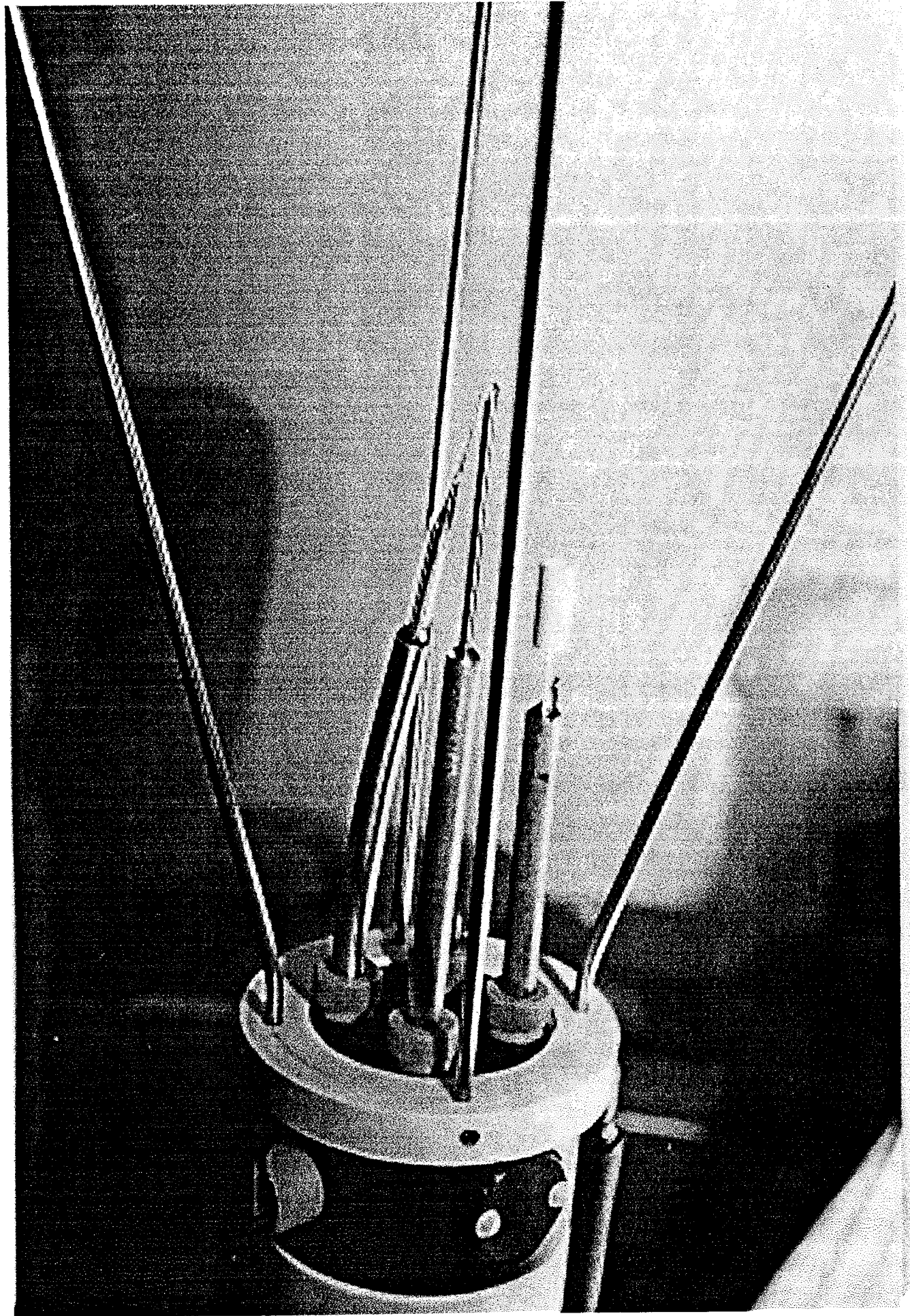


Figure 2.1: Bathymetric map of Lake Erie. The star denotes the approximate sampling site. Contours shown are in meters.



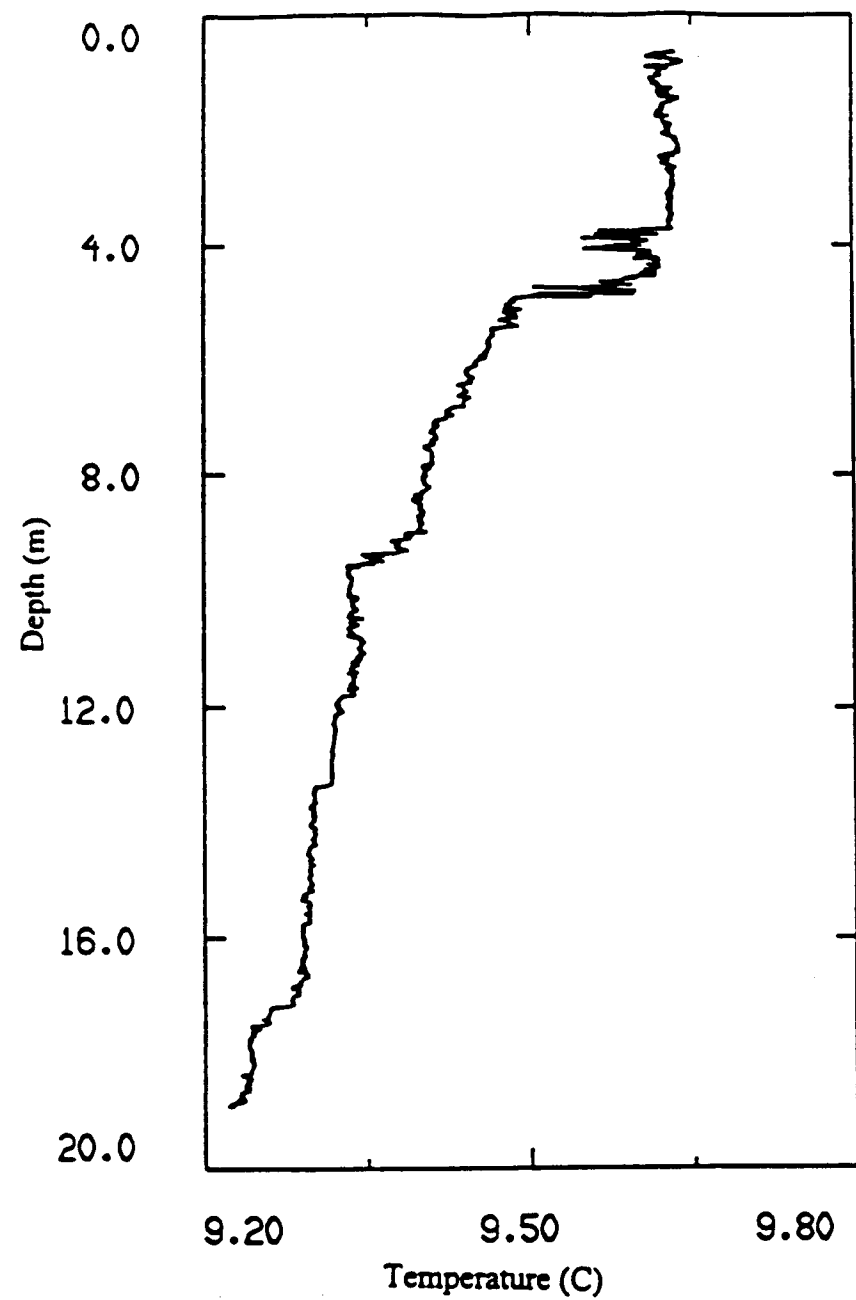


Figure 2.3: Temperature profile from May sampling trip taken in the early afternoon. A small diurnal thermocline is evident at about 4.5 meters and an even smaller seasonal thermocline has begun to form at approximately 9 meters. Notice the overturns, evidence of turbulence, at 4 meters.

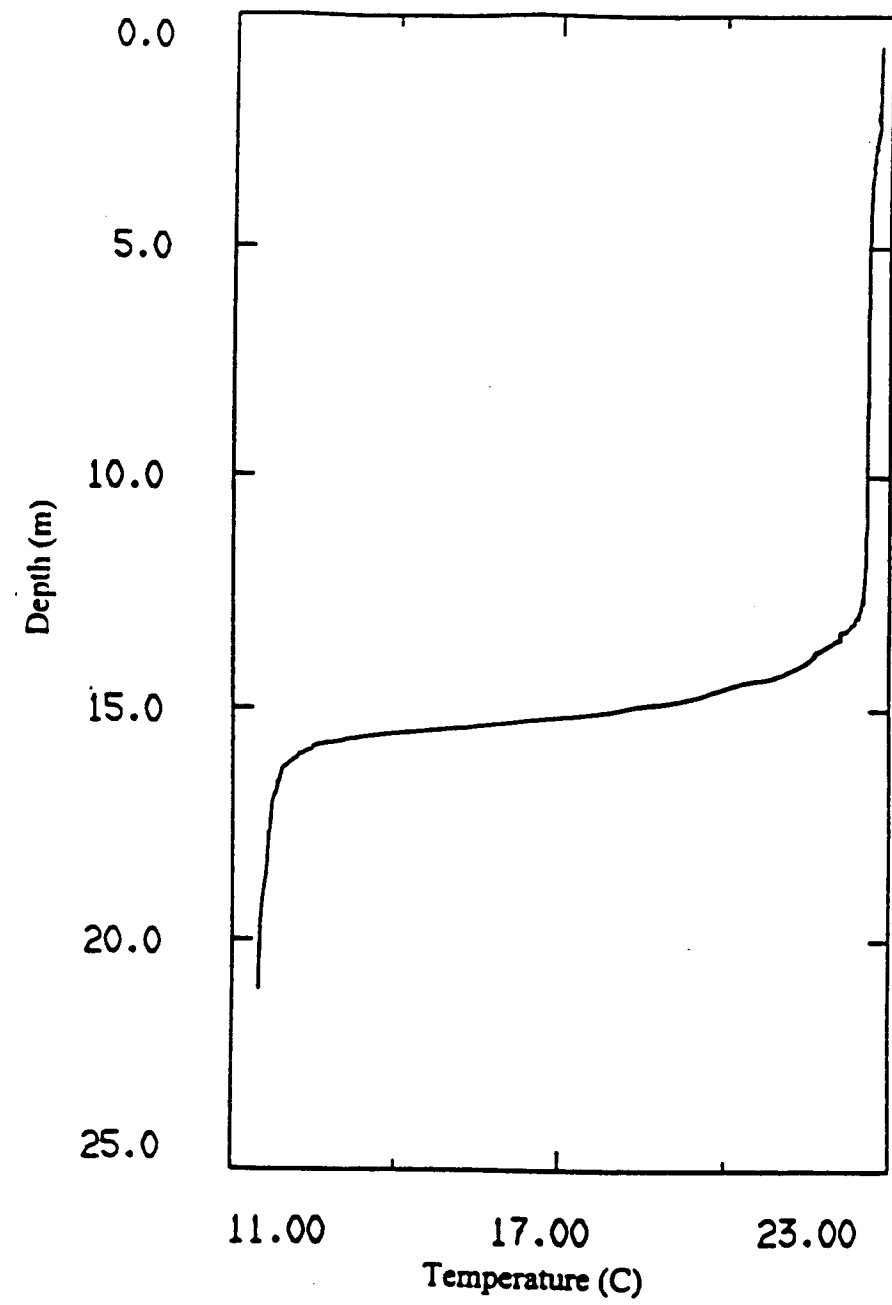


Figure 2.4: Temperature profile from August sampling trip taken in the early afternoon. Both the epilimnion and the hypolimnion are well mixed, separated by a strong density gradient at 15 meters.

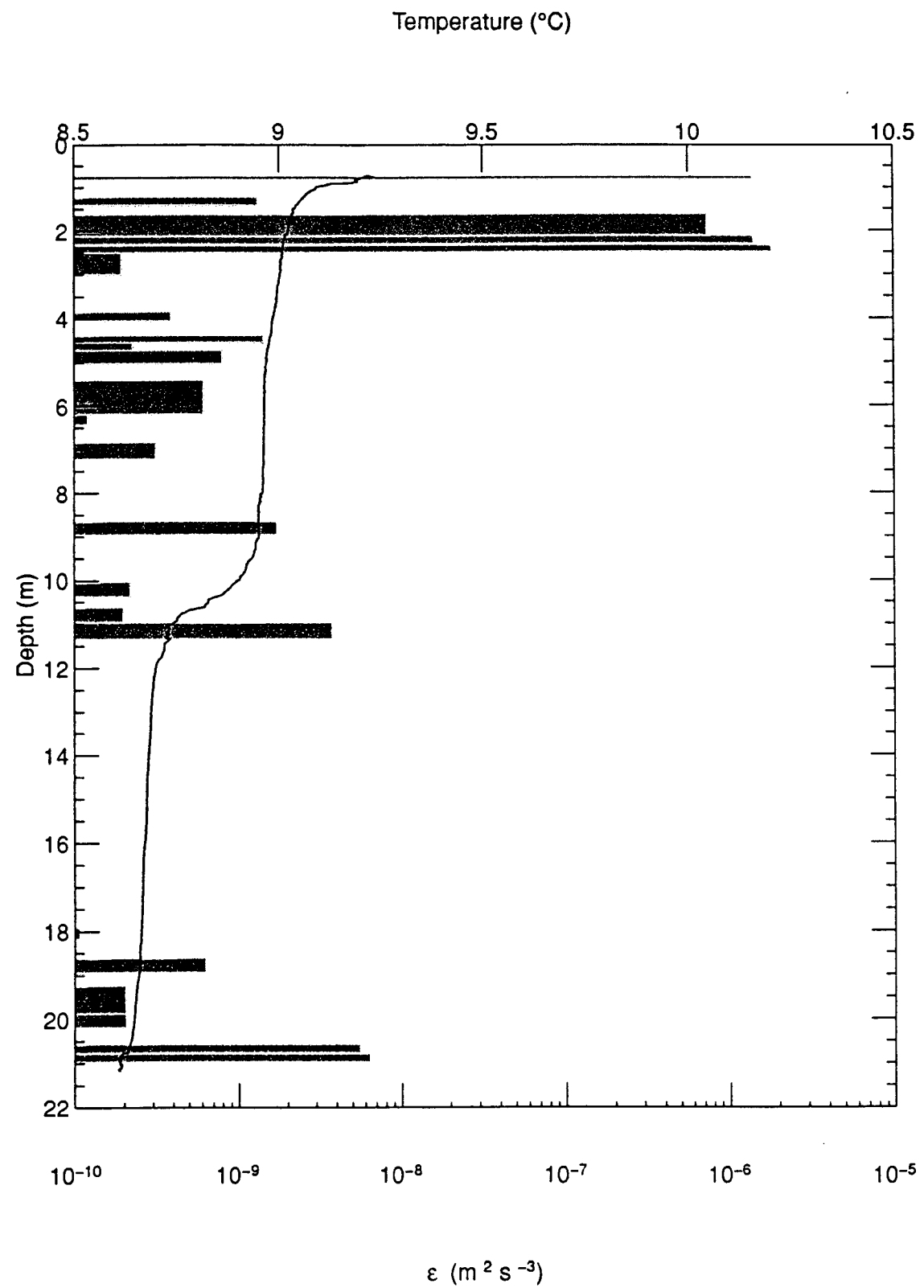


Figure 2.5: Profile at 9:29 AM 23 May 1997. The solid line is temperature. The bars are segments of turbulent kinetic energy. The length of the bar is the amount of TKE being dissipated in the segment. An overturn at the top of the column was too small to be plotted.

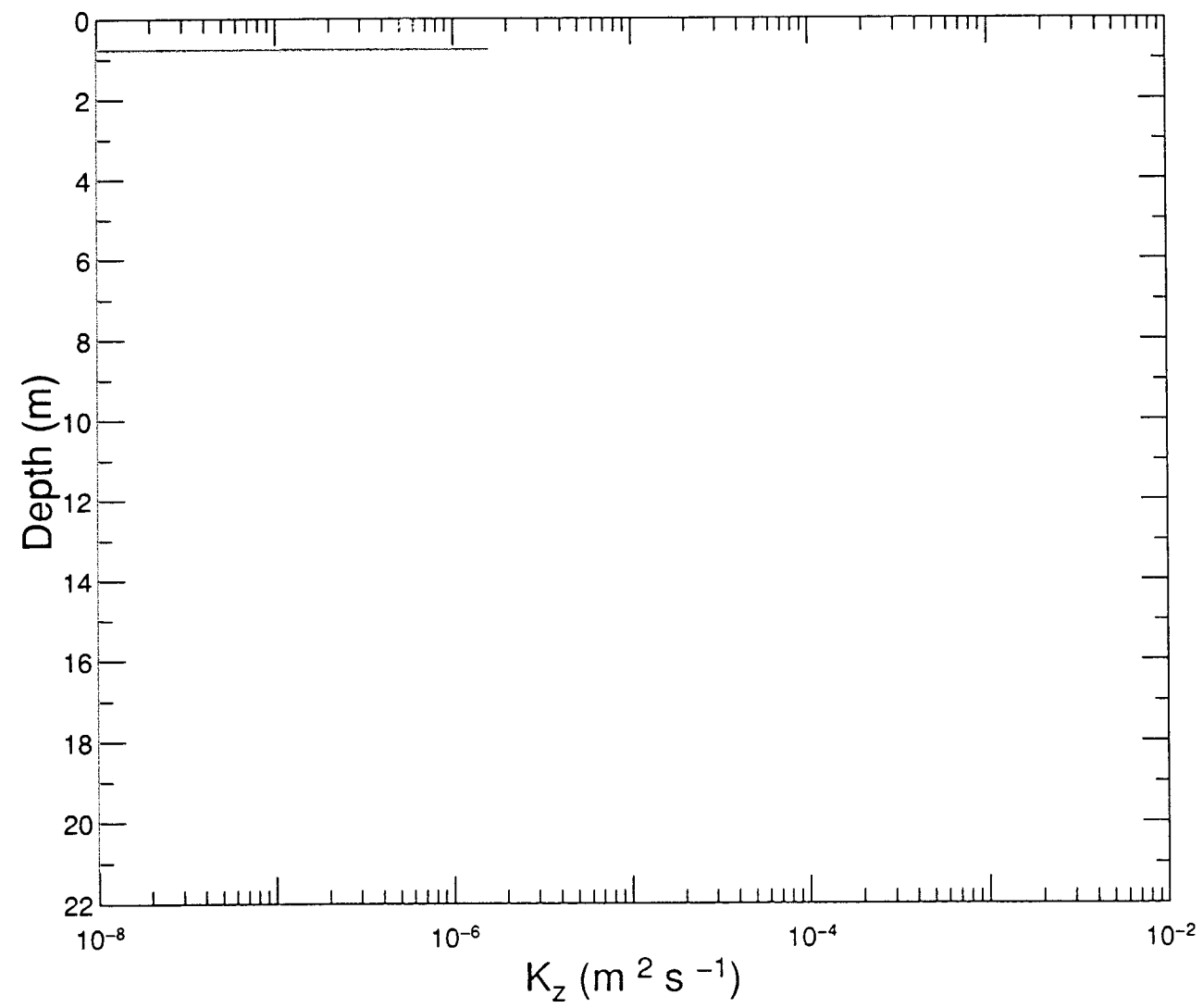


Figure 2.6: Eddy diffusivity at 9:29 AM on 23 May 1997.

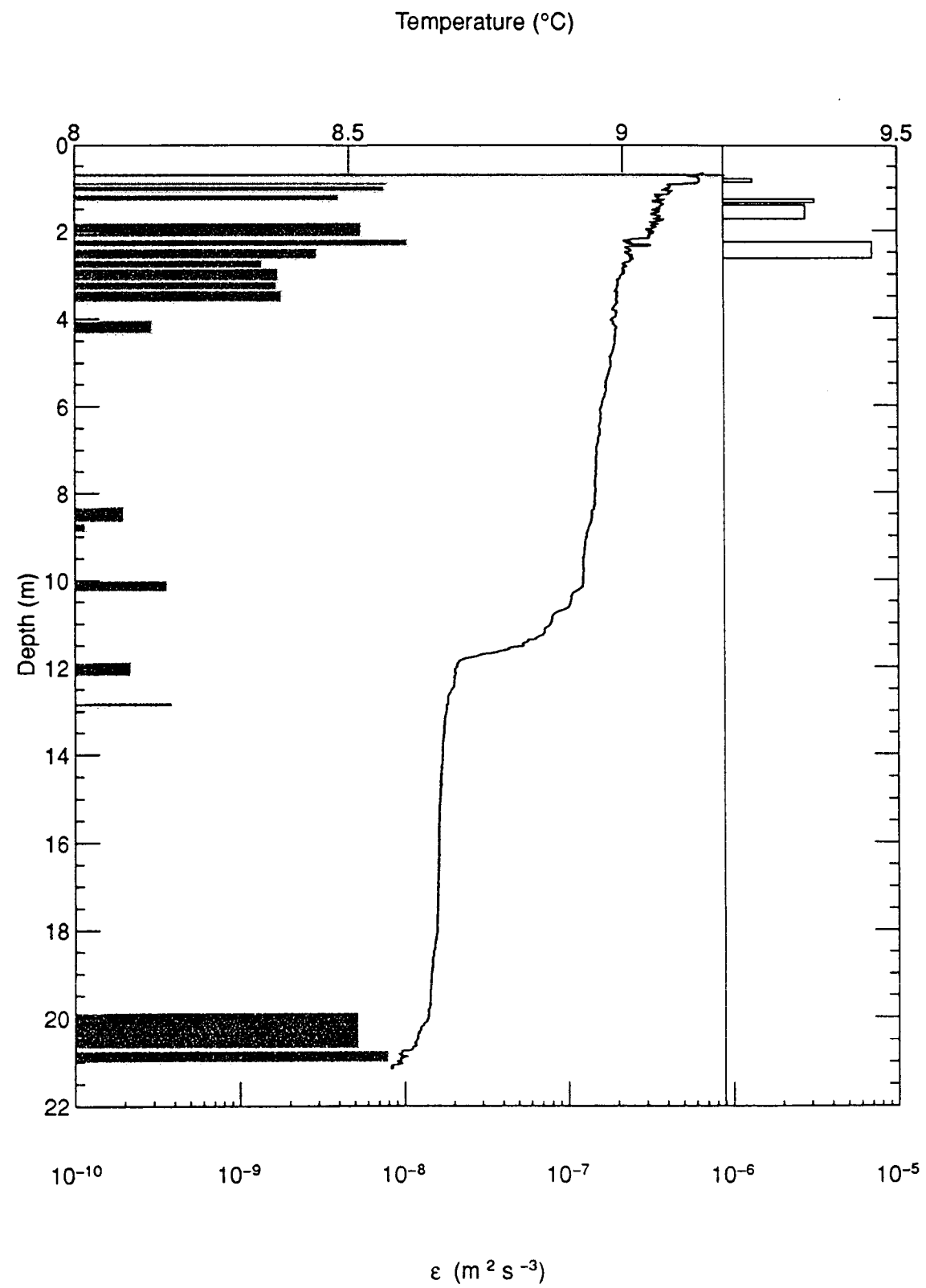


Figure 2.7: Variation in temperature and TKE dissipation at 10:23 AM on 23 May 1997. The bar at the right shows the presence of overturns.

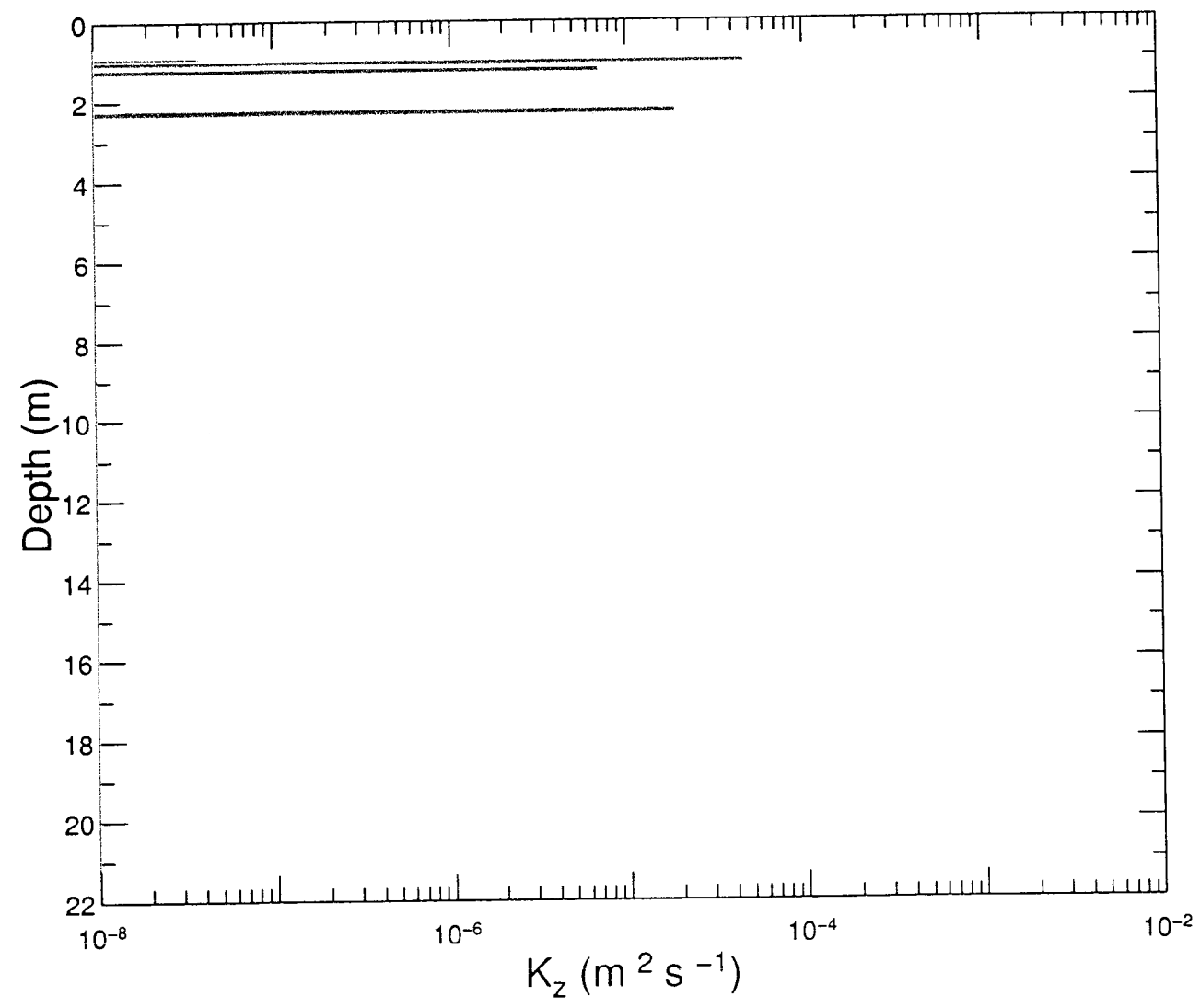


Figure 2.8: Eddy diffusivity at 10:23 AM on 23 May 1997.

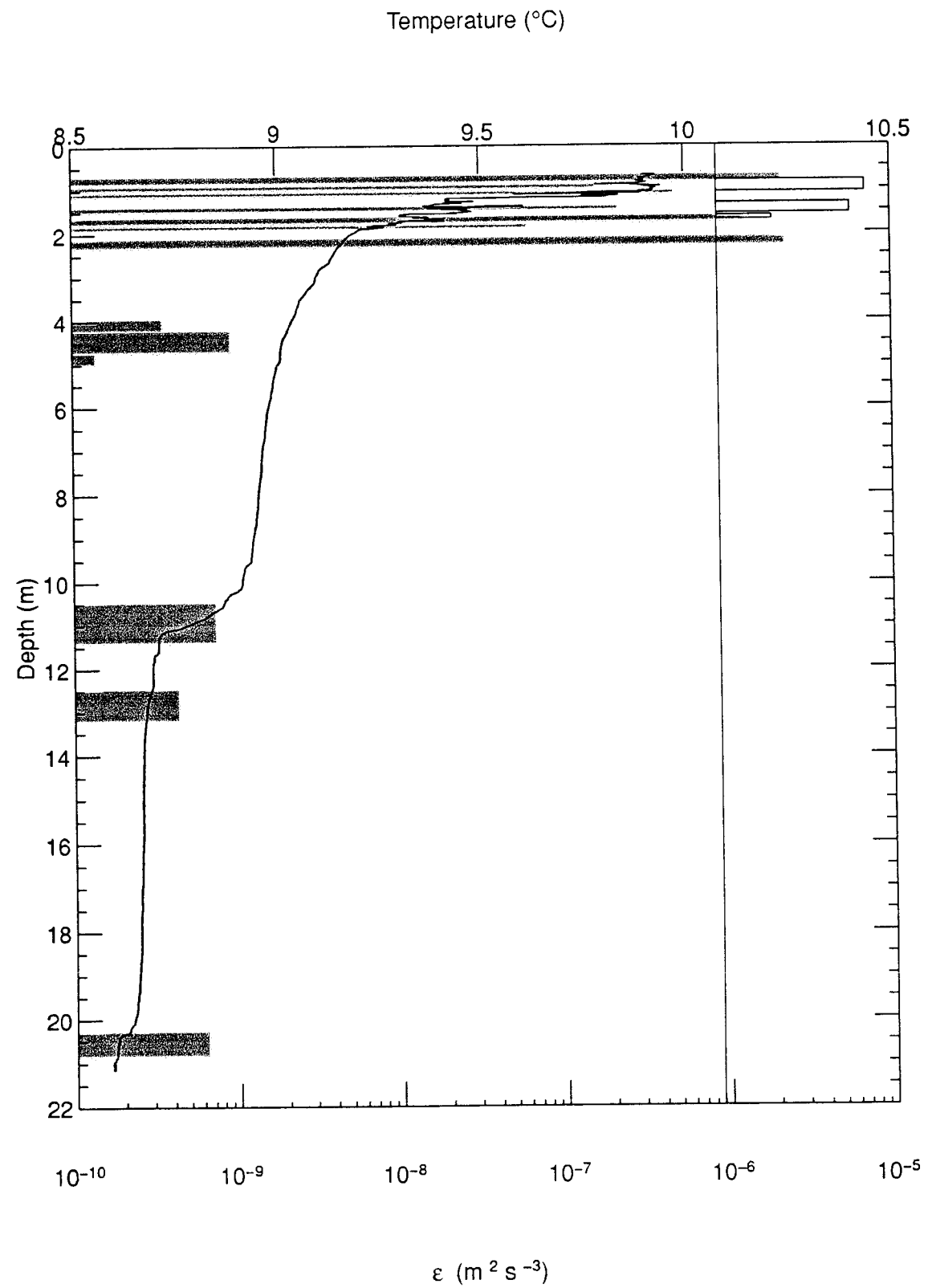


Figure 2.9: Variation in temperature and TKE dissipation at 1:26 PM on 23 May 1997. The bar at the right shows the presence of overturns.

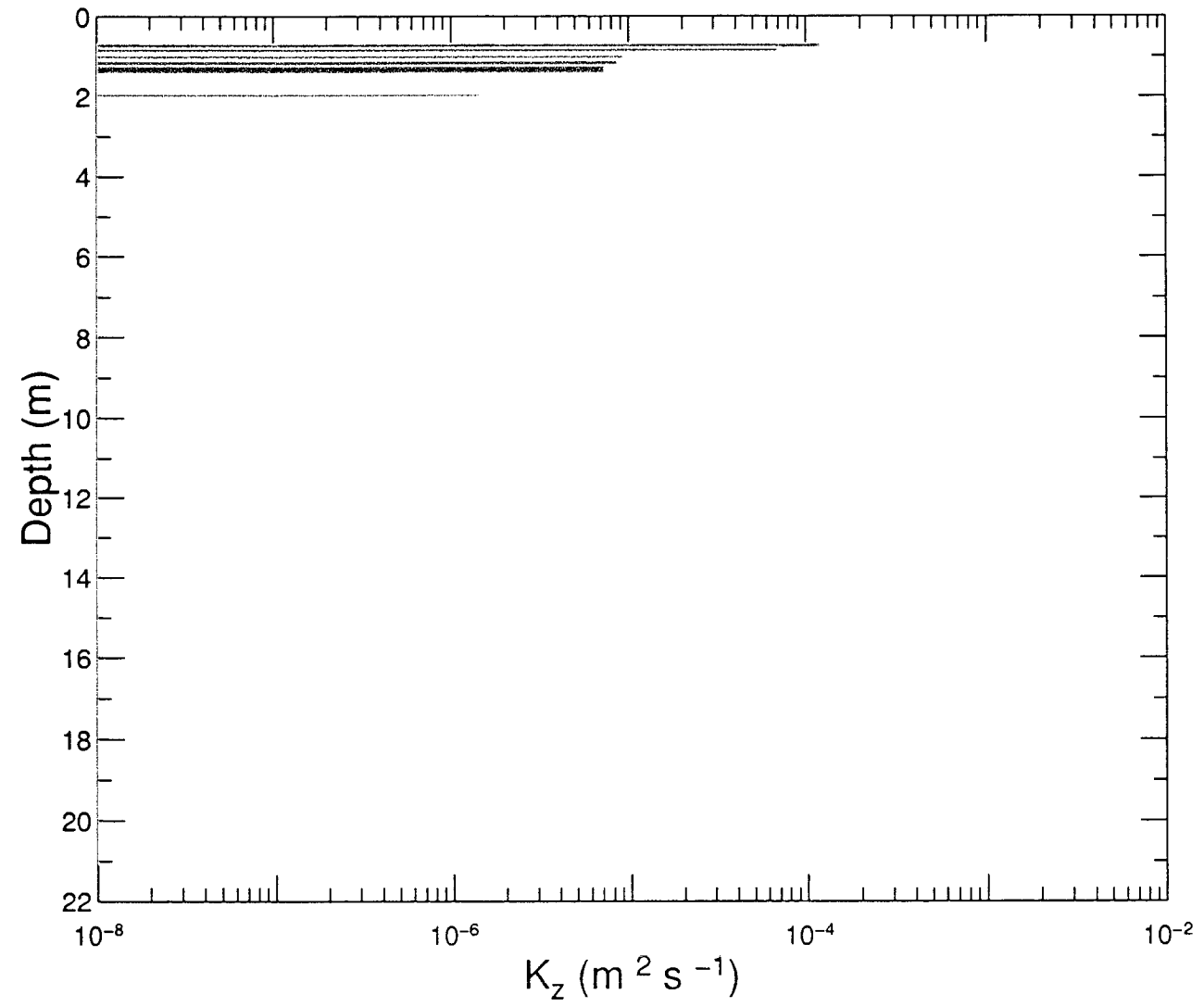


Figure 2.10: Eddy diffusivity at 1:26 PM on 23 May 1997.

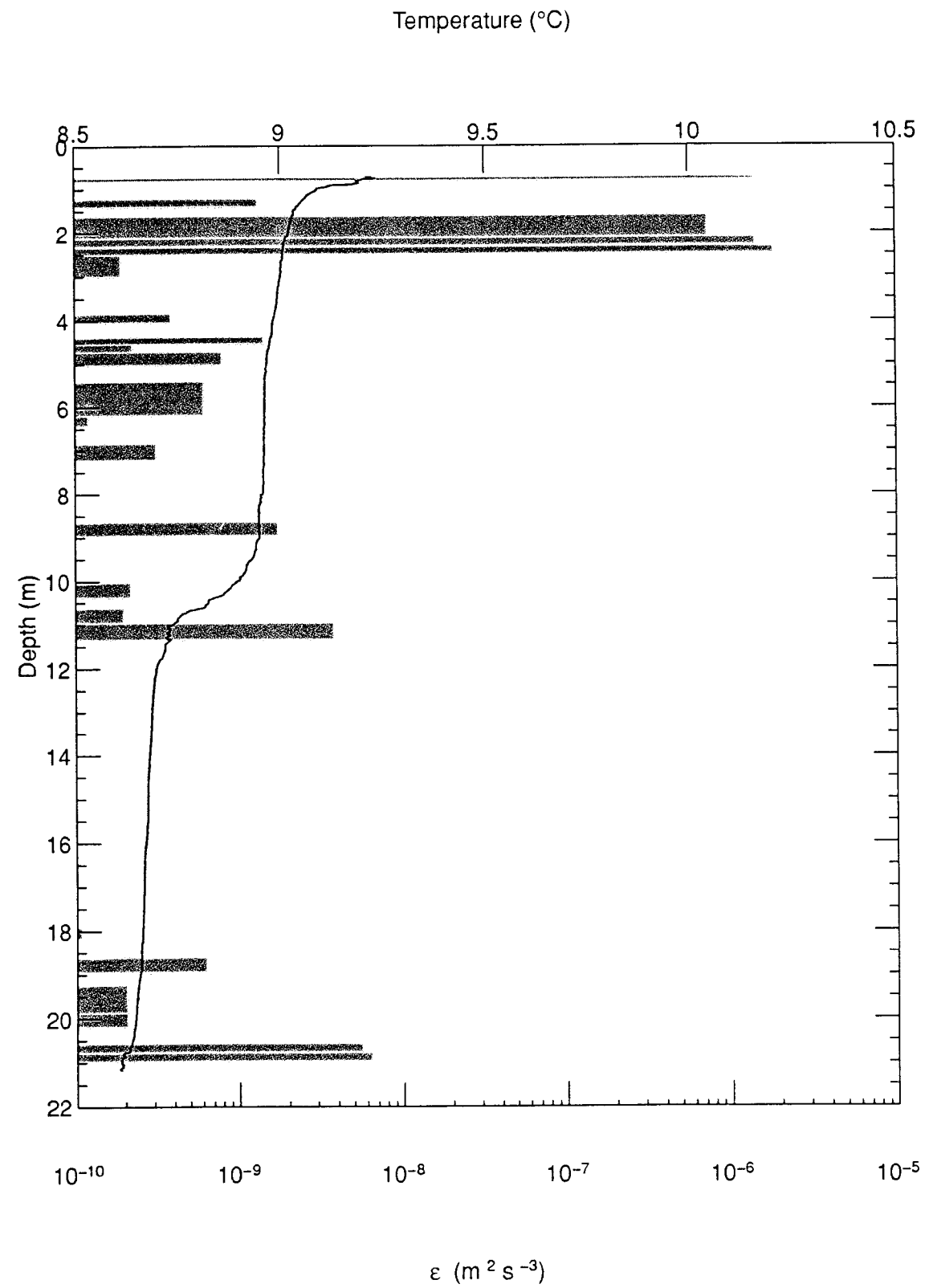


Figure 2.11: Variation in temperature and TKE dissipation at 2:26 PM on 23 May 1997. The bar at the right shows the presence of overturns.

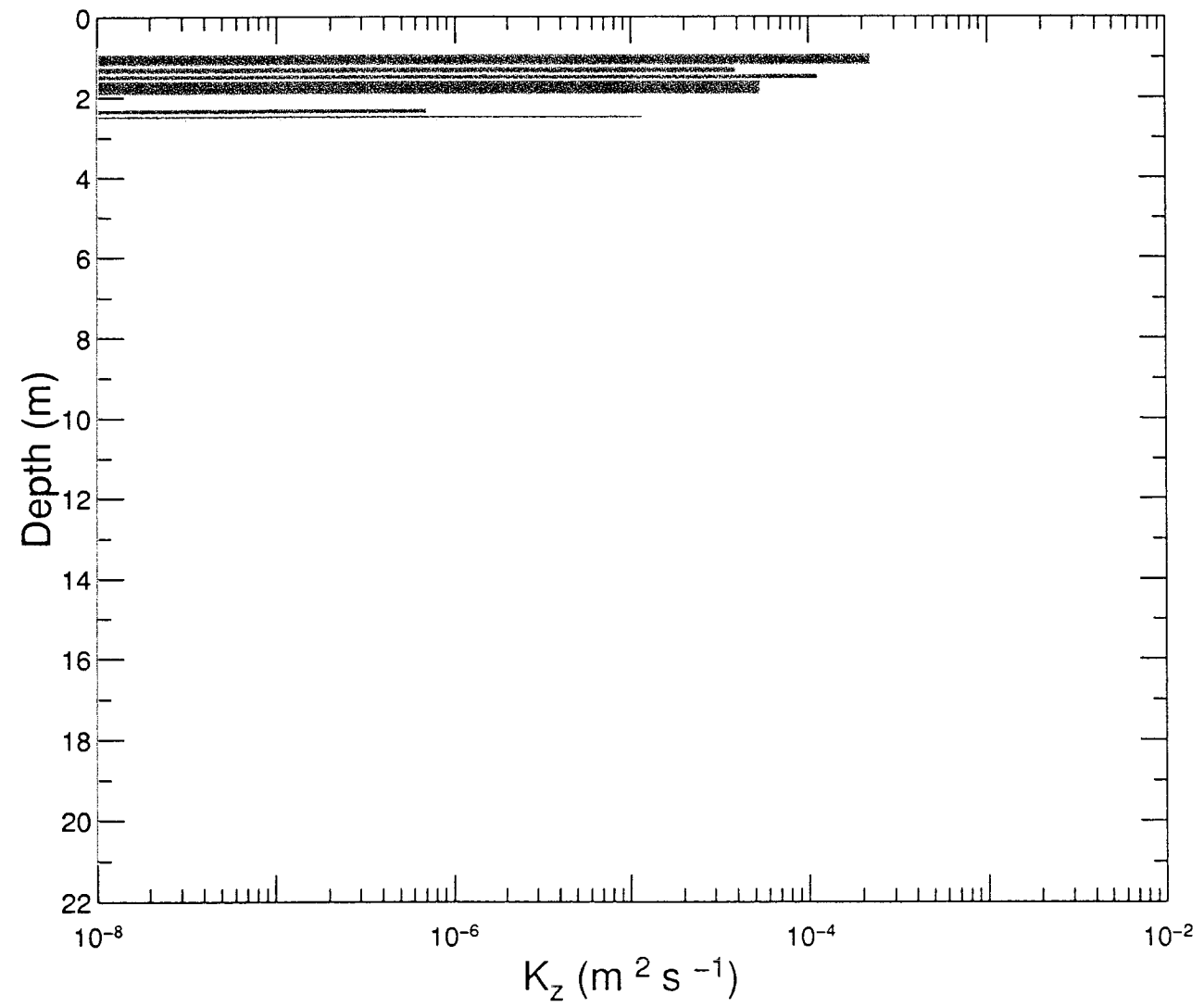


Figure 2.12: Eddy diffusivity at 2:26 PM on 23 May 1997.

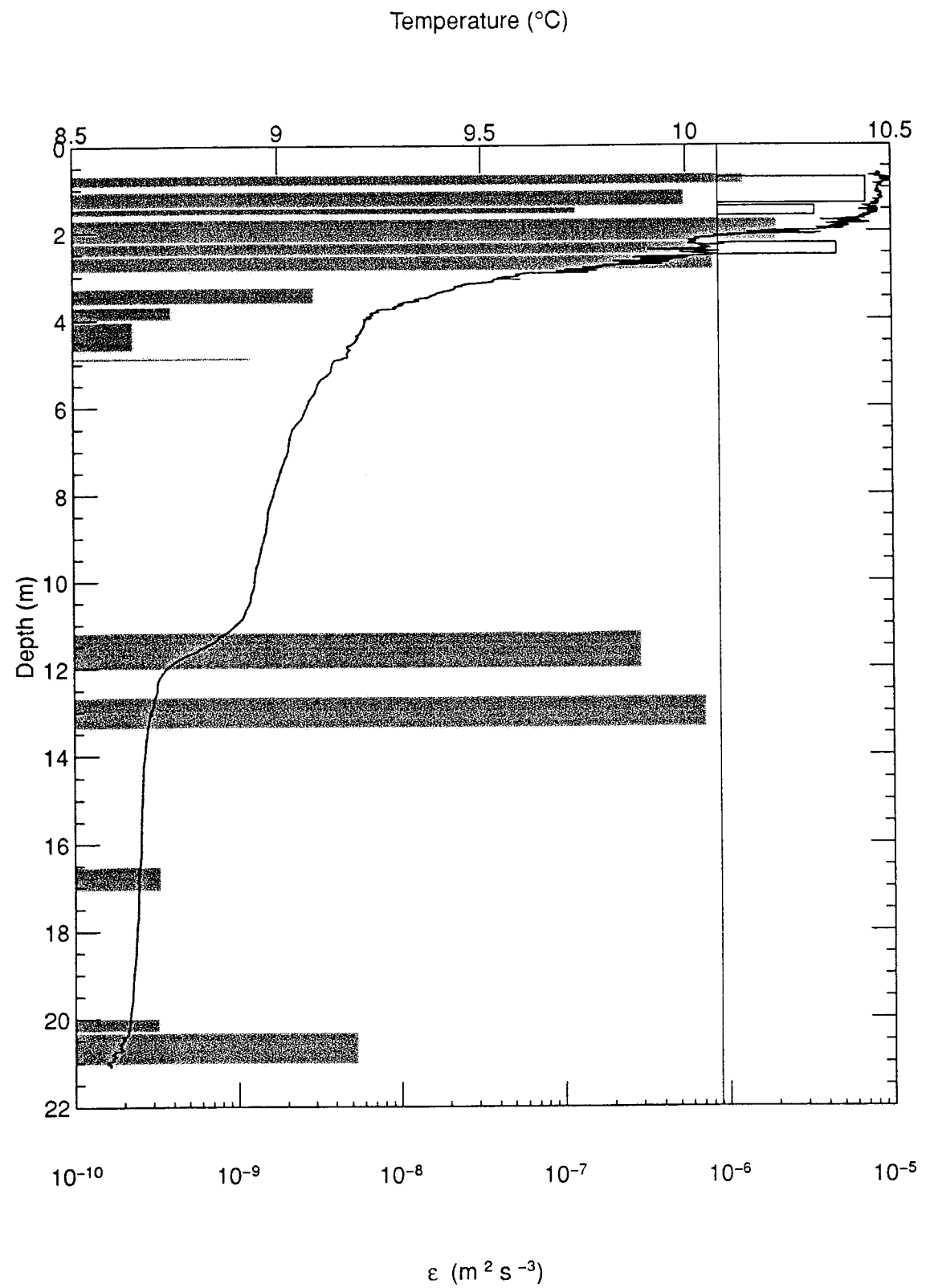


Figure 2.13: Variation in temperature and TKE dissipation at 5:39 PM on 23 May 1997. The bar at the right shows the presence of overturns.

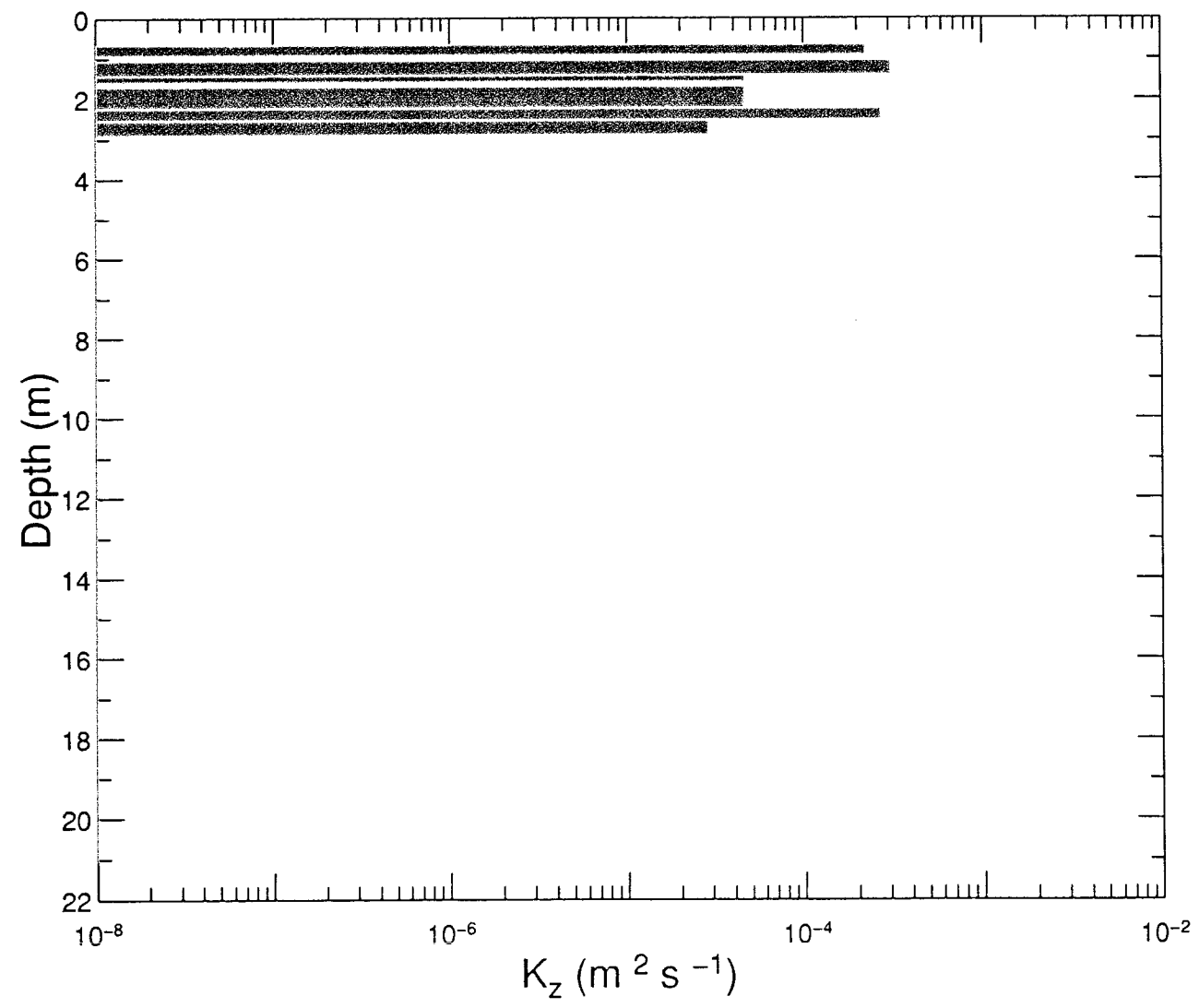


Figure 2.14: Eddy diffusivity at 5:39 PM on 23 May 1997.

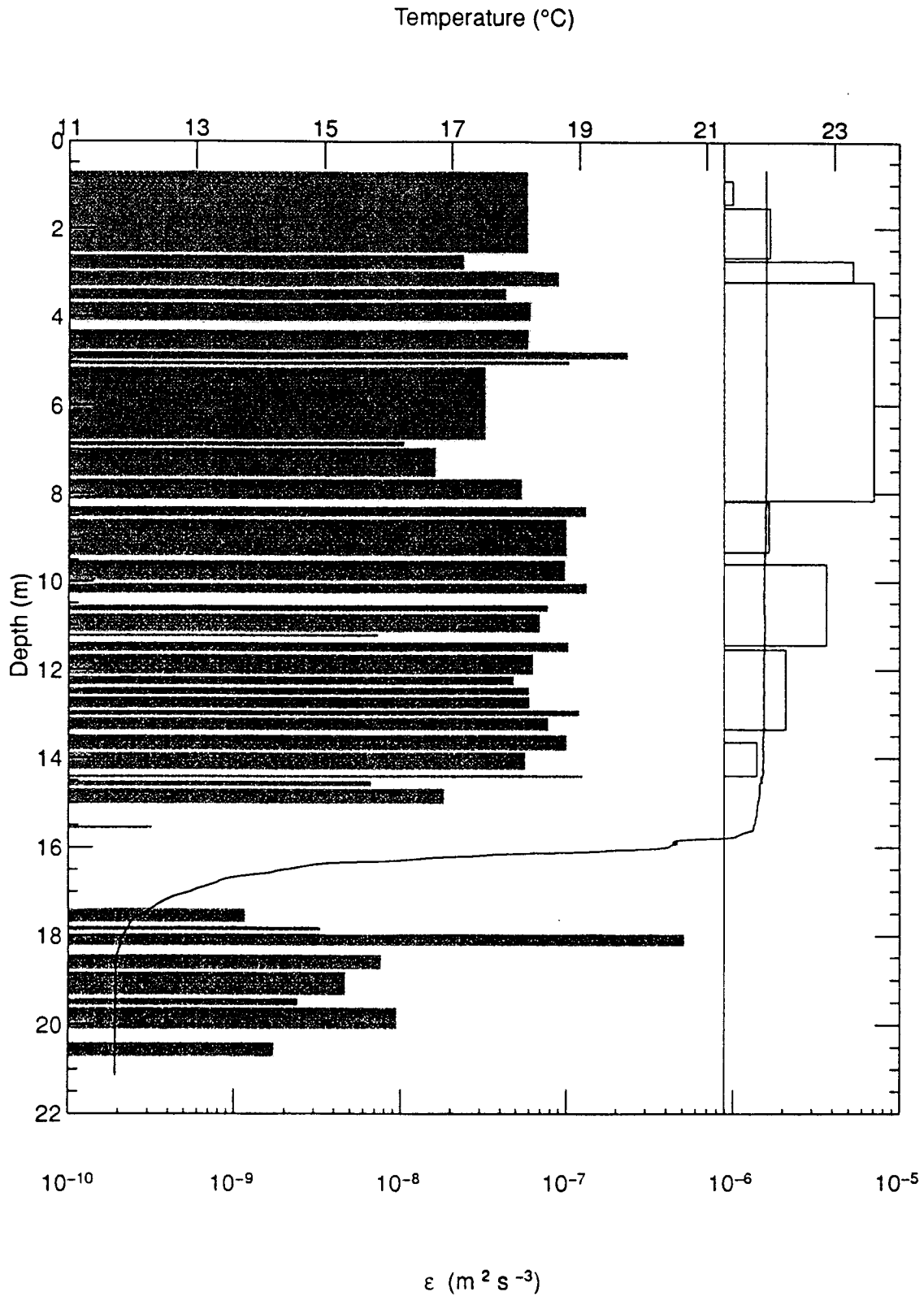


Figure 2.15: Variation in temperature and TKE dissipation at 6:37 AM on 8 August 1997. The bar at the right shows the presence of overturns.

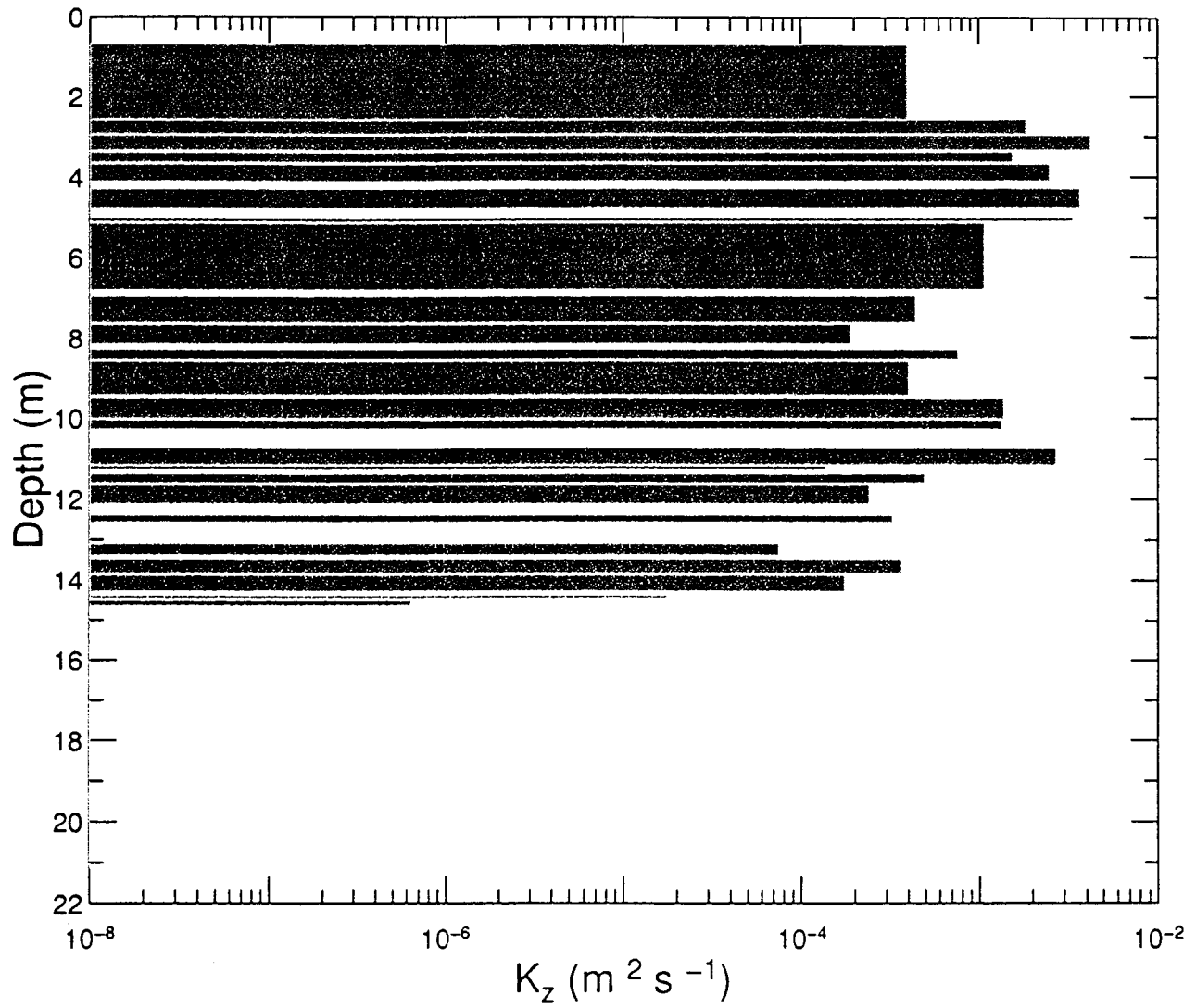


Figure 2.16: Eddy diffusivity at 6:37 AM on 8 August 1997.

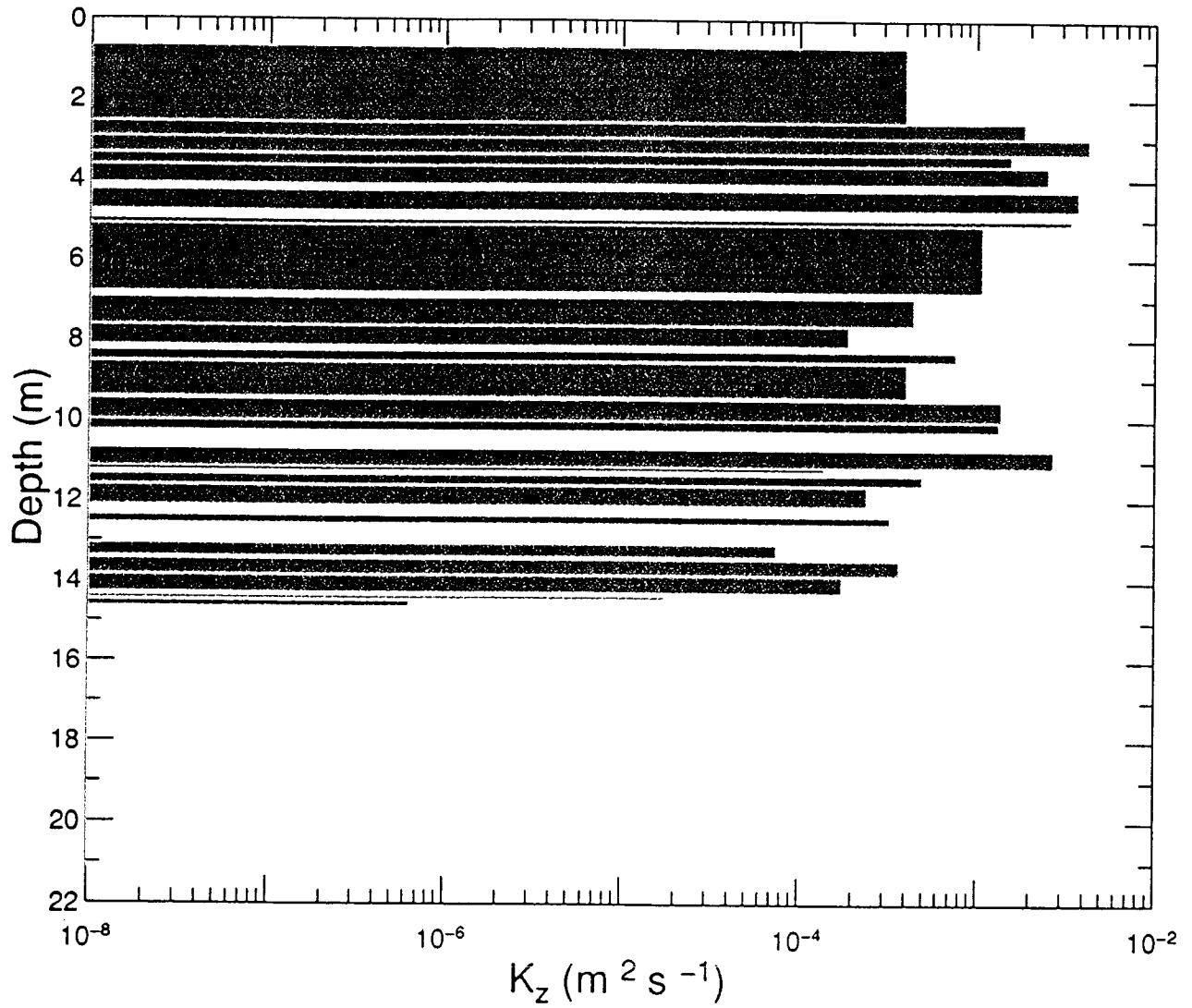


Figure 2.16: Eddy diffusivity at 6:37 AM on 8 August 1997.

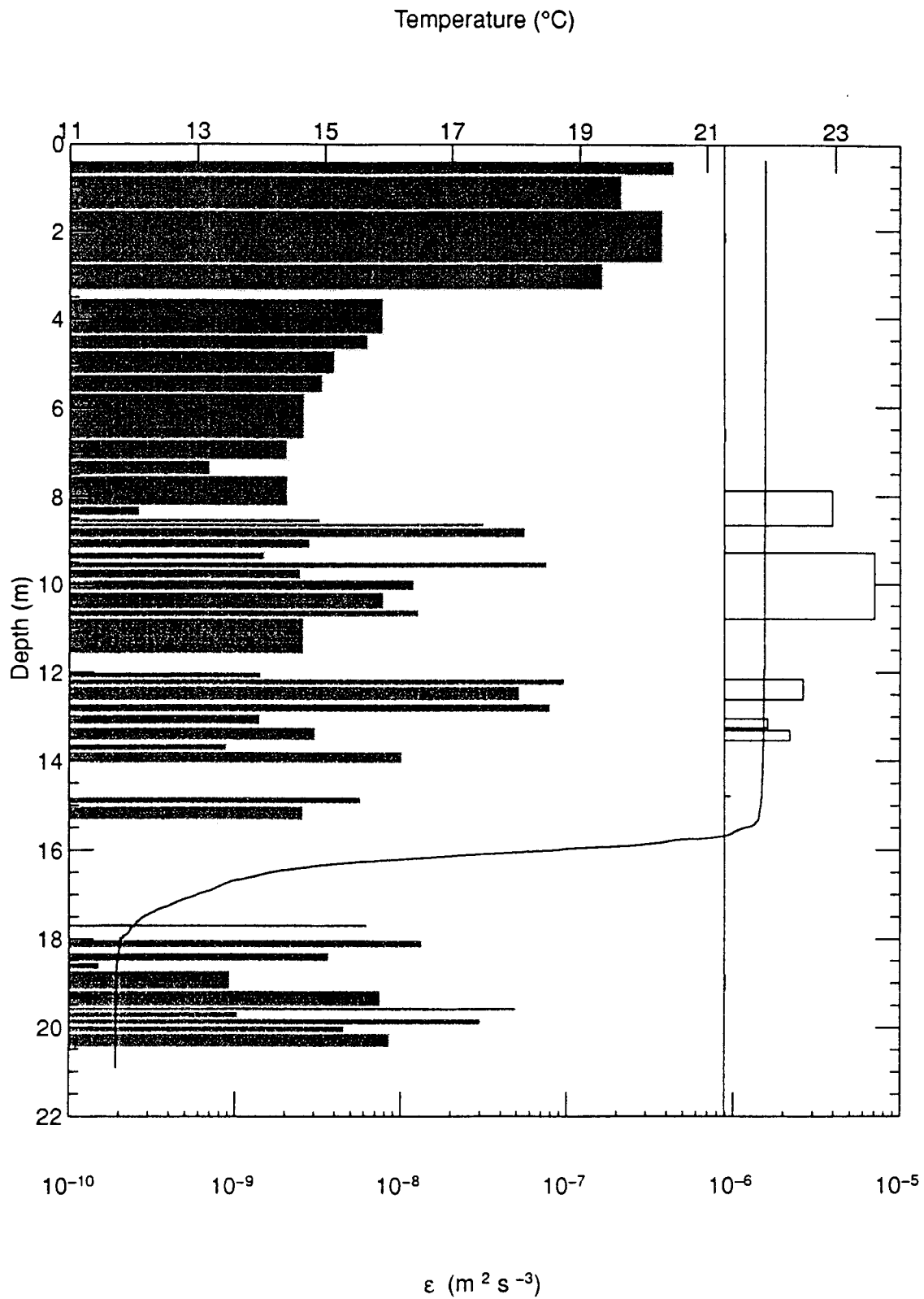


Figure 2.17: Variation in temperature and TKE dissipation at 8:56 AM on 8 August 1997. The bar at the right shows the presence of overturns.

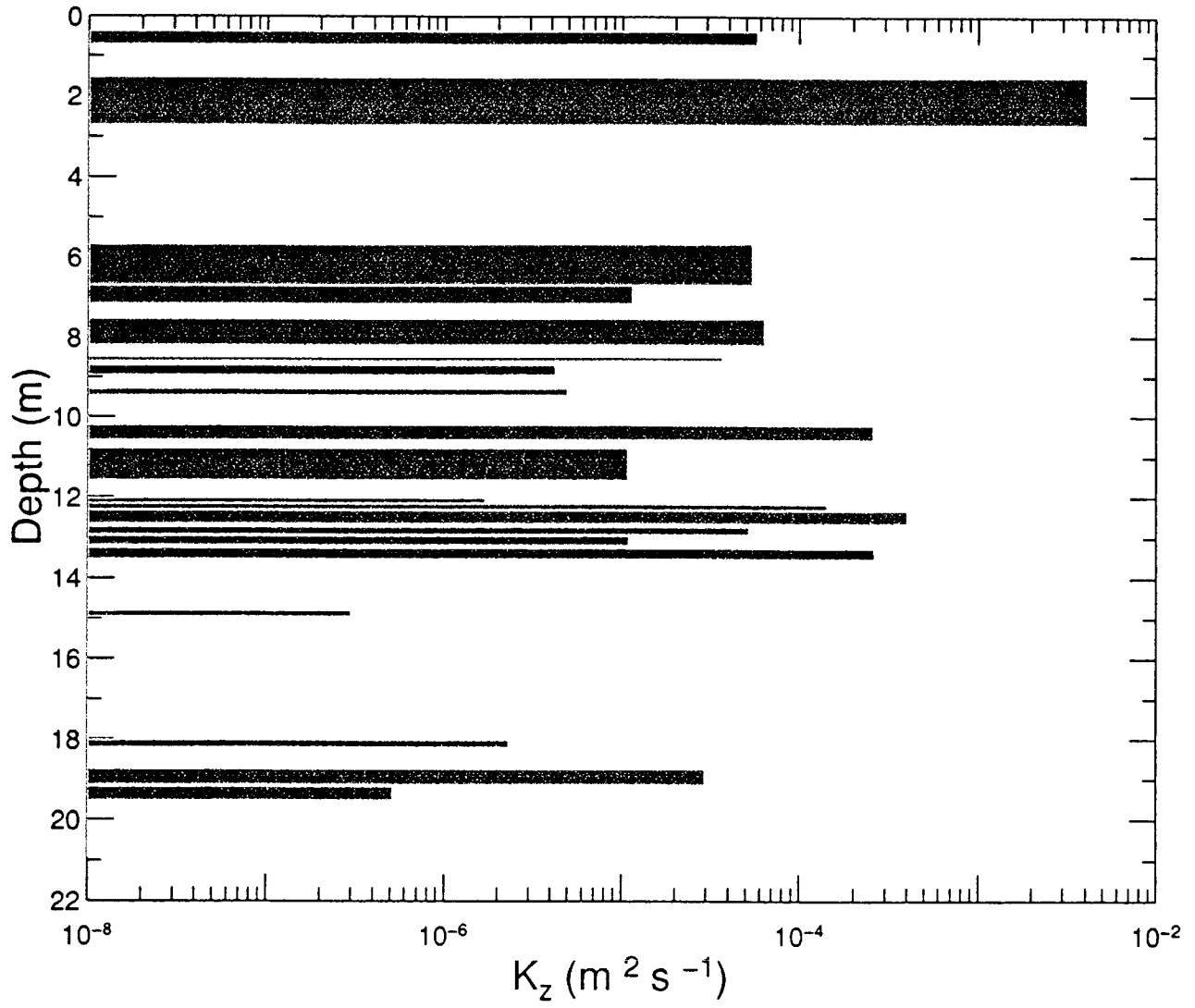


Figure 2.18: Eddy diffusivity at 8:56 AM on 8 August 1997.

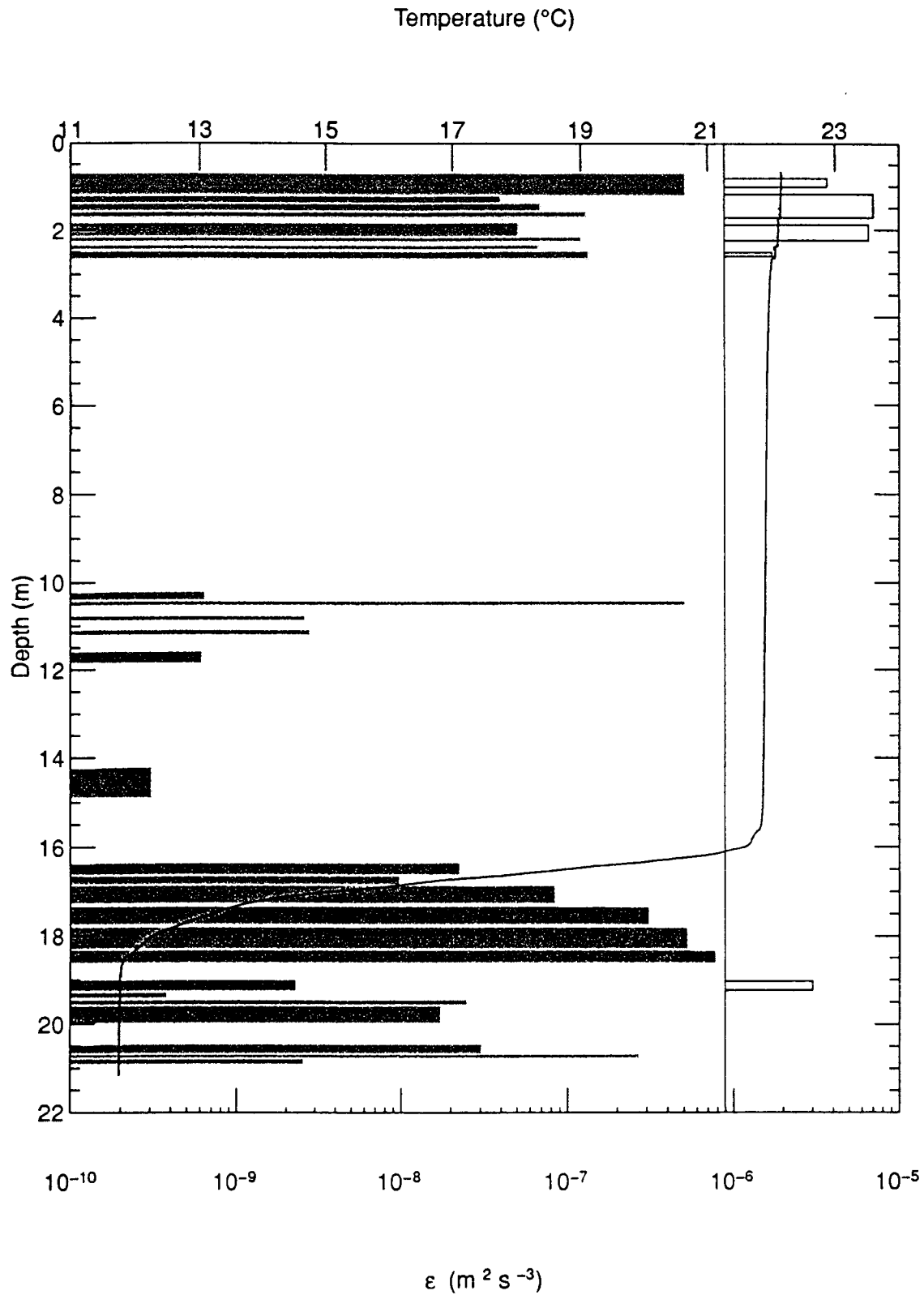


Figure 2.19: Variation in temperature and TKE dissipation at 11:26 AM on 8 August 1997. The bar at the right shows the presence of overturns.

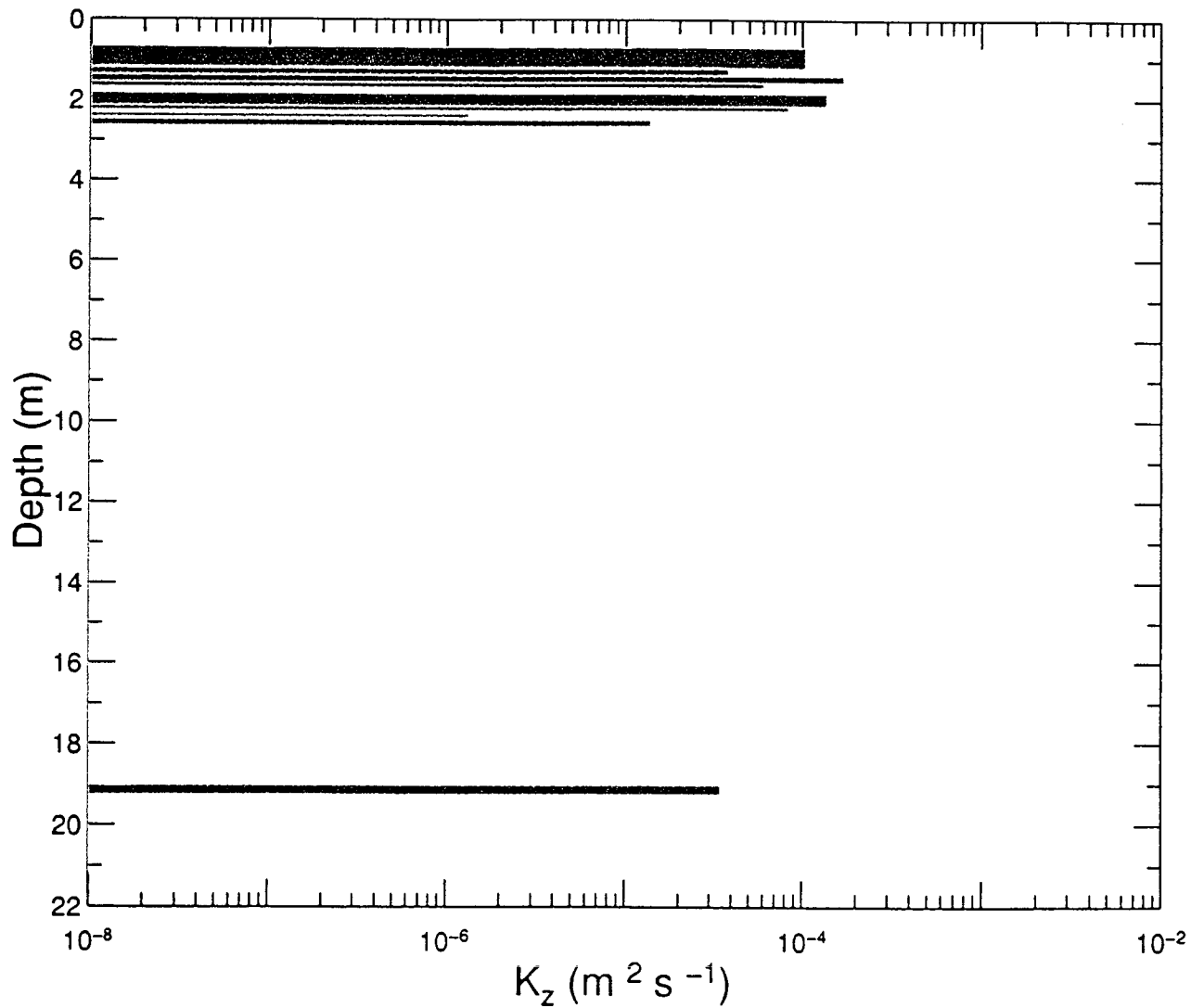


Figure 2.20: Eddy diffusivity at 11:26 AM on 8 August 1997.

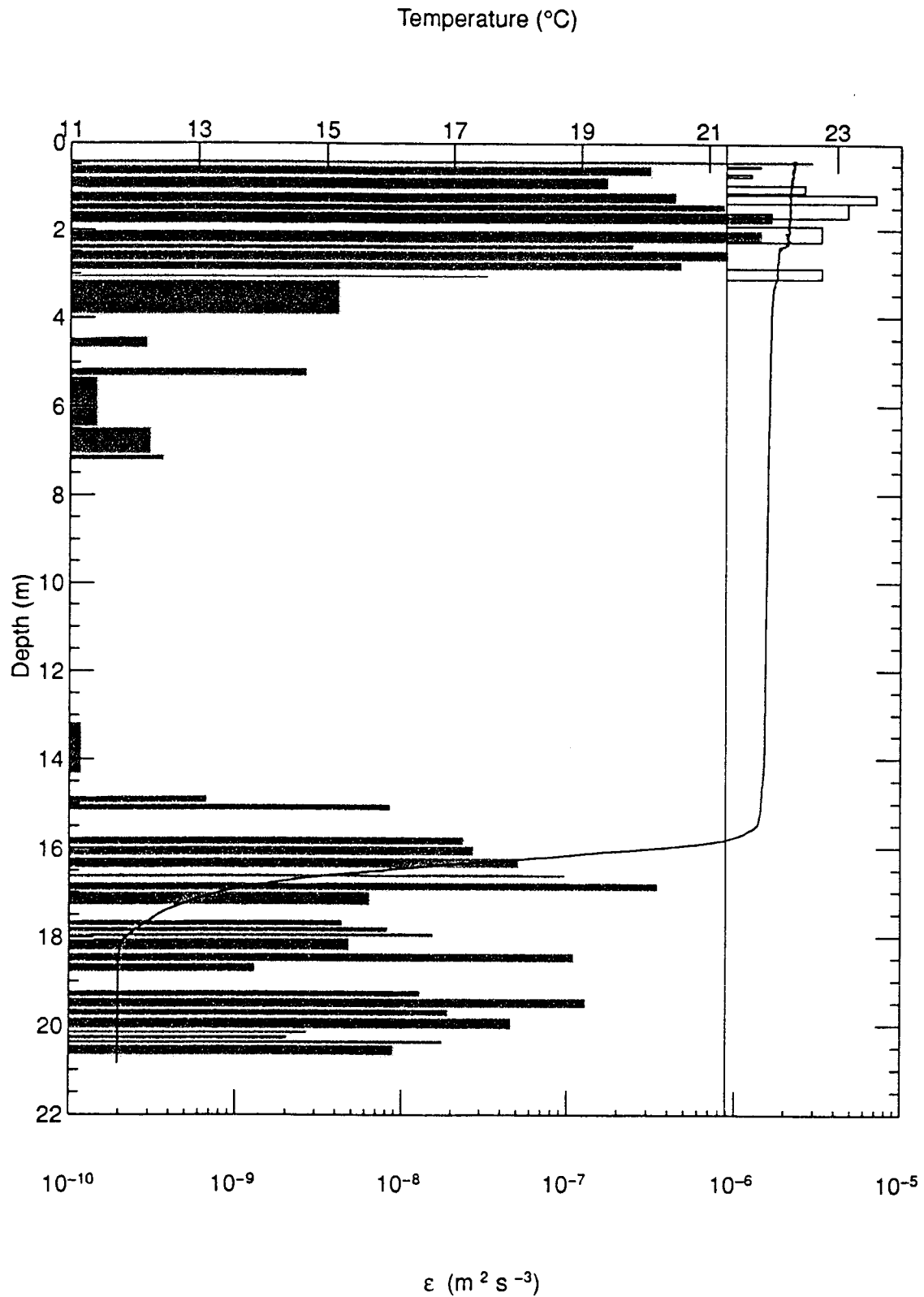


Figure 2.21: Variation in temperature and TKE dissipation at 12:30 PM on 8 August 1997. The bar at the right shows the presence of overturns.

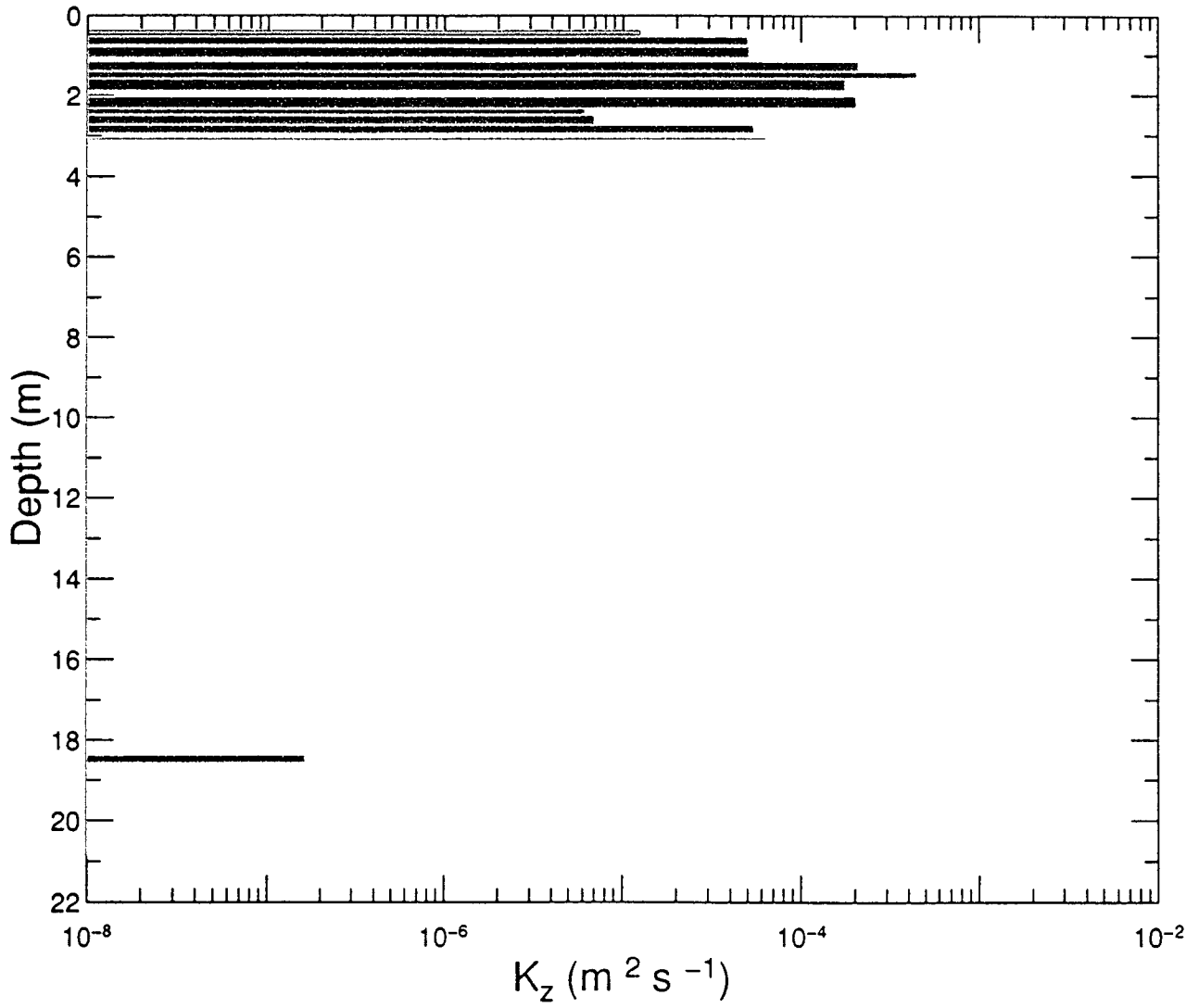


Figure 2.22: Eddy diffusivity at 12:30 PM on 8 August 1997.

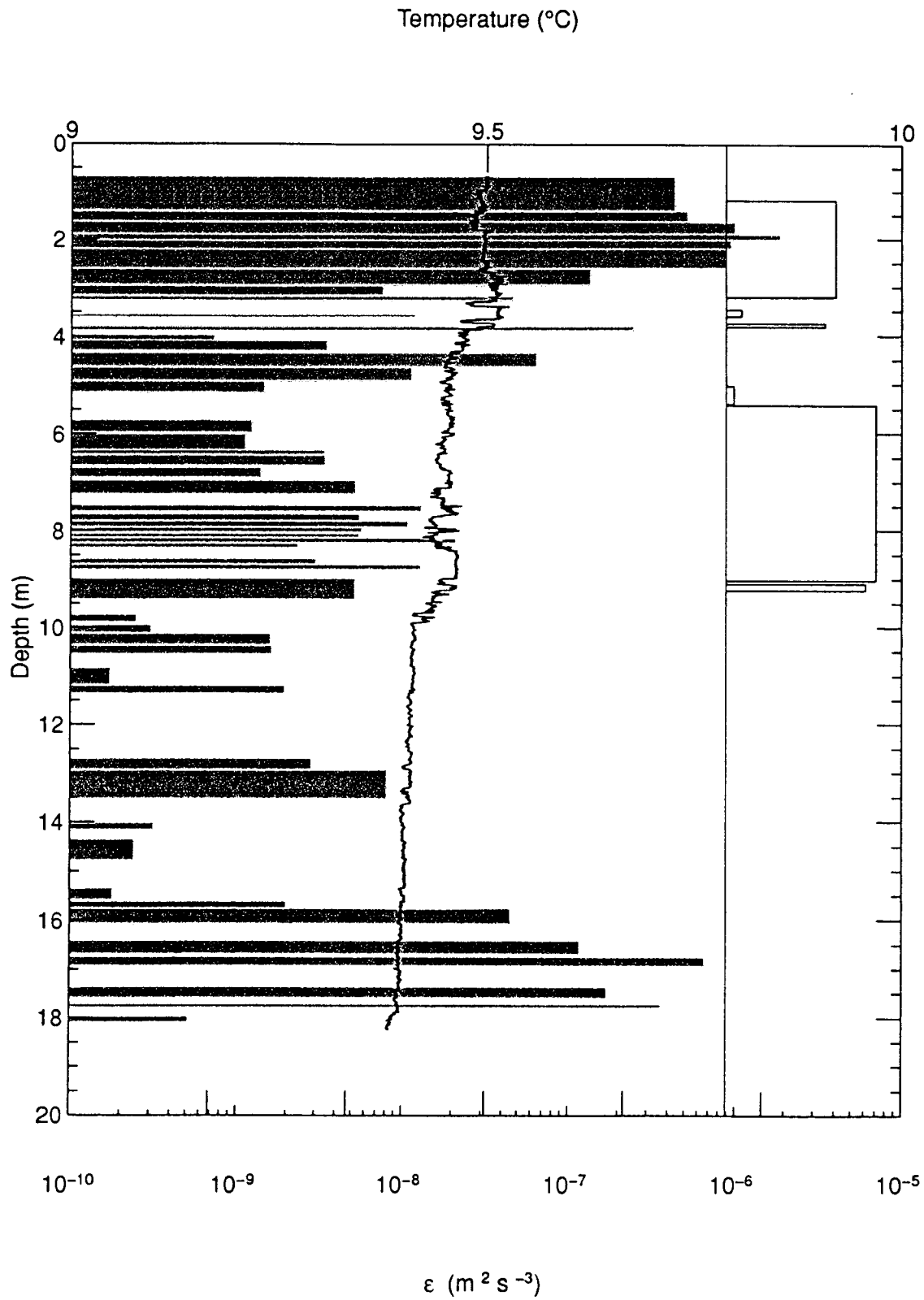


Figure 2.23: Variation in temperature and TKE dissipation at 12:28 PM on 21 May 1997. The bar at the right shows the presence of overturns.

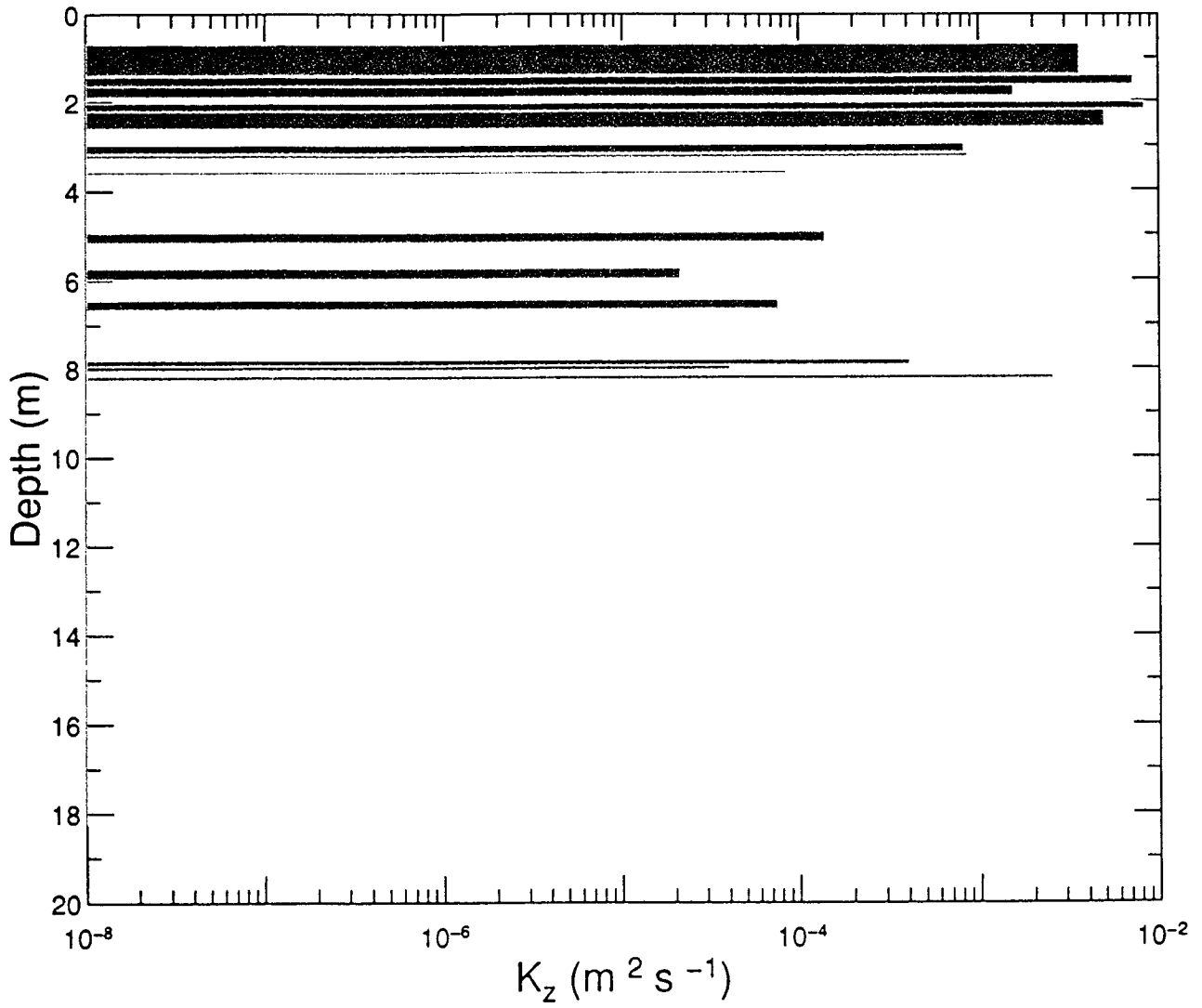


Figure 2.24: Eddy diffusivity at 12:28 PM on 21 May 1997.

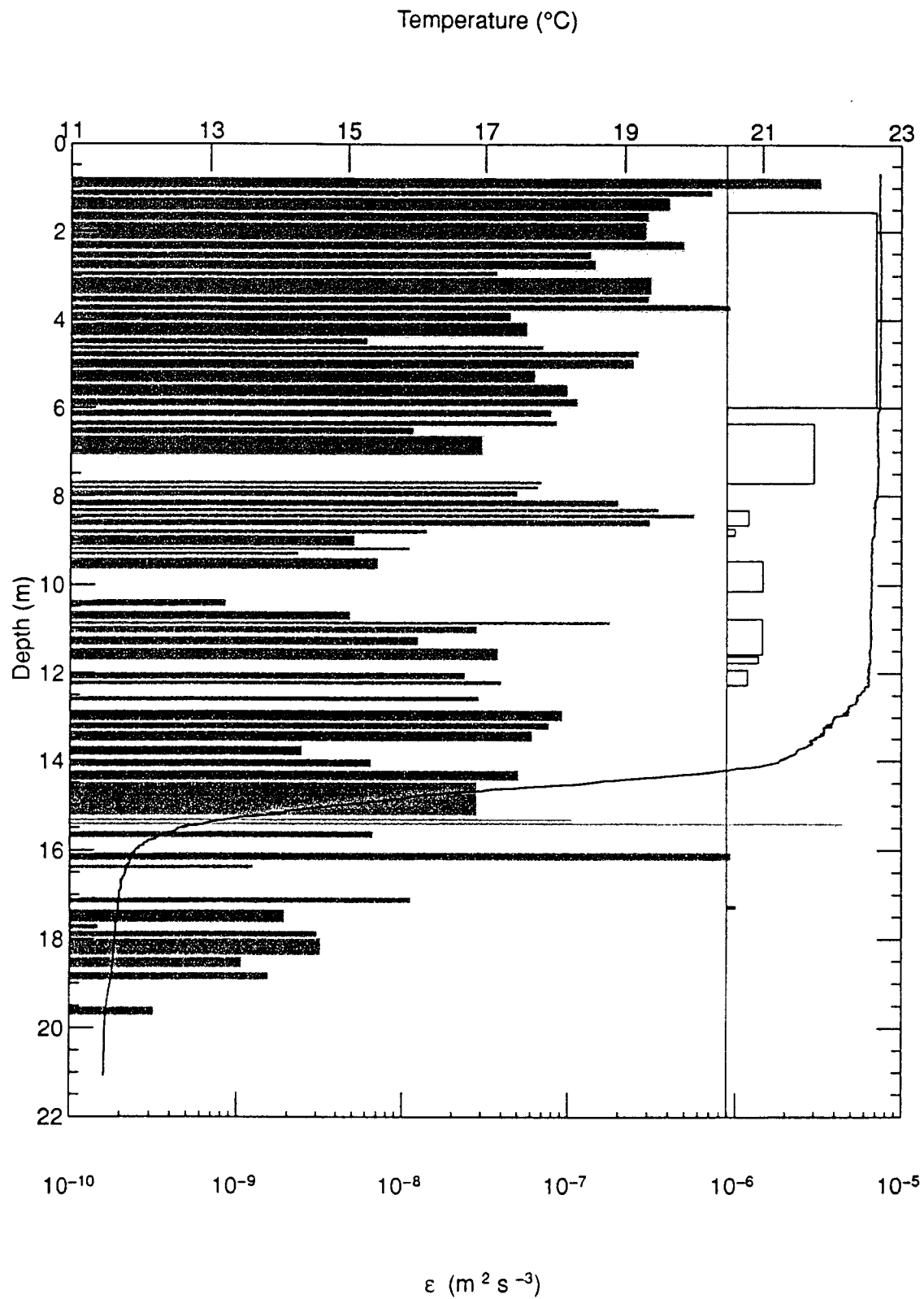


Figure 2.25: Variation in temperature and TKE dissipation at 12:43 PM on 4 August 1997. The bar at the right shows the presence of overturns.

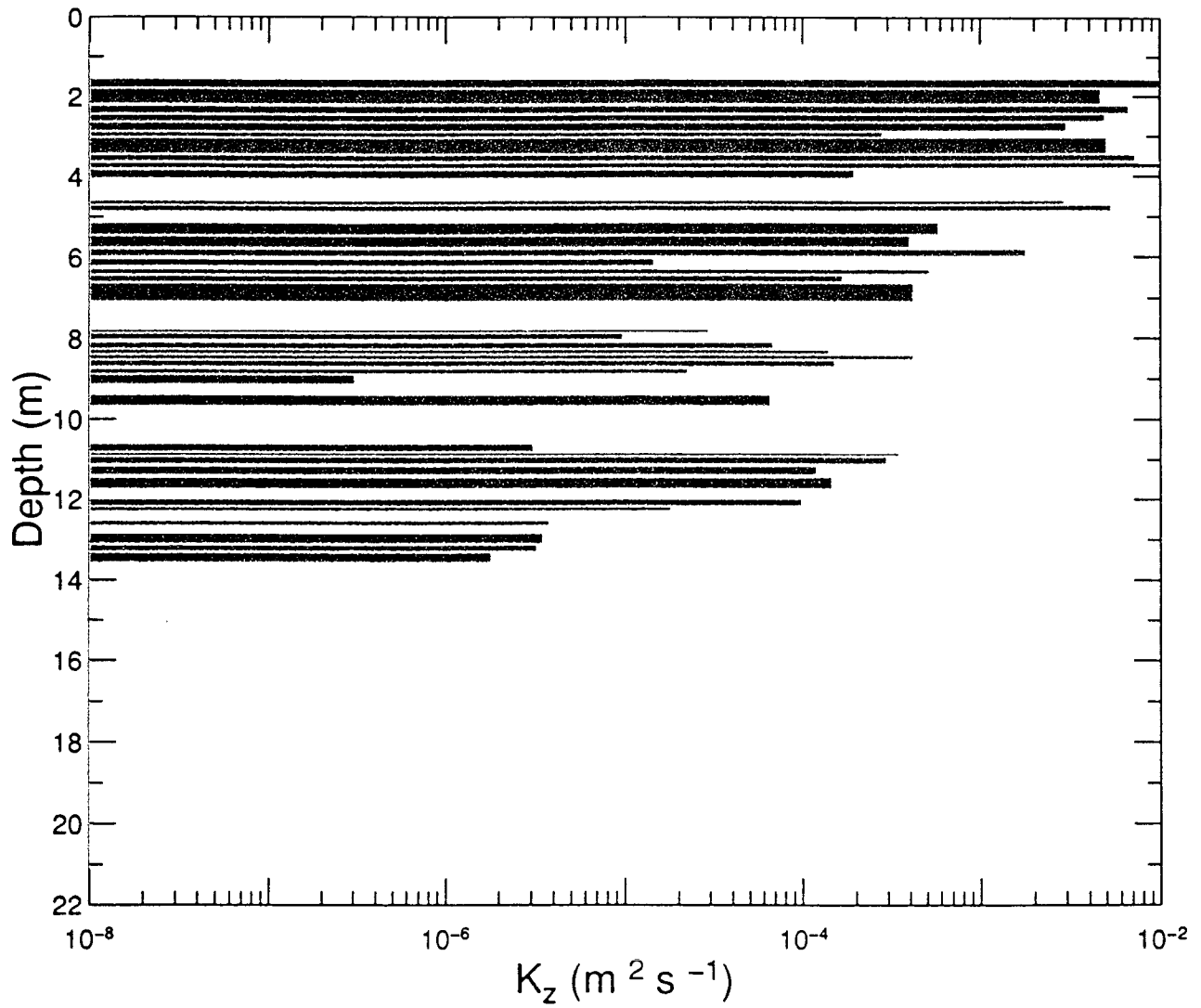


Figure 2.26: Eddy diffusivity at 12:43 PM on 4 August 1997.

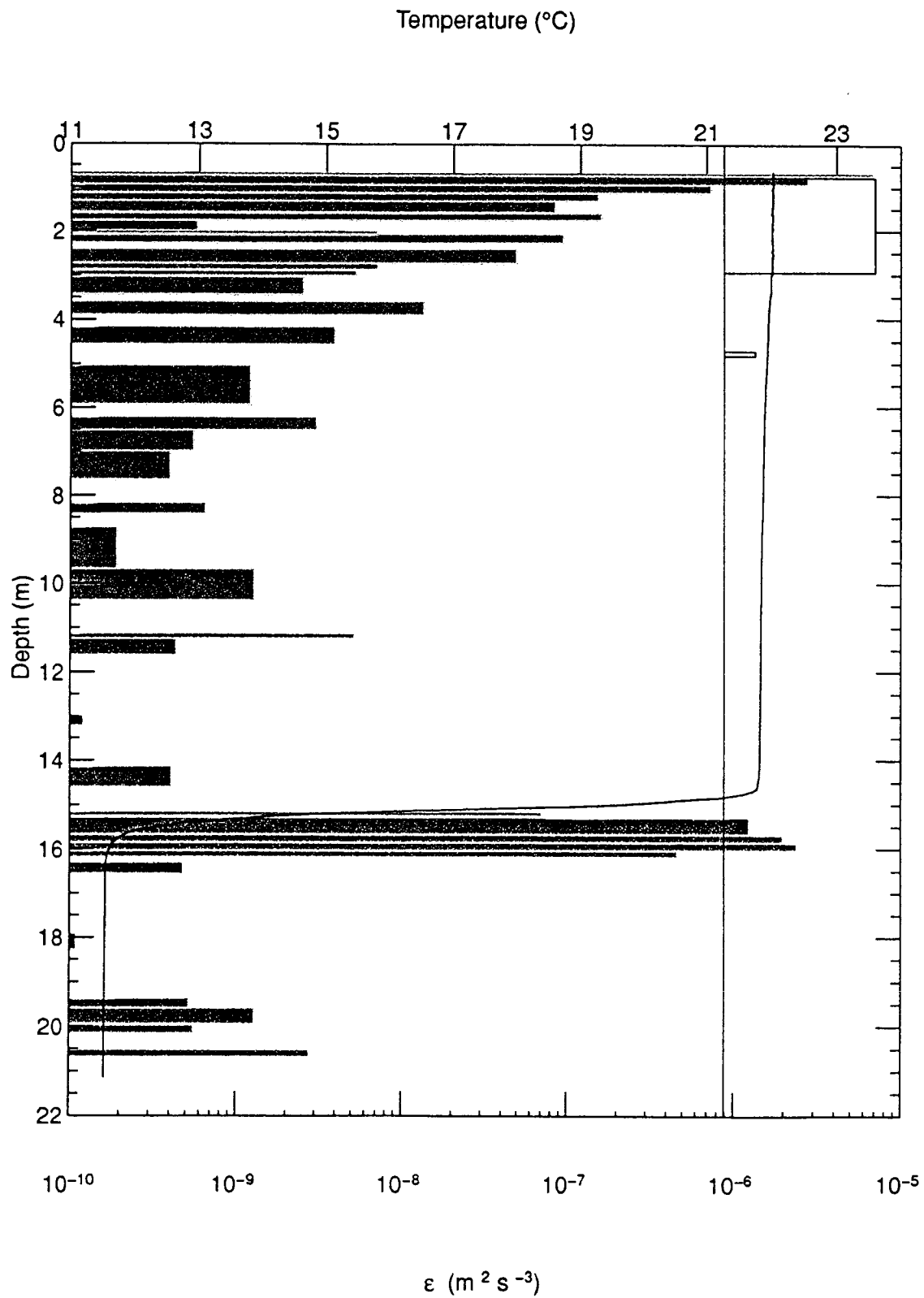


Figure 2.27: Variation in temperature and TKE dissipation at 1:00 PM on 6 August 1997. The bar at the right shows the presence of overruns.

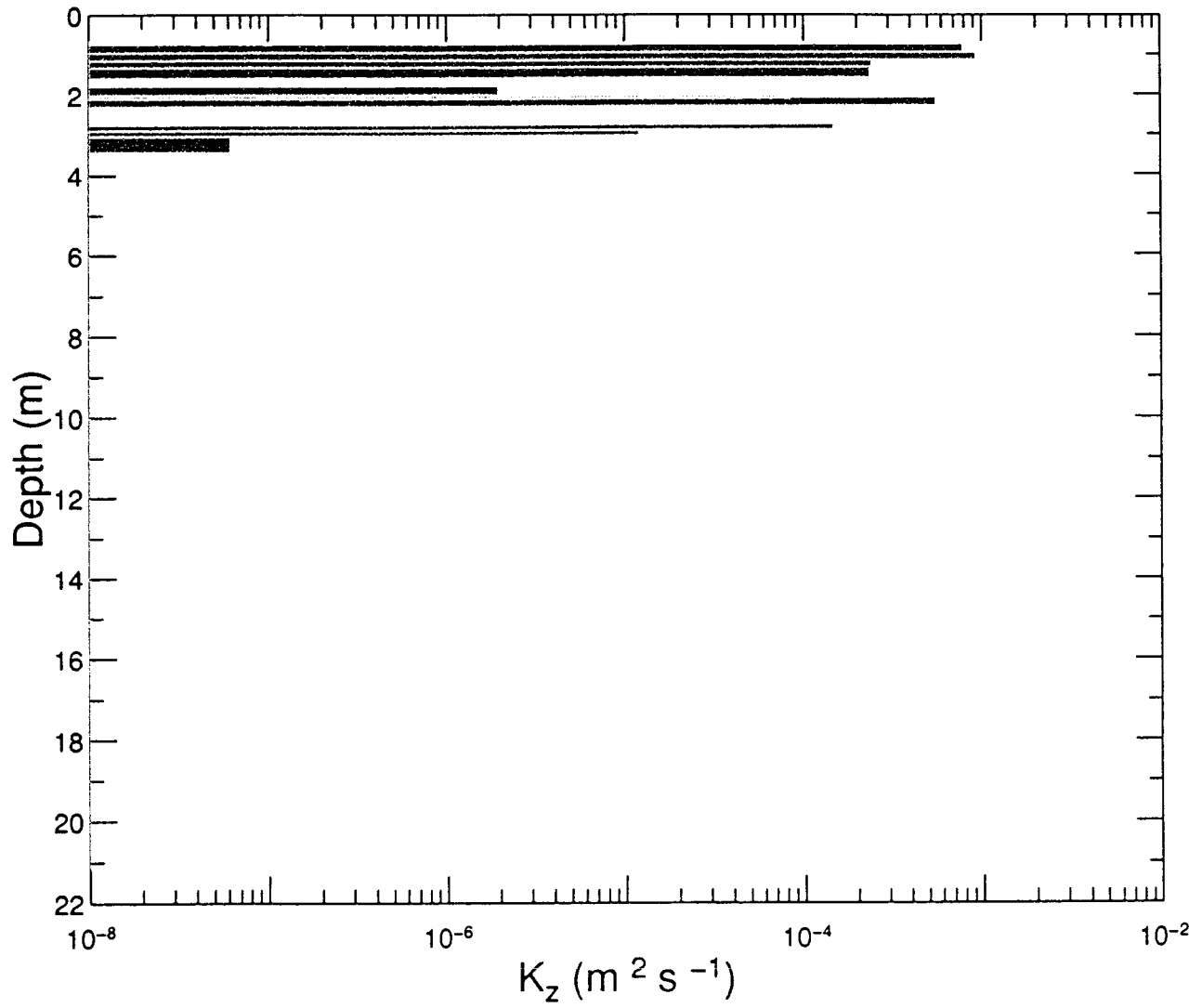


Figure 2.28: Eddy diffusivity at 1:00 PM on 6 August 1997.

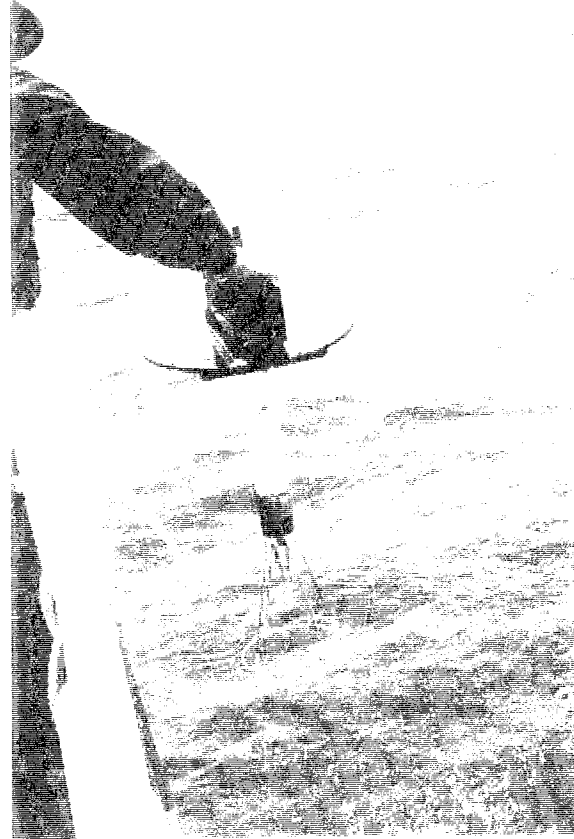
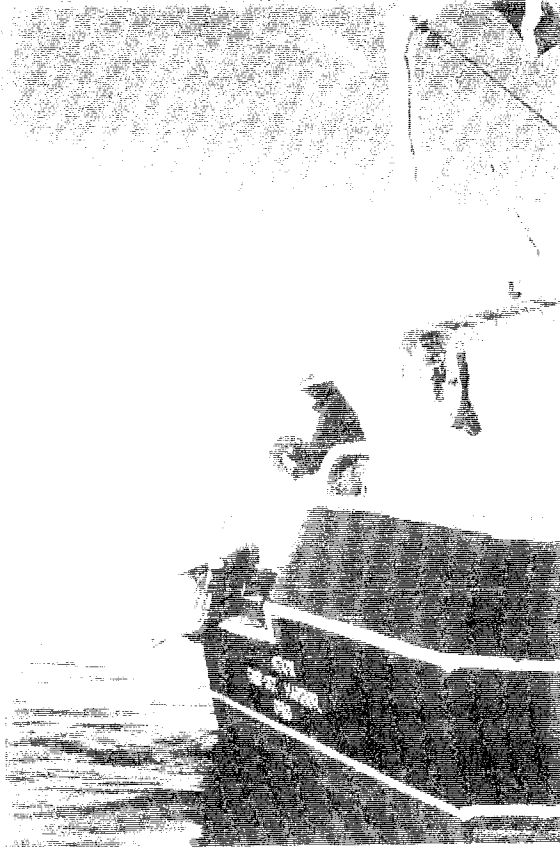


Figure 2.29: Deployment of the SCAMP in downward mode off the ODW Grandon in the central basin of Lake Erie

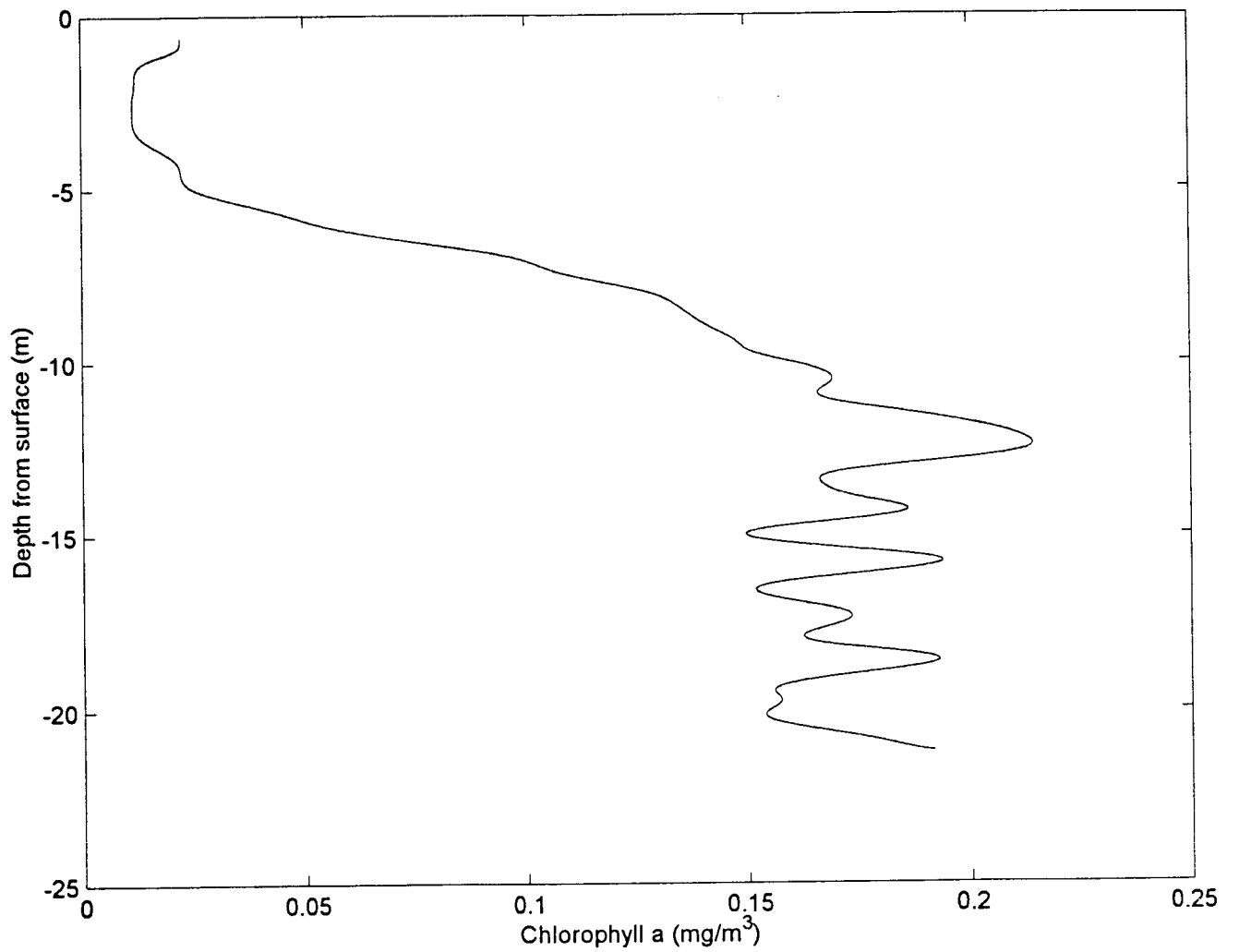


Figure 3.1: Variation in Chlorophyll a (mg/m^3) on 23 May 1997 at 11:25 AM.

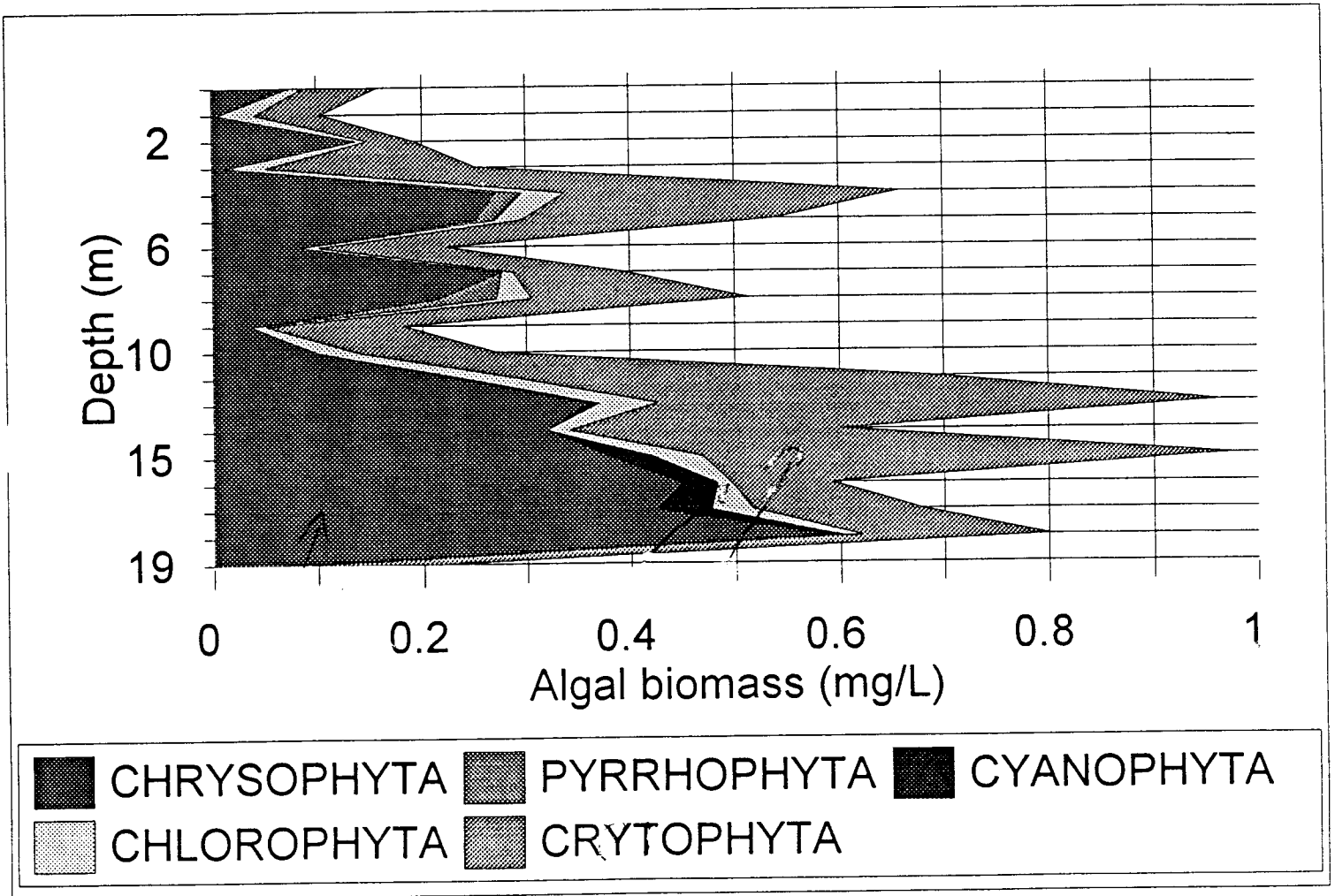


Figure 3.2: Variation in algal biomass on 23 May 1997 at 12:00 PM. This profile was sampled using a 0.5 m long Van Dorn sampler.

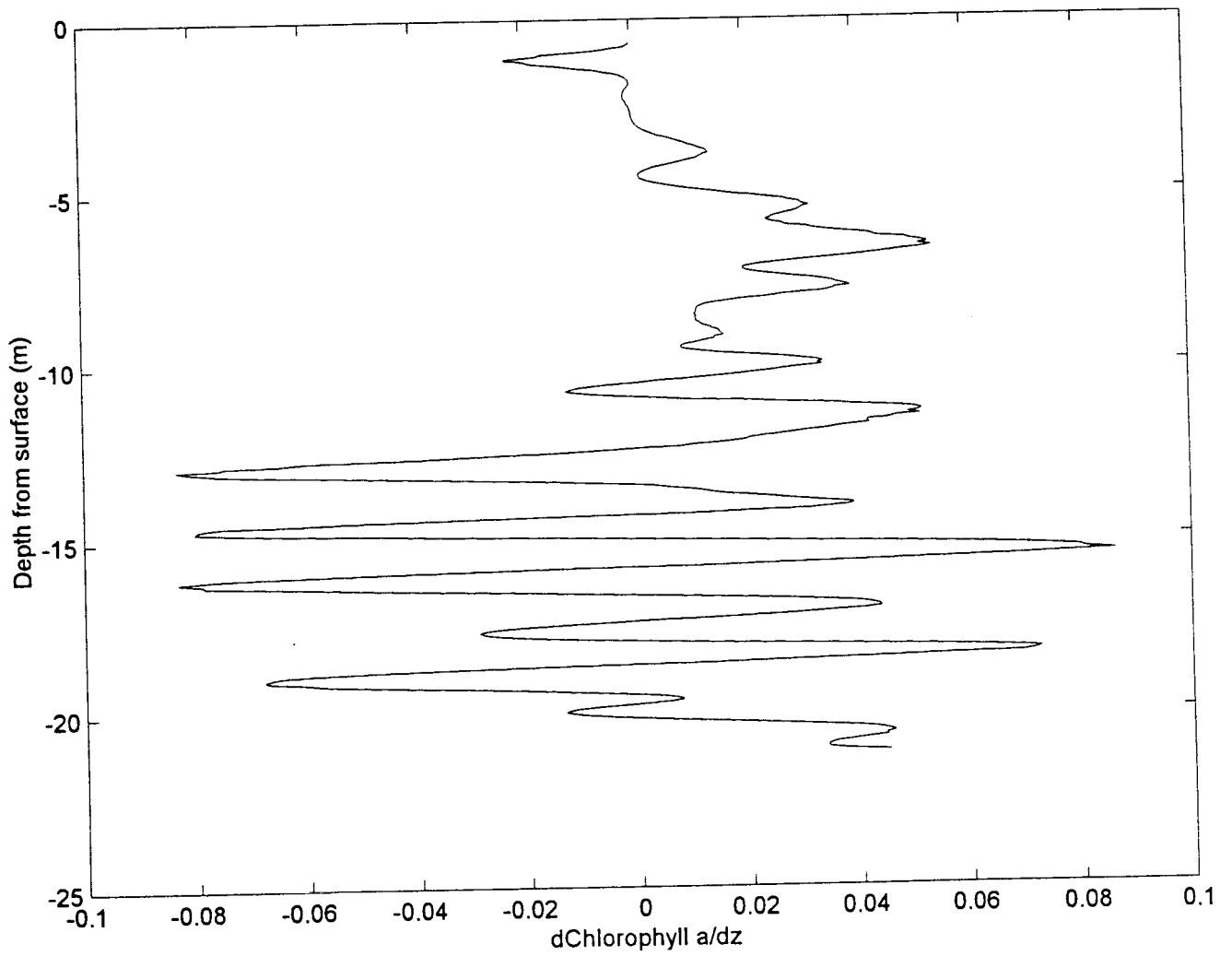


Figure 3.3: The gradient of chlorophyll a with respect to depth on 23 May 1997 at 11:25 AM.

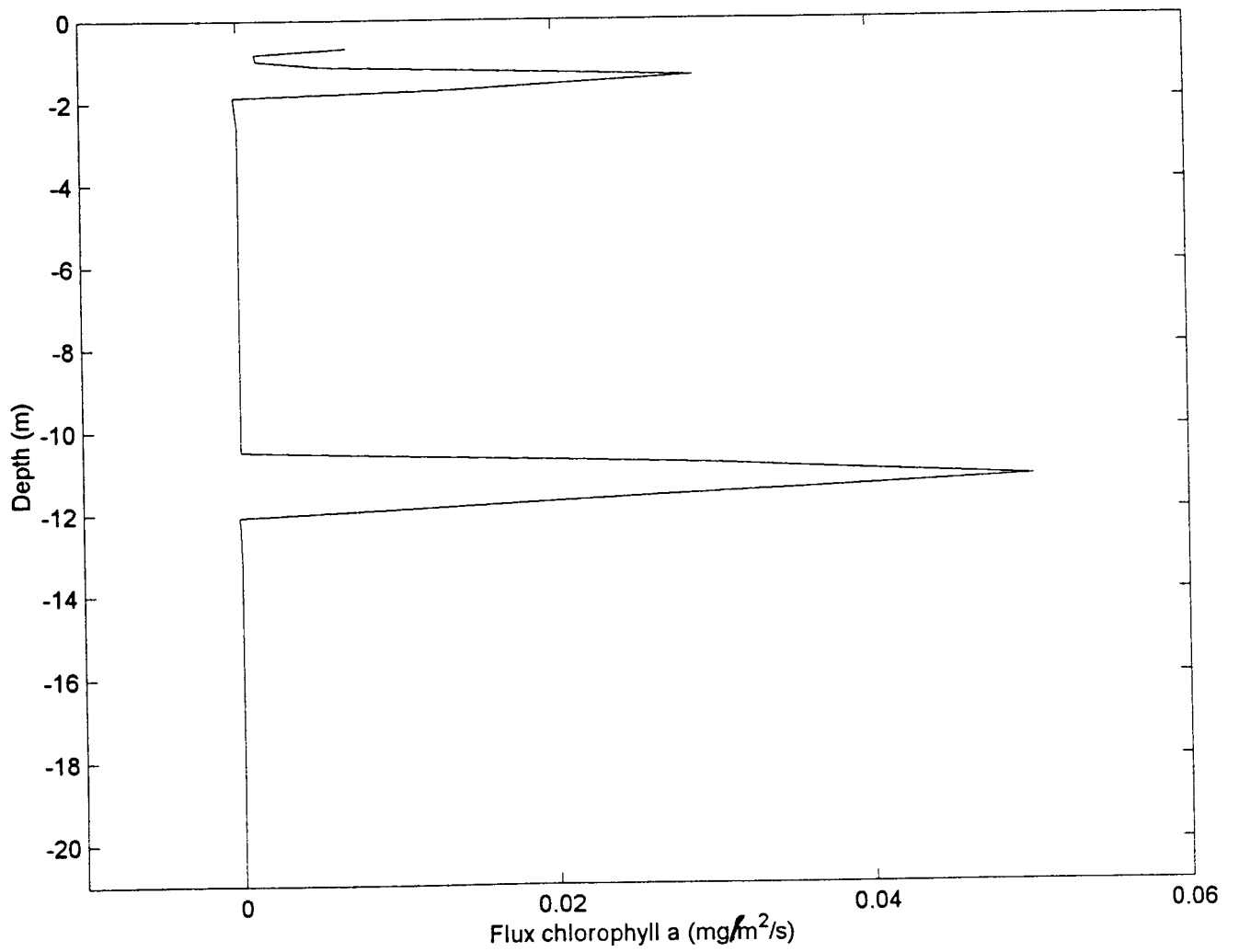


Figure 3.4: The Flux of chlorophyll a with respect to depth (mg/m²/s) on 23 May 1997 at 11: 25 AM.

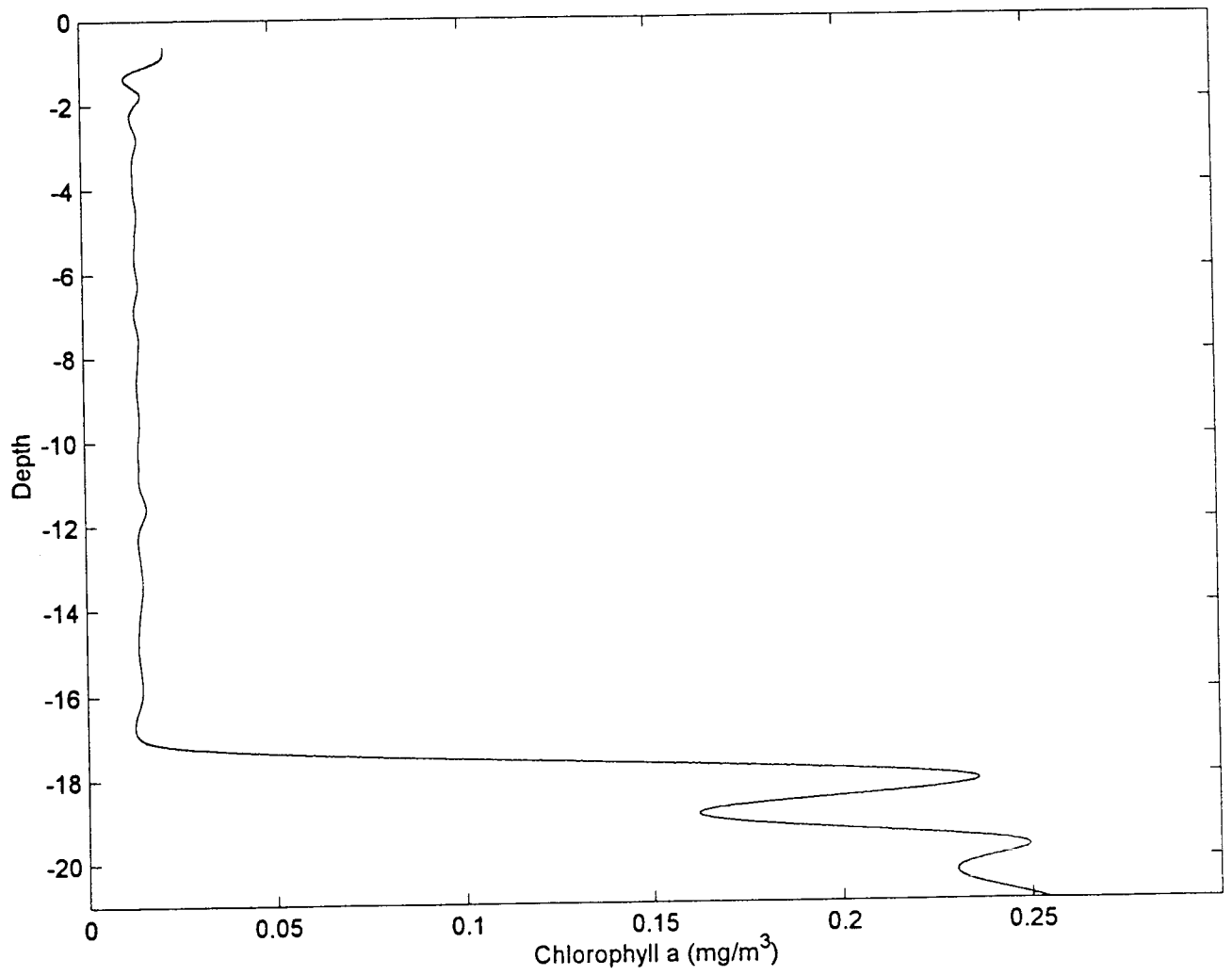


Figure 3.5: Variation in Chlorophyll a (mg/m³) on 8 August 1997 at 6:37 AM.

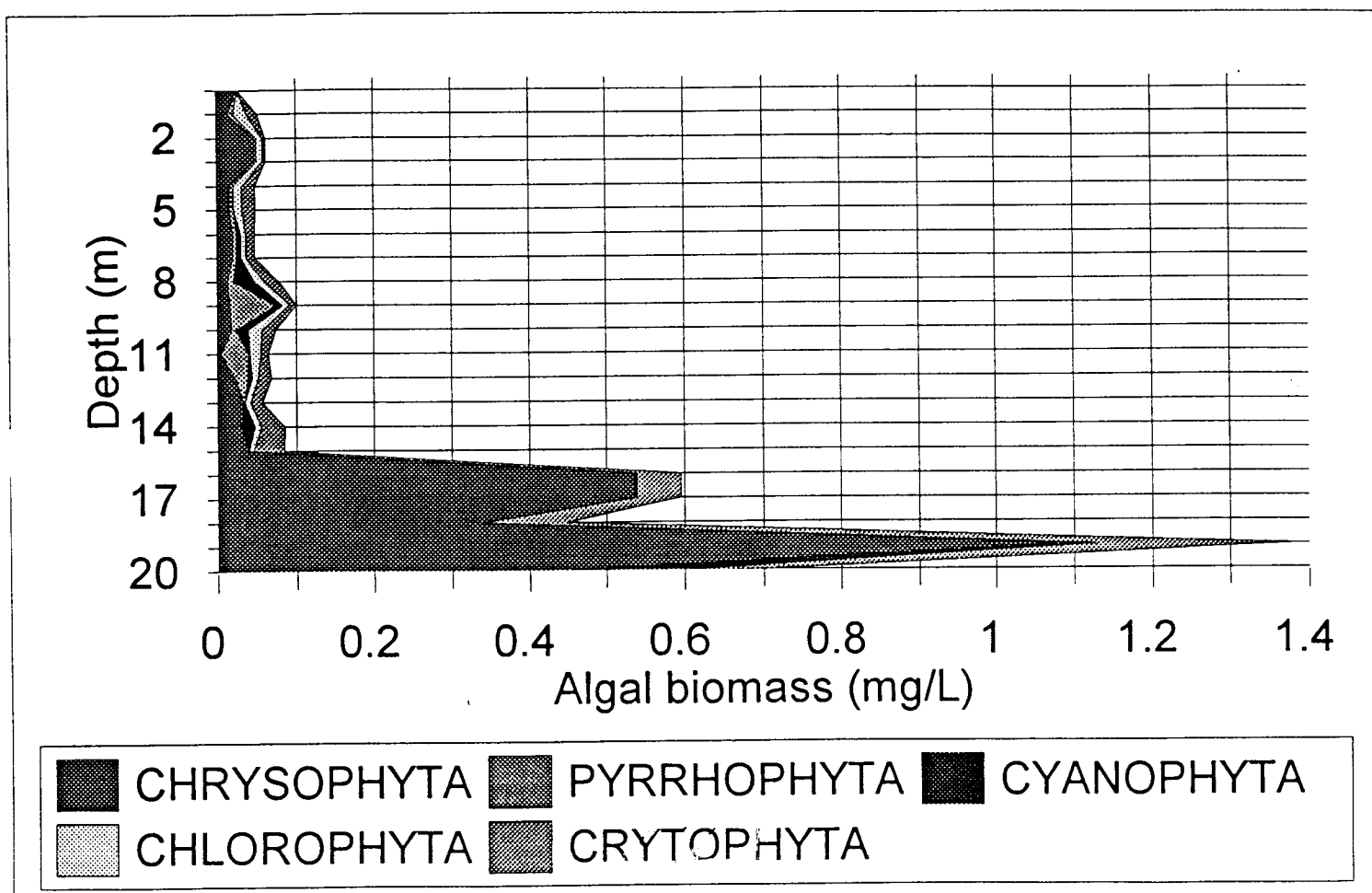


Figure 3.6: Variation in algal biomass on 8 August 1997 at 12:00 PM. This profile was sampled using a 0.5 m long Van Dorn sampler.